Universidad
Autónoma de Madrid

Facultad de Ciencias

Departamento de Física Teórica

Consejo Superior
de Investigaciones Científicas

Instituto de Física Teórica

IFT–UAM/CSIC

Applications of Holography to Strongly Coupled Hydrodynamics

Irene Rodríguez Amado,

Madrid, Mayo 2010.

Universidad
Autónoma de Madrid

Facultad de Ciencias

Departamento de Física Teórica

Consejo Superior
de Investigaciones Científicas

Instituto de Física Teórica

IFT–UAM/CSIC

Applications of Holography to Strongly Coupled Hydrodynamics

Memoria de Tesis Doctoral realizada por
Dña. Irene Rodríguez Amado,
presentada ante el Departamento de Física Teórica
de la Universidad Autónoma de Madrid
para la obtención del Título de Doctor en Ciencias.

Tesis Doctoral dirigida por
Dr. D. Karl Landsteiner,
Científico Titular del Consejo Superior de Investigaciones Científicas.

Madrid, Mayo 2010.

Contents

Preface

This thesis is about the application of the AdS/CFT correspondence to the dynamics of strongly coupled gauge theories, paying special attention to the hydrodynamic behavior of these systems. In particular, we study the response to small external perturbations of a strongly coupled quark-gluon plasma (sQGP) using holographic techniques, with an special interest in the exploration of the validity of the hydrodynamic approximation in such a system. We also study the hydrodynamic regime of high T_c superconductors within the frame of the gauge/gravity duality.

The AdS/CFT correspondence establishes an equivalence between a quantum field theory and string theory in a curved background with the peculiarity of being a strong-weak coupling duality. When the gauge coupling is taken to be large, the field theory is in a non-perturbative regime, whereas the string theory can be approximated by its classical low energy limit, supergravity. It provides us with a theoretical tool to describe the dynamics of strongly interacting gauge theories. Of particular interest is the strongly coupled quark-gluon plasma (sQGP) discovered in the Relativistic Heavy Ion Collider (RHIC) at Brookhaven. The sQGP behaves as a nearly perfect fluid and can be described in terms of hydrodynamics in the low energy long-wavelength limit. The RHIC accelerator creates very dense and hot matter, mostly made of quarks and gluons, by colliding heavy nuclei. The created fireball rapidly thermalizes, expands and cools down coming back to the hadronic gas phase, but in the meanwhile, when it is a quark-gluon plasma, it reproduces the conditions of the primordial plasma in the first microseconds after the Big Bang. At the end of the Grand Unification era (10^{-36} seconds) the universe was filled with a soup of free particles that was expanding and cooling down. Around 10^{-11} seconds after the explosion, the electroweak force decoupled from the strong force and particle interactions were energetic enough to create particles such as the Z and the W bosons. The Early Universe was then filled by the quark-gluon plasma, still cooling and expanding, until it reached a temperature of about 200 MeV that is 2×10^{12} K, when the confinement/deconfinement phase transition took place. The QGP hadronized forming protons and neutrons. This happened a couple of microseconds after the Big Bang. Few minutes after that, the temperature was low enough to allow the binding of hadrons, thus the formation of light nuclei started. The state of the Early Universe just before the quark/hadron phase transition is roughly reproduced at RHIC, and soon it will also be tested at the ALICE experiment in the LHC at CERN. These experiments give valuable information about QCD in the deconfined phase and the physics of the primordial plasma.

Having a theoretical understanding of them is a hard, challenging and interesting task, and it seems that holography can help us in this venture.

Recently, the AdS/CFT correspondence has emerged as a very useful tool in the frame of condensed matter physics as well, since there is a wide number of strongly correlated condensed matter systems that cannot be treated using the conventional paradigms, like for instance quantum critical systems. There are many strongly coupled materials that can be engineered and studied in laboratories that are challenging for condensed matter theory and for which seems possible that the gauge/gravity duality can be helpful to gain some insight into them. The high T_c superfluids and superconductors are expected to belong to this family of condensed matter theories to which holographic techniques might be applied. On the other hand, this large number of condensed matter systems also provides us with an enormous and rich variety of effective Lagrangians. Therefore it might as well be that using experimental techniques a material with a known gravity dual can be engineered, leading to experimental AdS/CFT and allowing for a better understanding of quantum gravity through atomic physics, thus reversing the usual direction of the correspondence. Consequently, the study of AdS/CM correspondence appears as a very exciting and rich topic. In this thesis we will apply the correspondence to model simplified condensed matter systems and see what kind of information we can get from it.

This thesis is organized in two parts. The first part is devoted to present the background ingredients and tools that will be used later on, namely, the properties of strongly coupled systems and the holographic techniques:

Chapter 1: We present the main features and issues of strongly coupled systems, centered on the sQGP phase of QCD, exposing some of the most relevant results at RHIC experiment that point to the strong coupling behavior of the formed plasma, and on the phenomena of quantum criticality, specially for the case of high temperature superconductivity and superfluidity. We also present some basics on linear response theory and hydrodynamics, the main tools to study perturbations in those setups.

Chapter 2: This chapter is devoted to explain the basics of the AdS/CFT correspondence, avoiding as far as possible to enter in technical details that will not be useful in what follows. We center on those aspects of the correspondence and its extensions more relevant for applications to the systems already mentioned: how to add temperature and how to add finite chemical potentials to the gauge theory.

Chapter 3: The power of the gauge/gravity duality relies on the ability to perform real-time computations. In this chapter we present the main computational tool for the

rest of the thesis: a prescription to holographically compute thermal correlators. We also present some results of the correspondence concerning the singularities of the propagators and the spectrum of quasinormal modes of black holes and the constraints that stability imposes on their location.

In the second part of the thesis, we present applications of the correspondence concerning strongly interacting physics:

Chapter 4: We examine an interesting property of the duality related to the quasinormal spectra of black holes: in the large frequency limit, the location of the poles of retarded correlators can be explained in terms of null rays bouncing in the black hole background, thus the quasinormal spectrum is related to the causal structure of the black hole geometry. This relation is consistent with the prescription given in the previous chapter for computing thermal correlators.

Chapter 5: The physics of near-equilibrium processes in the gauge theory is encoded in real time two-point correlation functions of operators and is completely determined by its singularities. Holographic correlators only have poles as singularities. We compute the quasinormal spectrum and the corresponding residues for different types of perturbations to measure the contribution of each collective mode in a gluon plasma. We present the results for the hydrodynamic modes and study the regime of validity of a hydrodynamic description based on those modes alone. We also are able to define a lower limit of the thermalization time for the plasma.

Chapter 6: The simplest model of holographic superfluidity is studied: the spontaneous symmetry breaking (SSB) of a global symmetry through the formation of a Bose condensate is holographically realized by a charged scalar condensing in a charged AdS black hole background. For small temperature the scalar field develops an expectation value and the system enters the superfluid phase. We find the expected Goldstone boson appearing at the SSB of a global $U(1)$ symmetry and follow it into the broken (superfluid) phase. Below the critical temperature it propagates as a sound mode: the second sound of the superfluid component.

The first part of this work is basically a compendium of many papers and reviews on the corresponding topics. The original work presented here corresponds to the second part of this doctoral thesis. It is based on our published papers [1–4].

Part I

Background: Strongly Coupled Systems and Holography

Chapter 1

Strongly coupled systems

Most of our understanding of quantum field theories relies on the possibility of performing perturbative analysis. This is guaranteed when ever the system is weakly interacting. The fact that an effective weakly interacting quasiparticle description can be valid in some theories even when the microscopic degrees of freedom are strongly interacting has led to a considerable progress in the understanding of strongly coupled systems. But problems appear when such a perturbative description is lacking and purely non-perturbative methods are needed. This is the case of non-Abelian gauge theories, as Quantum Chromodynamics (QCD): for processes that involve energies of order $\Lambda_{\rm QCD}$ the gauge coupling becomes strong thus making the perturbative analysis unreliable. Strongly coupled gauge theories can be studied using lattice simulations when one is interested in the static properties of the system, but they are not suitable (or require a huge effort) for the study of real-time dynamical processes.

A different framework where inherently strongly coupled physical phenomena are present is condensed matter physics. In general, correlated electron materials can be described in terms of order parameters, when a broken symmetry is present, and quasiparticles, when long-lived excitations are involved. Then, field-theoretical methods allow to determine the dynamics of the system. However, there are many examples that cannot be described using the usual paradigms. The absence of well-defined quasiparticle excitations implies that kinetic theory does not completely determine the transport properties of the system, so a different approach is needed. One family of systems for which this is the case corresponds to systems close to quantum critical points. Their dynamics can be described in terms of *quantum criticality* but anyway a non-perturbative analysis is required in order to fully determine their transport coefficients. This is the case, for instance, for systems that exhibit 'non-Fermi liquid' behavior, and also for some systems with a superfluid/superconductor-insulator transition, like cuprate superconductors (also called high T_c superconductors).

In this chapter we try to flash the main properties of these two kinds of physical systems for which new non-perturbative methods must be developed in order to have a description of dynamical processes. We will see in the next chapter that the AdS/CFT correspondence provides us with such a tool for studying strongly interacting field theories, or at least for

studying some simplified models that might nevertheless give useful information about real world physical systems. In particular here we center on the strongly coupled quark-gluon plasma and in the non conventional superconductors. We also present some field theory results related to the hydrodynamics of these systems.

1.1 Quark-Gluon Plasma

Quantum Chromodynamics (QCD) is the theory that describes the strong nuclear interactions between quark matter. This theory does not only exist in vacuum, moving around the phase diagram by changing temperature and baryon chemical potential, one finds a rich variety of phases some of them not fully understood yet. The ultrarelativistic heavy ion collision experiments taking place at RHIC, and the upcoming experiment at the LHC, have made the quark-gluon plasma (QGP) phase of QCD accessible. Quarks and gluons appear deconfined. For a long time it was expected that the QGP was in a weakly coupled regime. In contrast, experiments at the Relativistic Heavy Ion Collider (RHIC) at Brookhaven seem to indicate that around the deconfinement temperature the plasma remains in a strongly coupled regime. Developing methods to describe this state and the dynamical processes in it is really appealing and an important challenge. Strongly coupled QCD at equilibrium is usually studied using lattice simulations, that have proved to be a very successful tool to extract static quantities. However, studying real-time dynamical phenomena is much more involved since in general simulations are run in Euclidean time. Hence for most of the cases, lattice computations are not suitable for out-of-equilibrium processes and new methods are needed. For us the solution to this problem will be using the gauge/gravity duality to study such phenomena in sQGP-like models.

QCD phase diagram.

QCD is a non-Abelian gauge theory with local internal symmetry group $SU(3)$. Each quark comes in three colors and there are six different kinds of quarks, called flavors. The quark-quark interactions are mediated by gluon exchange, where the gluons are the carriers of the force. There are eight different gluons corresponding to the possible different color and anti-color combinations. In contrast to what happens for the electromagnetic and the weak nuclear interactions, the individual matter constituents of QCD, the quarks, are not observed isolated in nature, only colorless states can appear as free states: baryons and mesons, what is usually refereed to as *quark confinement*. The gluons also carry color, so they can interact among themselves, unlike photons in QED. Therefore they will appear confined in color invariant combinations as well, the so-called glueballs. Thus we may better talk about *color confinement* rather than quark confinement. Another property of QCD that is not observed for the other interactions is the fact that strong nuclear

interactions turn off when the momentum transfer is large, it is refereed to as *asymptotic freedom*.

These two properties can at first sight seem surprising in comparison with the other particle interactions, though they are built into the quantum character of the field theory[1]. The general approach to field theories is perturbation theory. As a quantum theory it is likely that corrections in the loop expansion are divergent, thus to make sense of the perturbation series, renormalization of the physical quantities is needed. This procedure implies that quantities like masses and couplings will depend on the energy scale of the processes in such a way that the renormalized action is invariant under changes in the regularization parameter. The *running coupling constant* is found to be

$$\Lambda \frac{\partial}{\partial \Lambda} g(\Lambda) = \beta(g)\,, \tag{1.1}$$

where the form of the beta-function $\beta(g)$ depends on the gauge theory under consideration. If $\beta > 0$, the coupling is increasing with the energy scale Λ, and the theory may run to a Landau pole in case that the coupling becomes divergent. On the other hand, if $\beta < 0$, the coupling decreases while increasing the momentum scale so the theory is asymptotically free. This is the case of non-Abelian gauge theories [6]. Assuming that the coupling is small, the beta-function can be written as a perturbative expansion in g. To leading order, the beta-function for $SU(N)$ with N_f flavors was obtained in [7, 8],

$$\beta(g) \approx \beta_0 g^3 = -\frac{g^3}{16\pi^2}\left(\frac{11}{3}N - \frac{2}{3}N_f\right)\,, \tag{1.2}$$

which for the case of QCD ($N = 3$, N_f=6) is negative. The strength of the interactions is actually given by $\alpha_s = g^2/4\pi$. From the running coupling constant to leading order it is given by

$$\alpha_s(\Lambda) = \frac{1}{1/\alpha_s(\Lambda_0) - 8\pi\beta_0 \log(\Lambda/\Lambda_0)}\,, \tag{1.3}$$

where Λ_0 is the arbitrary renormalization scale. For large transfer momentum Λ, the strength of the interactions is small, leading to ultraviolet asymptotic freedom, in the limit that the coupling vanishes the particles become free. For small energies, the strength of the interactions becomes large, thus the perturbative analysis is not reliable any more. One can expect that for energies such that $\alpha_s \sim \mathcal{O}(1)$, the interaction between quarks and gluons is strong enough to confine them together in hadrons, leading to infrared confinement. The scale at which this happens set the scale of non-perturbative interactions, known as $\Lambda_{\rm QCD}$.

A natural consequence of these two aspects of QCD, confinement in hadrons at low energy and ultraviolet asymptotic freedom, is that there should be a phase transition

[1]For a detailed explanation of these issues we refer the reader to any quantum field theory book. In particular we have followed [5].

between the two different phases of matter when the temperature is raised. Consider a hadron gas at zero baryon chemical potential. The dominant degrees of freedom at low temperature are pions and light mesons, that are the only excitations that can be easily produced for $T \leq 100$ MeV. When the temperature is increased above this value, more and more massive resonances start to contribute and eventually dominate. At some limiting temperature it will be easier to use the energy to excite new particles than to increase the temperature. It was found by Hagedorn that the limiting temperature for QCD is around 160 MeV [9]. The density of hadrons becomes large enough to consider the soup of hadrons not as made of composite particles but as a sea of quarks and gluons. The phase transition becomes apparent if one compares the pressure due to a hadron gas with the pressure due to a plasma made of free quarks and gluons. At some critical temperature the pressures coincide and the hadron gas and the plasma of constituents are in equilibrium. For temperatures above that critical temperature the initial gas of hadrons enters a new phase of matter, the deconfined quark-gluon plasma [10–12].

This transition has been investigated using lattice QCD computations at zero baryon chemical potential. In [13] it was found for various models with different number of light quarks that their thermodynamic quantities rise very steeply at some value of the temperature signaling the presence of a transition between two different matter phases. Furthermore, the results given in [14] point that there is actually no phase transition, but a continuous crossover. The critical temperature corresponds then to a region rather than to an exact value. It has been estimated to be between $150 - 190$ MeV for zero chemical potential [15].

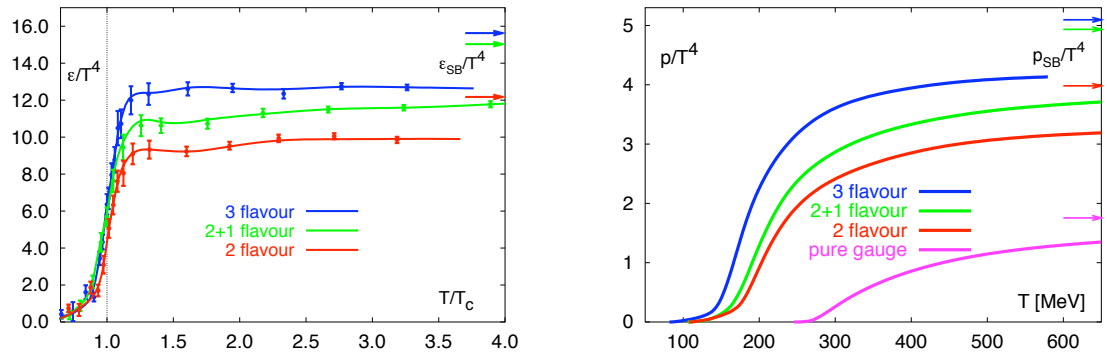

Figure 1.1: *Normalized energy density and pressure in various lattice QCD simulations. The arrows represent the corresponding asymptotic value given by the Stefan-Boltzmann result for an ideal free gas of quarks and gluons. Both plots from [13].*

Energy density and pressure as a function of temperature are shown in figure 1.1. If the system recovers asymptotic freedom at very high temperatures, it will become a free gas of quarks and gluons that can be studied using statistical perturbation theory. In fact,

its thermodynamic properties will correspond to the Stefan-Boltzmann predictions for an ideal non-interacting gas. Lattice simulations show that after the fast rising, the energy density reaches a plateau, remaining almost constant up to temperatures about $4T_c$, at roughly the 80% of the Stefan-Boltzmann result.

However, it is not completely clear if this result is pointing to a weakly or a strongly coupled regime of the deconfined phase. In the case that at temperatures close to the critical temperature $T \geq T_c$ the system remains strongly coupled a new paradigm of quark-gluon plasma will enter the scene, the strongly coupled quark-gluon plasma (sQGP). It should describe a liquid of deconfined quarks and gluons, and not a gas. Later on we will see some experimental results that seem to point in that direction.

So far we have only considered QCD at vacuum and at finite temperature but one can also introduce finite chemical potential and see how the picture changes. We can start examining the zero temperature, finite μ_B case. The initial ground state is the vacuum. As the chemical potential is increased the situation remains the same up to a critical value for which the appearance of bound nucleons in the ground state is favored. The baryon density becomes finite $n_B \neq 0$ for $\mu_0 \simeq 922$MeV. It corresponds to a first order phase transition that is expected to persist at finite temperature and finally end up in a critical point. If one continues increasing the chemical potential, hence the baryon density, at fixed low temperature, a phase transition is again expected from a phase in which matter exists in the form of nucleons to a phase described in terms of quarks, the so-called *color superconductor*, for which diquark condensates are formed. These very high baryon densities are relevant for the physics of compact neutron stars.

The case of finite temperature, finite chemical potential is more difficult to treat. Lattice simulations, proven so useful for finite temperature and $\mu_B = 0$, have very deep problems when dealing with finite chemical potential, though some improvements have been made that let one go to at least small values of μ_B [2]. Using that improvements, the crossover found at zero chemical potential is expected to extend to finite density for small values of μ_B and smoothly connect to a critical point in the (T, μ_B)-phase diagram. For larger values of the chemical potential, the phase transition is expected to be a first order phase transition.

In figure 1.2 the QCD phase diagram is shown as contemporary understood. We are interested in studying the possible sQGP appearing at small μ_B. Nowadays, this region of the phase diagram is being experimentally tested. Let us now comment what such experiments tell us about the matter phase just above the critical temperature.

[2] See for instance [16] and references therein for a summary of such methods.

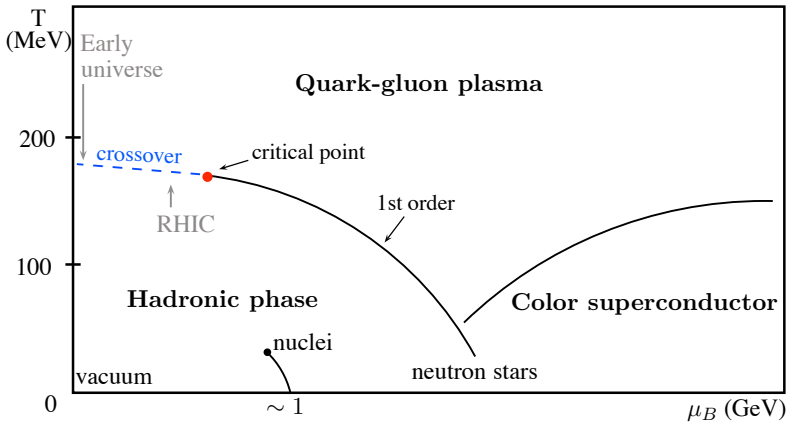

Figure 1.2: *Scheme of the QCD phase diagram.*

RHIC and the sQGP.

The plasma phase of QCD is explored at RHIC, where head-on collisions of gold nuclei at center of mass energy of order ~ 200 GeV/nucleon lead to the production of a tiny drop of quark-gluon plasma. Following [17], assuming thermalization, it is possible to prove that this energy will produce an energy density in the central region of the collision that is above the critical density, given by the density inside the hadrons, thus it is enough to deconfine the constituents in a plasma state. A comparison with the energy density found using lattice simulations in [13], suggests that the central region reaches a temperature about $T \sim 200$MeV, that from the analysis above is expected to be sufficient for QGP formation. The various stages of the collision are depicted in figure 1.3.

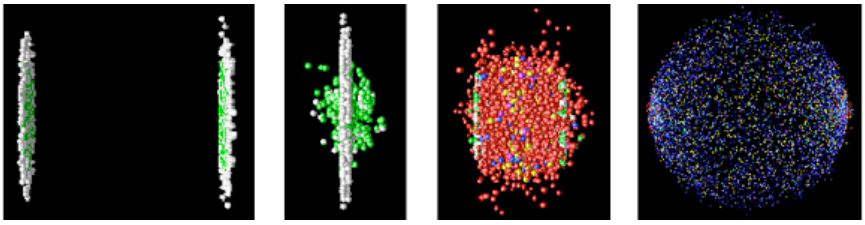

Figure 1.3: *The flattened ions due to relativistic effects approach each other. In the collision, part of the energy is transformed into heat and particles. For energetic enough collisions, the hadrons 'melt' and quarks and gluons are liberated: QGP drop in the central region. Expansion and cool down drive the system back to the hadronic phase. Figure from [18].*

The nuclei are accelerated to velocities corresponding to a Lorentz factor $\gamma \sim 100$, thus they are highly contracted in the direction of motion. In off-center collisions, the overlap region between the two flattened 'pancakes' is almond-shaped. In the initial inelastic collisions between nucleons, many particles are liberated in the high matter density medium, thus they can rescatter several times, leading to a very hot and dense 'fireball'

in which quarks and gluons are freed. This fireball then thermalizes through collisions between the particles, leaving us with a drop of QGP that can be well described in terms of hydrodynamics [17]. Finally, expansion and cooling drive the system to temperatures below the deconfinement T_c and hadronization of the plasma occurs. This effect implies the production of the jets of hadrons that are actually detected. Information about the fireball must be inferred from the emitted hadrons.

Hydrodynamics seem to provide a good description of the formed plasma (thermalized fireball), but in order to extract information from data some inputs are needed. A crucial one is the initial time from when on we expect the system to be well described by hydrodynamics. There are three contributions that must be taken into account from the impact of the two nuclei. The first one is the time scale of the collision. Its shortest value estimated as the overlapping time between the pancakes, turns out to be $t_{\text{min}} \sim 0.14$ fm/c. The fireball has a formation time associated to the creation of the large amount of particles that form it, that is expected to be about $t_{\text{form}} \sim 0.35$ fm/c. The last contribution comes from the thermalization time of the fireball. It is the hardest one to estimate. After thermalization, the system is expected to be described by a thermal distribution governed by collective excitations. Matching the data to the corresponding collective parameters coming from hydrodynamic simulations leads to a very fast thermalization, estimated to be $\tau_{\text{therm}} \sim 0.6-1.0$ fm/c. In section 1.3 we will briefly have a look at plasma hydrodynamics.

In off-center collisions there is an anisotropy effect in the formation of the fireball due to the almond-shape of the overlap region between the colliding nuclei. The production of particles is affected by the shape of the overlap region. Interactions between the produced particles generate a gradient of pressure larger in the collision direction than in the transverse one. This effect translates into an anisotropy in the distribution of transverse momenta. In principle, the anisotropy can be washed out by free streaming or result in a non uniform distribution of detected particles with respect to the interaction plane. Experimental data signal that the collective flow suffers the presence of pressure gradients that push the particles more in some directions, generating the so-called *elliptic flow*. The angular distribution of detected particles can be parametrized in terms of the elliptic flow parameter v_2. The experimental results for such parameter can be compared with hydrodynamic simulations parametrized by the shear viscosity to entropy ratio η/s [19]. Matching the measured parameter with hydrodynamic models seem to imply a very small shear viscosity, like the one of an almost perfect fluid [20–23]. This result supports the picture of a sQGP liquid rather than the description as a weakly interacting gas of quasi-particles.

Of course, many other properties of the QGP can be studied experimentally. However, performing theoretical predictions of such properties is very hard. The strongly coupled regime in which the plasma seems to be makes it compulsory to find non-perturbative

computational tools in order to give a reliable description of this new phase of QCD. Lattice simulations do its best for static properties but typically fail if a dynamical description is required. After thermalization one can try to exploit the hydrodynamic nature of the evolution, but at the end of the day one has to face the computation of correlators in a strongly coupled system, so the problem arises again.

Our proposal is to use the gauge/gravity duality, which gives a description of strongly coupled field theories in terms of classical supergravity. We will see in the next chapter that the correspondence typically involves a super Yang-Mills theory (SYM) in the gauge side. One can argue that SYM and QCD are very different theories and in fact they are, for instance, SYM is conformal, supersymmetric and not confining whereas QCD has a running coupling, is not supersymmetric and does confine. But this differences get diluted when one considers both theories at finite temperature, more concretely at RHIC temperatures, slightly above the critical temperature. Then, none of them is confining, nor supersymmetric, nor conformal and both display Debye screening and can be strongly coupled. Certainly, there are still differences in the matter composition and in some parameters, but there are strong similarities and one can expect that the AdS/CFT correspondence can help to gain some insight into real world sQGP.

1.2 Quantum phase transitions

There is another branch of physics that provides us with strongly correlated systems to which usual field-theoretical tools cannot be applied: quantum critical dynamics. There are more condensed matter examples that exhibit intrinsic strongly interacting behavior besides quantum critical systems. However, one reason for paying special attention to this kind of materials is that very simple holographic duals can be constructed to model their main characteristics, making the application of the holographic tools much easier. On the other hand, there are many examples of real materials that have been studied experimentally and that exhibit quantum criticality, so in principle they also give an arena in which the correspondence can be experimentally checked.

Within the large number of quantum critical systems in the market, let us center on non-conventional superfluids and superconductors, that are not described by the well established condensed matter paradigms. Superconducting materials are usually layered in the three dimensional crystal and couplings between layers are negligible, thus the physics is effectively two dimensional. For that reason we will focus on $2+1$-dimensional systems and on second order phase transitions, typical for superconducting-insulator transitions[3]. Let us start reviewing what is a quantum critical theory.

[3] A general discussion on quantum phase transitions can be found in [24].

Quantum criticality.

A quantum phase transition is a phase transition that takes place at zero temperature. The change between different phases of matter depends on the value of some physical parameter, as pressure, doping or magnetic field, and is driven by quantum fluctuations rather than thermal fluctuations. The quantum critical point is not necessarily the zero temperature limit of a finite temperature phase transition, in fact, it can become a crossover at finite temperature. Moreover, the Coleman-Mermin-Wagner-Hohenberg theorem [25–27] states that in $2+1$ dimensions there cannot be spontaneous breaking of continuous symmetries at finite temperature [4].

At $T = 0$ but away from the quantum critical point, the system is characterized by two quantities: the energy scale that measures the fluctuations about the ground state (or mass gap) and the coherence length that measures the scale over which correlation is lost. Typically, at the critical point we expect the energy to vanish and the coherence length to diverge with some scaling properties. The system becomes scale invariant and can be described in terms of an effective scale invariant field theory: the quantum critical theory. In general, the scaling of energy and length do not need to be inversely related and different relations correspond to different condensed matter systems. We are interested in a particular case in which the quantum critical theory is Lorentz invariant, thus time and space are going to scale in the same way.

Quantum critical points dominate a whole region in the phase diagram away from the quantum phase transition. The so-called quantum critical region is the finite temperature region of the diagram characterized by the requirement that the deformation away from critically due to some energy scale is small compared with the deformation due to finite temperature. The key observation is that the effective scale invariance at the critical point extends to the critical region thus the system there can be described by the generalization to finite temperature of the effective scale invariant quantum critical theory.

Figure 1.4 illustrates the typical phase diagram of a system that undergoes a quantum phase transition. The region between the dashed lines is the quantum critical region, that for a $2+1$-dimensional system is known to be described by a conformal field theory CFT_3. Notice that the imprint of the critical point grows as the temperature is increased. Of course, the system can also undergo thermal phase transitions or crossovers away from the critical point and outside of the QCR. Different low temperature phases will be separated in the phase diagram by the quantum critical region.

There are many physical examples of quantum critical systems whose quantum criti-

[4] In some $2+1$-dimensional theories it is possible to have a Berezinsky-Kosterlitz-Thouless transition, that is an infinite order phase transition. Normal second order phase transitions are only allowed when fluctuations are strictly suppressed. In chapter 6 we have an example of such transition.

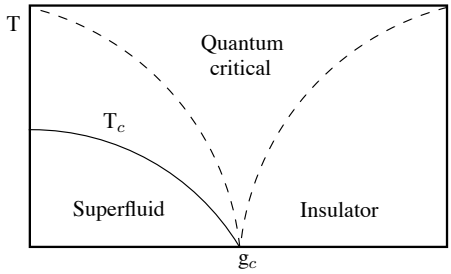

Figure 1.4: *Typical phase diagram near a quantum phase transition. Solid line denotes a possible thermal phase transition or crossover between the two low temperature phases, which are also separated by the scale invariant region (QCR) delimited by the dashed lines.*

cal theory is strongly coupled and whose phase diagram is basically given by figure 1.4. For instance, $2+1$-dimensional antiferromagnets and boson Hubbard models have both a quantum phase transition between an ordered and a disordered low temperature phases. In the first case, the phase transition between coupled pairs of spins and decoupled dimers is driven by the ratio between the two different strengths for neighbor interactions (see for example [28]). In the second case, the phase transition corresponds to a superfluid-insulator transition induced by tunning the ratio between repulsion and hopping interactions of the bosons [29].

One can try to exploit the proximity to a quantum phase transition to describe the dynamics of condensed matter systems for which a weakly interacting description is not valid, at least close to the quantum critical region. For the case of superfluid-insulator transitions, a theory of quantum critical transport has been developed in [30,31], based on weak coupling perturbative analysis. However, this theory is only valid in a small region of the parameter space and cannot be generalized, thus a general theory of transport in strongly interacting superfluids is lacking.

Another example for which quantum phase transitions are believed to be relevant is the description of superconducting-insulator transitions in thin metallic films, whose effective description is again $2+1$-dimensional. Common superconductors are described by BCS theory [32], where charged fermions condense forming Cooper pairs due to an attractive interaction between quasiparticles that is mediated by phonons and becomes strong at very low energies [33]. But there are examples in nature of superconducting materials that do not fit in this description. This is the case of cuprate high T_c superconductors, whose typical phase diagram is depicted in figure 1.5.

Typically, the parent compound of a cuprate superconductor is not superconductor but an antiferromagnetic insulator. When it is doped, by replacing some atoms in the lattice of the layer, it can turn into a superconductor at low temperatures. Over doped high temperature superconductors behave as Fermi liquids above the critical temperature,

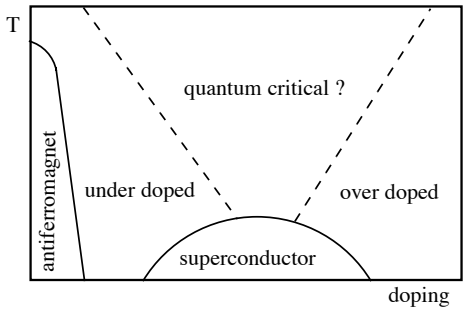

Figure 1.5: *Schematic phase diagram of a cuprate superconductor. The solid lines denote thermal phase transitions. The dashed lines delimit a possible QCR in case that there is a quantum critical point beneath the dome.*

thus they have an effective description in terms of weakly interacting quasiparticles. The phase transition appearing when the temperature is lowered is fairly well described by the BCS theory and the Cooper pairing mechanism. On the contrary, under doped high T_c superconductors are expected to be described by strongly interacting degrees of freedom and it is still not clear which is the correct description just above the superconducting to normal phase transition. It is expected that electrons remain in bound states and disordering of the phase of the condensate is involved, since such a transition takes place from a ordered phase to a disordered one [34]. The under doped region is usually refereed to as pseudogap. It is also expected that the system has a quantum critical point hidden under the superconducting dome in the phase diagram [35,36]. If there is such a quantum critical point, the quantum critical region (between dashed lines in figure 1.5) should describe the so-called strange metal state. This state experimentally shows an unexpected resistivity, which is linear with the temperature. It seems reasonable that the hypothetic quantum phase transition is important to describe the dynamics of high T_c superconductors in the under doped and in the strange metal regions.

Therefore, quantum critical physics plays an important role in the understanding of some strongly coupled systems, in particular for some superfluid/superconductor-insulator transitions, but they are certainly not enough to determine the dynamics of such systems. One can think that lattice simulations might be useful since many superconducting materials are actually crystals, so discretization appears naturally. But as in the case of strongly coupled plasmas above, it is a very hard task to deal with non-equilibrium physics, so lattice methods will not be a powerful tool to get information related to quantum critical transport either. In chapters 2 and 3 we will see that the AdS/CFT correspondence provides us with a new toolkit for studying the dynamics of strongly interacting systems and that it is possible to construct holographic models of superfluidity/superconductivity that, though they are quite vanilla models, reproduce the most representative characteristics of such systems. But, what are the defining properties of superfluids and superconductors?

Superfluids and Superconductors.

Superconductivity and superfluidity show up in condensed matter physics as the low temperature phase of disordered to ordered phase transitions. The ordered phase appears as an instability of the vacuum under the formation of a condensate, thus under spontaneous symmetry breaking of some gauge or global symmetry of the system [5].

Superfluidity is associated with a global $U(1)$ symmetry that is spontaneously broken, thus a massless Goldstone boson is present in the broken phase. The simplest example in which this happens is the complex ϕ^4 theory,

$$\mathcal{L} = \partial_\mu \phi^* \partial^\mu \phi + m^2 |\phi|^2 + \lambda |\phi|^4 \,. \tag{1.4}$$

The Lagrangian is invariant under global transformation of the phase of the field $\phi = \varrho e^{i\varphi}$. If $m^2 < 0$, the scalar field can take a non trivial expectation value and the symmetry will be spontaneously broken by fluctuations. The field φ becomes a massless field in the Lagrangian, as expected from the Goldstone mechanism. Following Landau's theory of superfluidity one expects that the broken phase has a two fluid description, since not all the system develops superfluidity at the same time. This implies that there are two sets of transport coefficients, those related to the normal phase, also present in the broken phase, and those related to transport in the superfluid component. We will comment a bit on these coefficients in the next section. The main characteristics of superfluids are then the appearance of a new massless boson (the Goldstone), a second sound velocity and of course the absence of resistance to flow.

On the other hand, superconductivity is associated with the spontaneous symmetry breaking of a gauge $U(1)$ symmetry, thus with a Higgs mechanism. This implies the appearance of a massive photon in the broken phase. Promoting the above Lagrangian to have a gauge $U(1)$ symmetry under local transformations of the phase of ϕ,

$$\mathcal{L} = (\partial_\mu + iqA_\mu)\phi^* (\partial^\mu - iqA^\mu)\phi + m^2 |\phi|^2 + \lambda |\phi|^4 - \frac{1}{4} F^2 \,, \tag{1.5}$$

one can again have a non trivial expectation value for the scalar and the symmetry will be spontaneously broken. Now writing the field has $\phi = \langle \phi \rangle + (\phi_1 + i\phi_2)/2$ it is possible to gauge away the second field ϕ_2 and end up with a Lagrangian in which there is still a real massive scalar but also the gauge field becomes massive. Considering a static scenario and assuming that the fluctuations on the field are very small (something expected at low temperature), the current will be given by the London equation $\vec{j} = -2q \langle \phi \rangle \vec{A}$. Since the electric field is $\vec{E} = -\partial_t \vec{A} = 0$, combining the Ohm's law $\vec{E} = R\vec{j}$ and the London equation one finds the well known characteristic of superconductors: $R = 0$ zero resistance to conduct electricity, thus an infinite DC (zero frequency) conductivity. The

[5] For a detailed explanation on the features of superfluids and superconductors see [37] and [38].

other characteristic of superconductivity is the Meissner effect, the expulsion of magnetic fields from the superconductor. It is a consequence of having a massive photon in the broken phase. It can be easily deduced taking the curl of Ampere's law $\vec{\nabla} \times \vec{B} = \vec{j}$ combined again with the London equation. The result is an equation for the magnetic field,

$$\nabla^2 \vec{B} = 2q \langle \phi \rangle \vec{B} \,, \tag{1.6}$$

whose solution, in one spatial direction, is given by $B_x = B_0 \mathrm{e}^{-kx}$, where $k = \sqrt{2q \langle \phi \rangle}$. Thus the magnetic field only penetrates the sample a finite distance, it exponentially decays inside the superconductor. Its characteristic penetration depth is $1/k$, and it is easy to show that k is actually the mass acquired by the photon.

Photons can be neglected when the electromagnetic interaction is weak or when it is screened in the charged medium. In such cases, one can consider that the effective degrees of freedom are charged particles, not photons, thus effectively the electromagnetic symmetry can be treated as a global symmetry. This implies that the underlying physic of superfluids and superconductors will be effectively the same. Therefore, the main characteristic of superfluid/superconducting-insulator transitions that we are going to take into account are the formation of a spontaneous symmetry breaking condensate, the appearance of a Goldstone boson and new transport coefficients in the broken phase and infinite conductivity at zero frequency. In chapter 6 we give a concrete holographic realization of these properties.

1.3 Linear response and Hydrodynamics

In the previous two sections we have seen two very different systems of non-perturbative nature for which the usual field-theoretical methods are not applicable and for which known non-perturbative approaches are not enough to describe their dynamics and transport. In order to study the transport physics of any thermal system one shall study the evolution of propagating fluctuations on such system. In a thermal medium, properties of elementary particles are modified since they are 'dressed' by their interactions and one should talk about collective modes. These collective excitations or quasiparticles, are characterized by a mass and a damping rate. The dispersion relation of collective modes is related to the transport coefficients of the theory.

Evolution of collective excitations is given by the response of the medium to small external perturbations, where small is meant for perturbations that do not change significantly the state of the system. In this near-equilibrium situation, linear response theory is enough to determine the time evolution of such fluctuations. Consider the time evolution of a state $|\Psi_{\mathrm{S}}(t)\rangle$ in a quantum system where we introduce a small perturbation that can be expanded in terms of a potential term $V_{\mathrm{H}}(t)$. The subscripts S and H stand for the

Schrödinger and Heisenberg pictures. In linear approximation, the state in the perturbed system is

$$|\bar{\Psi}_{\rm S}(t)\rangle = {\rm e}^{-iHt}\left(1 - i\int_{t_0}^{t} {\rm d}\tau V_{\rm H}(\tau) + \dots\right)|\Psi_{\rm S}(0)\rangle\,, \tag{1.7}$$

where bars refer to states in the perturbed system. Of course, if one switches off the perturbation, unperturbed evolution is recovered. The effect of the perturbation on an observable is given by the subtraction

$$\delta\langle\mathcal{O}(t)\rangle = \langle\bar{\Psi}_{\rm S}(t)|\mathcal{O}|\bar{\Psi}_{\rm S}(t)\rangle - \langle\Psi_{\rm S}(t)|\mathcal{O}|\Psi_{\rm S}(t)\rangle\,. \tag{1.8}$$

From the relation between the state suffering the perturbation and the initial state, the linear response in the operator $\mathcal{O}$ is

$$\delta\langle\mathcal{O}(t)\rangle = -i\int_{t_0}^{\infty} {\rm d}\tau\langle\Psi_{\rm H}|\,\theta(t-\tau)\,[\mathcal{O}_{\rm H}(t), V_{\rm H}(\tau)]\,|\Psi_{\rm H}\rangle + \dots\,. \tag{1.9}$$

Therefore the linear response is given by the retarded commutator of the perturbation and the operator. An special case is this in which the perturbation is given by an external source like $V(\tau) = \int {\rm d}^3\xi j(\tau,\boldsymbol{\xi})\mathcal{O}_{\rm S}(\boldsymbol{\xi})$. In such a case, the linear response reduces to the convolution of the source with the retarded two-point Green function

$$\delta\langle\mathcal{O}(t,\mathbf{x})\rangle = -\int {\rm d}\tau{\rm d}^3\boldsymbol{\xi} G_{\rm R}(t-\tau,\mathbf{x}-\boldsymbol{\xi})j(\tau,\boldsymbol{\xi})\,. \tag{1.10}$$

Of course, one should have expected that the response is given by the retarded correlator and not any other known thermal correlator since causality has to be satisfied. As we will see in chapter 3, different kind of sources are related to different effects on the plasma. For instance, sources localized in time will involve dissipation, how energy is lost in the system as a function of time, whereas periodic sources localized in space will involve absorption, related with spatial correlations in the system. There can also be diffusion effects when conserved charges are present, the charge cannot dissipate but it spreads over the medium. In such case, the collective excitations associated with that conserved charges are massless and will govern the late time evolution of the perturbed system, that will be described in terms of hydrodynamics.

Hydrodynamics.

Hydrodynamics gives an effective description of the near-equilibrium real-time macroscopic evolution of a given system, provided that the evolution is both slow in time and space compared to the typical scale set by the underlying microscopic theory. For thermal quantum field theories as the ones we are interested in, this microscopic scale is given by the inverse of the temperature. Therefore, the hydrodynamic description will be valid when the characteristic energy and momentum of the involved processes are small compared to

the temperature of the system, i. e. $(\omega, k) \ll T$, or equivalently it describes the dynamics at large time scales and large distances. It is formulated in terms of a few relevant fields, their equations of motion and the so-called constitutive relations. The reason for not using an action principle and work directly with the equations of motion is the dissipative character of thermal media. The relevant fields, or hydrodynamic fields, are associated to the conserved charges of the system, since they can fluctuate at arbitrarily long times. In fact, the existence of a hydrodynamic description relies on the existence of this kind of modes. The equations of motion are then the continuity equations for the conserved charges. The constitutive relations encode the dissipative behavior and relate the currents with the characteristic parameters of the system. As an effective theory, we can make an expansion order by order in gradients of these parameters, namely, in temperature and local fluid velocity gradients. Here we just consider first order hydrodynamics.

Consider the simple example of a system with a conserved charge. The current conservation equation and the constitutive relation are

$$\partial_\mu j^\mu = 0\,, \tag{1.11a}$$

$$j^\mu = \rho u^\mu - D\left(g^{\mu\nu} + u^\mu u^\nu\right)\partial_\nu \rho = \rho u^\mu - D P^{\mu\nu}\partial_\nu \rho\,, \tag{1.11b}$$

where ρ is the charge density, u^μ is the local fluid velocity and D is the diffusion constant. The coefficients in the constitutive relation, like D, are the so-called transport coefficients of the theory. They can be deduced from the retarded two-point correlation functions that determine the response in the corresponding fields. In particular, transport coefficients are given in terms of the Green-Kubo formulas. For instance, the diffusion constant will be given by the current-current correlator,

$$D \propto \lim_{\omega\to 0}\frac{1}{\omega}\,\mathrm{Im}\,G_{\mathrm{R}}^{j\,j}(\omega, \mathbf{k}=0)\,. \tag{1.12}$$

One can also find the location of the poles of the retarded Green functions looking for normal modes that are plane waves. The solutions give us the dispersion relation of the corresponding collective excitations that in this low frequency low momentum limit are called *hydrodynamic modes*. The dissipative effects imply that the dispersion relations allow complex $\omega(\mathbf{k})$. For the case of charge diffusion,

$$\partial_t \rho - D\nabla^2\rho = 0\,, \tag{1.13}$$

there is a pole in the current-current correlator at $\omega = -iDk^2$. This particular mode encodes the dissipative behavior of the charge in the system.

More interesting is the case of transport coefficients associated to the energy-momentum conservation. The conservation equations and first order constitutive relations are

$$\partial_\mu T^{\mu\nu} = 0\,, \tag{1.14a}$$

$$T^{\mu\nu} = T^{\mu\nu}_{\mathrm{ID}} - P^{\mu\alpha}P^{\nu\beta}\left[\eta\left(\partial_\alpha u_\beta + \partial_\beta u_\alpha - \frac{2}{3}g_{\alpha\beta}\partial_\lambda u^\lambda\right) + \zeta g_{\alpha\beta}\partial_\lambda u^\lambda\right]\,, \tag{1.14b}$$

where the transport coefficients are the shear viscosity η and the bulk viscosity ζ. If one considers perturbations with momentum in the direction $\mathbf{k} = (0, 0, k)$, the hydrodynamic modes appearing as poles of the correlators between different elements of the energy-momentum tensor can be computed in the same way as that for the charge density example. There are two different types of hydrodynamic modes for the stress-energy tensor: the *shear* modes, related with diffusion of the momentum in the transverse directions, and the *sound* modes, related with longitudinal propagation of the energy density.

The *shear* modes correspond to fluctuations of T^{0i} and T^{3i} where $i = 1, 2$ labels the transverse directions. Both are related by the constitutive equation, so the evolution can be encoded in one of them and it turns out that it satisfies a diffusive equation similar to (1.13)

$$\partial_0 T^{0i} - \frac{\eta}{\epsilon + P} \partial_3^2 T^{0i} = 0 \,. \tag{1.15}$$

The dispersion relation for the shear mode is given by

$$\omega = -i \frac{\eta}{\epsilon + P} k^2 \,. \tag{1.16}$$

The *sound* modes correspond to fluctuations of T^{00}, T^{03} and T^{33}. The three fluctuations are related by two conservation equations now. They can be diagonalized leading to a dispersion relation for the sound mode

$$\omega = v_s k - \frac{i}{2(\epsilon + P)} \left(\frac{4}{3} \eta + \zeta \right) k^2 \,, \tag{1.17}$$

where v_s is the sound velocity at which this sound wave propagates and is given by $v_s^2 = \frac{\mathrm{d}P}{\mathrm{d}\epsilon}$, where the energy density is defined by $\epsilon + P = sT$.

The hydrodynamic modes are massless modes in the sense that their dispersion relations satisfy $\lim_{k \to 0} \omega = 0$. We have already seen that they appear associated to conserved charges of the system. It is also known that the phases of order parameters of second order phase transitions behave as hydrodynamic modes. So the massless Goldstone boson that appears at spontaneous continuous symmetry breaking should also be identified as a hydrodynamic mode.

For the simple model of superfluidity given by (1.4), the hydrodynamic equations of an ideal relativistic superfluid were worked out in [39]. In addition to the energy-momentum tensor and the $U(1)$ current conservation, the evolution of the condensate phase φ satisfies a Josephson equation. The equations of motion are then

$$\partial_\mu T^{\mu\nu} = 0 \,, \tag{1.18a}$$

$$\partial_\mu j^\mu = 0 \,, \tag{1.18b}$$

$$u^\mu \partial_\mu \varphi - \mu = 0 \,, \tag{1.18c}$$

where μ is the chemical potential associated to the charge density n of the conserved current. These equations form a coupled system, since the constitutive relations for the current and the energy-momentum tensor are modified in the presence of a condensate. From the equation of state, the conjugate variables of the hydrodynamic parameters T, μ, φ are

$$\mathrm{d}P = s\mathrm{d}T + n\mathrm{d}\mu + V^2\mathrm{d}\left(\frac{1}{2}(\partial_\mu\varphi)^2\right) , \tag{1.19}$$

where V^2 is the condensate density associated to the chemical potential for the order parameter φ. The constitutive relations are

$$T^{\mu\nu} = (\epsilon + P)u^\mu u^\nu + Pg^{\mu\nu} + V^2\partial^\mu\partial^\nu\varphi\,, \tag{1.20a}$$

$$j^\mu = nu^\mu + V^2\partial^\mu\varphi\,, \tag{1.20b}$$

where the energy density is now defined by $\epsilon + P = sT + n\mu$. This supports the picture of a two fluid model in the superfluid phase. The current and the stress-energy tensor have a *normal fluid* component given by the ideal fluid current and stress tensor but they also have a field contribution due to the motion of the condensate that leads to the *superfluid* component. The velocity u^μ is interpreted as the fluid velocity of the normal component, that in the two fluid model is the only one carrying entropy. It is possible to study fluctuations in this superfluid model to find the hydrodynamic modes. In the broken phase, two different sound modes appear with dispersion relations $\omega^2 = v_s^2k^2$ and $\omega^2 = v_2^2k^2$. The propagation velocities are given by [75]

$$v_s^2 = \frac{\partial P}{\partial\epsilon}\,, \tag{1.21a}$$

$$v_2^2 = V^2\left[\left(1 + \frac{n\mu}{sT}\right)\left(\frac{\partial^2 P}{\partial\mu^2} - \frac{n + \mu V^2}{s}\frac{\partial^2 P}{\partial T\partial\mu}\right)\right]^{-1} . \tag{1.21b}$$

Hence, v_s is the sound velocity of the normal component whereas v_2 is interpreted as the velocity of the so-called second sound of the superfluid component. Of course, in the absence of a condensate, $V = 0$, the second sound mode disappears and its velocity vanishes. In chapter 6 we will come back to the second sound of superfluids and using holographic techniques we will be able to take into account also the dissipative behavior of the thermal medium, that here has been neglected.

Chapter 2

The AdS/CFT correspondence

The *Holographic principle* states that a theory of quantum gravity in a region of space can be described in terms of a non-gravity theory living on a lower dimensional space that has one or less degrees of freedom per Planck area [40, 41]. The concept of holography is well known from the study of black hole physics, where the entropy given by all the possible microstates of a black hole is determined by the area of its horizon, leading to the celebrated Bekenstein-Hawking bound [42].

A decade ago, Maldacena conjectured that superstring theory (or supergravity in the low energy limit) in a negatively curved space is equivalent to a certain class of conformal field theories living on the boundary of this space, yielding the so-called AdS/CFT correspondence [43]. The strong version of this duality states that a *quantum gravity* theory in an asymptotically anti-de Sitter spacetime is equivalent to a *quantum field* theory in a lower dimensional space. Hence, the correspondence can then be interpreted as a *holographic* realization of quantum gravity.

A connection between gauge theories and strings was first proposed by 't Hooft [44] in an attempt to understand strong interactions giving an approximate qualitative description of the QCD flux tubes in terms of effective strings. The AdS/CFT correspondence is a precise implementation of this idea as an exact duality in terms of real strings.

In this chapter we briefly present the basic properties of the original Maldacena conjecture and also some of the generalizations of the duality. In particular we show how to implement finite temperature and finite chemical potential, achieved by the introduction of a black hole in the geometry and by the addition of a Maxwell field coupled to gravity, respectively. We emphasize those aspects of the duality that are more relevant for the applications considered in this thesis. More detailed explanations about the original proposal and its extension to finite temperature can be found in the original papers [43, 45, 46] and in the exhaustive reviews [47, 48] and references therein. For the case of finite chemical potential with applications to condensed matter systems see the reviews [49, 50].

2.1 The Conjecture

Before describing the concrete example worked out by Maldacena, let us present two different ways in which the connection between quantum gauge theories and gravity theories shows up. First we will review the 't Hooft argument, that claims that gauge theories have an effective description in terms of strings in some certain limits. Afterwards, departing from a string theory scenario, which incorporates gravity in a natural way, we will see that it is possible to include gauge interactions through the addition of new objects called Dp-branes and derive the duality in a more straightforward way.

Large N and strings.

In [44] 't Hooft proposed that gauge theories could be described in terms of 'string' theories. Although the analysis suggested a duality between both theories, there were no proposals for an explicit formulation of such duality. The first problem that arises in doing so is that there are no consistent phenomenologically relevant string theories in less than ten dimensions.

In order to see how this duality arises we can consider a $SU(N)$ Yang-Mills theory with schematic Lagrangian

$$\mathcal{L} \sim \frac{1}{g_{\mathrm{YM}}^2} \mathrm{Tr}\left[(\partial\Phi)^2 + V(\Phi)\right] . \tag{2.1}$$

In the large N limit, the effective coupling parameter of such theory is the 't Hooft coupling $\lambda = g_{\mathrm{YM}}^2 N$. Eventually we will take the *'t Hooft limit*, i. e. infinitely large number of colors $N \to \infty$ while keeping the 't Hooft coupling fixed and finite.

The fields Φ transform in the adjoint representation of the gauge group and can be written in matrix notation, so Feynman diagrams can be written in a double line notation in which any adjoint field is represented by a direct product of a fundamental and an anti-fundamental field, see figure 2.1. In this double line representation, we can order the diagrams as an expansion in powers of N by noticing that each vertex introduces a factor $1/g_{\mathrm{YM}}^2 = N/\lambda$, propagators are proportional to $g_{\mathrm{YM}}^2 = \lambda/N$ and each closed line sums over the index in the loop so gives a factor of N. The diagrams can be viewed as the simplicial decomposition of two-dimensional surfaces: the loops represent faces and the propagators edges. The order on powers of N of a diagram with E edges, V vertices and F faces is

$$N^{F+V-E}\lambda^{E-V} = N^{\chi}\lambda^{E-V} , \tag{2.2}$$

where $\chi = F + V - E = 2 - 2g$ is the Euler character and g is the genus of the compact, closed and oriented Riemann surface described by the diagram.

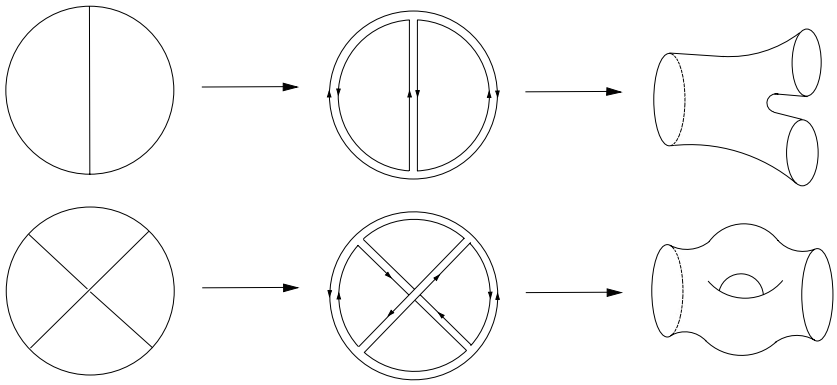

Figure 2.1: *Feynman diagrams (left) rewritten in double line notation (middle) interpreted as Riemann surfaces (right).*

Therefore, the $SU(N)$ Yang-Mills theory diagrammatic expansion in the 't Hooft coupling can be interpreted as an expansion in Riemann surfaces with Euler character equal to the power of N in the corresponding diagram, see figure 2.1. It is clear that the larger the genus the more suppressed the diagrams, so in the 't Hooft limit only the planar diagrams ($g = 0$) will contribute.

The amplitude of any process in this gauge theory is given by a double expansion in the number of colors and in the coupling, leading to a partition function

$$\log Z = \sum_{g=0}^{\infty} N^{2-2g} f_g(\lambda)\,, \tag{2.3}$$

where $f_g(\lambda)$ represents the sum over all the possible Feynman diagrams with a given genus. This expression is the same that one finds when performing a perturbative expansion of a closed oriented string theory upon identification of the string coupling constant to be $g_{\rm s} \propto 1/N$. In the limit of large N the string theory is weakly interacting and since the genus can be interpreted as the number of string loops, the planar diagram description of the gauge theory can be identified with the tree level of the string theory.

This 'derivation' of the 'duality' is based on perturbation theory and in order to claim that this relation is rigorous one should be able to match also non-perturbative effects on both sides. Another problem is the matching of dimensionality of the gauge and the string theories. Naively one would expect that starting with a 4-dimensional gauge theory one gets a closed string theory living in a 4-dimensional space, but this cannot be the case since string theories are not consistent in less than ten dimensions, so one is forced to include extra-dimensions [51, 52] and guess the string theory. The AdS/CFT correspondence is a realization of this idea, although it appears naturally when one considers strings theories with additional objects, Dp-branes.

Open strings vs. closed strings.

The key point that led to the discovery of the gauge/gravity duality was the identification of the Dp-branes as the full string theoretical description of the supergravity extremal p-branes made by Polchinski [53].

String theories include gravity in a natural way, they contain closed strings whose low energy excitations include a massless graviton and some other fields that amount to the matter content of ten dimensional supergravity. But it is known that string theories can also contain solitonic 'membranes' of different dimensionalities called D(irichlet)-branes.

A Dp-brane is a $p+1$ dimensional object in the ten dimensional spacetime where open strings can end, even when only closed string are allowed to propagate in the bulk (like in type IIB theory). The ends of the strings can move freely on the brane hyperplane, but Dirichlet boundary conditions are imposed on the transverse directions. They are dynamical objects that can fluctuate due to excitations of the open strings. A very nice property of D-branes is that the massless excitations of open strings living on a D-brane are gauge fields in an Abelian gauge group. Non-abelian gauge groups can be obtained with stacks of parallel branes. If one considers N coincident Dp-branes the gauge group living on their world-volume will be $U(N)$, since the endpoints of the open strings can be attached on different branes and all the combinations are possible. Therefore the low energy theory living on the world-volume of a (stack of) branes is a (non-)abelian gauge theory. It is worth to notice that in general this theory will come with a number of supersymmetries that depends on the precise arrangement of branes.

The D-branes are massive objects with tension, or energy density, proportional to $1/g_{\mathrm{s}}$, thus they couple to gravity. This implies that open strings on the brane couple to closed strings on the bulk. The backreaction on the geometry due to the presence of these massive hyperplanes effectively curves the spacetime. It was shown by Polchinski that the low energy limit of Dp-branes are extremal p-branes in supergravity [53]. Black p-branes are massive $p+1$-dimensional solutions of supergravity (gravity with local supersymmetry) analogous to black holes in general relativity. They are called extremal if the area of the horizon goes to zero. So the low energy limit of the string theory with D-branes is supergravity on a spacetime curved by the presence of a heavy source, the extremal p-branes.

We have presented two different pictures of the same configuration, the D-brane cartoon and the curved background cartoon, that of course must be completely equivalent. In general we do not know how to deal with stringy effects, so a natural limit in which compare these two approaches is one where these effects are negligible. This corresponds to the low energy limit, $E \ll l_{\mathrm{s}}^{-1}$.

The action of the system is given by the contribution of the branes, the bulk and the interactions between them. The interactions between brane modes and bulk modes are proportional to positive powers of the gravitational constant $\kappa \sim g_s l_s^4$. Since taking the low energy limit is equivalent to take the string length to zero, the open string sector living on the brane decouples from the close string sector living on the bulk. Moreover, the interactions between closed strings are also proportional to κ, thus the bulk theory is free. If we look know to the massless spectrum, we find that in the low energy limit we have two decoupled theories: a supersymmetric gauge theory living on the stack of branes and free supergravity in the bulk.

On the other hand, we can consider that the system is described by only closed strings in a curved spacetime. The D-branes act as the source that curves the space, generating a throat (near-horizon region) close to their location but asymptotically flat far away from it. From the point of view of an asymptotic observer, any excitation living in the near-horizon region has very small energy due to the redshift suffered when we bring it closer and closer to the branes. So excitations of arbitrary energy in the throat are compatible with the low energy limit when measured by an observer at infinity. In the flat region we will have again free supergravity. This is so because in the low energy limit, bulk excitations have wavelengths large enough to ignore the effect on the geometry of the stack of branes, while excitations in the near-horizon region cannot escape to the asymptotic region. Then finally we end up with free supergravity in the bulk but with closed string theory in the throat.

If we compare the resulting limits and take into account that the departing theory was the same, we can match the free supergravities in the bulk for the two descriptions and also identify the gauge theory on the branes with the string theory on the throat leading to the strong version of the celebrated Maldacena conjecture: *a quantum gravity theory in asymptotically AdS is dual to a quantum gauge theory in its conformal boundary.*

The canonical example.

For the sake of clarity we will center on a concrete example, the original proposal and the simplest realization of the gauge/string duality first found in [43]:
$\mathcal{N} = 4$ $SU(N)$ super Yang-Mills theory in four dimensional Minkowski space is dual to type IIB superstrings theory on $\mathrm{AdS}_5 \times \mathrm{S}^5$ *with N unit of R-R 5-form flux on the sphere.*

Let us consider a stack of N coincident D3-branes in type IIB string theory in flat ten dimensional Minkowski space. The low energy limit world-volume theory on the branes is given by $\mathcal{N} = 4$ $SU(N)$ super Yang-Mills theory in $3 + 1$ dimensions [54, 55]. This theory is conformally invariant with conformal group $SO(4, 2)$ and contains a unique vector multiplet, that consists of a gauge field, four Weyl complex fermions and six real

scalars, so in addition to the conformal symmetry it has a $SO(6)$ R-symmetry that rotates the scalar fields into each other. All the fields are in the adjoint representation of the gauge group and are connected by supersymmetric transformations.

On the other hand, the metric of the D3-branes is given by

$$\mathrm{d}s^2 = \left(1+\frac{L^4}{r^4}\right)^{-1/2} \mathrm{d}x_\mu \mathrm{d}x^\mu + \left(1+\frac{L^4}{r^4}\right)^{1/2} \left(\mathrm{d}r^2 + r^2 \mathrm{d}\Omega_5^2\right) , \tag{2.4}$$

where the coordinates x_μ correspond to the Minkowski space filled by the branes, r is the radial coordinate of the transverse space and the parameter L is proportional to the string length and is defined as

$$L^4 = 4\pi g_\mathrm{s} N l_\mathrm{s}^4 . \tag{2.5}$$

Far away from the location of the branes $r \gg L$ ten-dimensional Minkowski space is recovered since the metric is asymptotically flat. We can instead look to the geometry very close to the brane position. For $r \to 0$ the metric appears to be singular. In the low energy limit, an asymptotic observer sees excitations close to the source very redshifted. The throat can be defined as the region where excitations of arbitrary energy are seen as low energy excitations by this outside observer. The relation between the energy measured at infinity and the proper energy is

$$E_\infty \sim \sqrt{-g_{00}}\, E_\mathrm{p} = \left(1+\frac{L^4}{r^4}\right)^{-1/4} E_\mathrm{p} \;\Rightarrow\quad \text{for}\quad r\to 0\;:\quad E_\infty \sim \frac{r}{L} E_\mathrm{p} . \tag{2.6}$$

Hence the throat or near-horizon region corresponds to $r \ll L$. Notice that in this limit the spacetime is not singular but develops a negative constant curvature. The metric in the near-horizon limit is then

$$\mathrm{d}s^2 = \frac{r^2}{L^2}\left(-\mathrm{d}t^2 + \mathrm{d}\vec{x}^2\right) + \frac{L^2}{r^2}\mathrm{d}r^2 + L^2 \mathrm{d}\Omega_5^2 . \tag{2.7}$$

This metric describes the product space $\mathrm{AdS}_5 \times \mathrm{S}^5$, where the parameter L plays the role of both the anti-de Sitter space radius and the 5-sphere radius. The symmetries of this spacetime are the AdS_5 group of isometries $SO(4,2)$ and the $SO(6)$ rotation group of the sphere. The anti-de Sitter space is the maximally symmetric solution of Einstein's equations with negative cosmological constant.

Following the arguments exposed above, one is tempted to say that these two theories are physically equivalent, though this equivalence has not been proven yet. We do not have a non-perturbative description of string theory and we do not know how to quantize it in a curved space, so we may better consider the correspondence just as a conjecture. Much effort has been made to obtain the spectrum beyond the supergravity approximation and progress has been made for special operators in some limits. For instance, exploiting the integrability of the system the spectrum of large spin operators has been resolved [56–58].

Nevertheless, there are strong indications that the duality should be valid in its strong version coming from the spectrum of some particular operators, supersymmetry protected correlators and in general coupling independent properties.

One can start examining the gauge and global symmetries that of course do not depend on the coupling constants. Coming back to the isometries of $\mathrm{AdS}_5 \times \mathrm{S}^5$, it has spacetime symmetry groups $SO(4,2)$ and $SO(6)$. Superstring theories living on anti-de Sitter have 32 supercharges since the space is maximally symmetric. All these symmetries combine in the super-Lie group $SU(2,2|4)$. The $\mathcal{N}=4$ Yang-Mills theory is conformal so in four dimensions it has a $SO(4,2)$ conformal symmetry group. It also has a R-symmetry group $SO(6)$ due to supersymmetry. $\mathcal{N}=4$ in four dimensional space has 16 supercharges, but the conformal superalgebra doubles the number of supersymmetry generators, giving a total of 32 supercharges. The symmetries again combine in the superconformal group $SU(2,2|4)$. We can finally conclude that gauge symmetries of the gravity side map to global symmetries of the gauge side.

There is still a non-perturbative symmetry shared by both theories. The Montonen-Olive duality states that the $\mathcal{N}=4$ Yang-Mills theory is invariant under $SL(2,\mathbb{Z})$ S-duality transformations acting on the complex gauge coupling $\tau = \frac{\theta}{2\pi} + i\frac{4\pi}{g^2_{\mathrm{YM}}}$, where θ is the instanton angle. In type IIB string theory the same S-duality acts on the axion-dilaton complex coupling $\tau = \frac{\chi}{2\pi} + i\mathrm{e}^{-\Phi}$, where the dilaton field is $\mathrm{e}^{\Phi} = g_{\mathrm{s}}$. Identifying the two complexified parameters, we can extract the relation between the coupling constants of the gauge and the gravity theory to be $g^2_{\mathrm{YM}} = 4\pi g_{\mathrm{s}}$, that can also be found from the Born-Infeld action of the branes.

The key feature of the correspondence that makes it so attractive for applications to strongly interacting systems is that it is a strong/weak duality. The supergravity approximation of string theory is valid when the spacetime is weakly curved, this happens when the radius of curvature L of the AdS space, of the throat, becomes large compared with the string length. On the other hand, a perturbative analysis of the Yang-Mills theory is reliable when the 't Hooft coupling λ is small. From (2.5) and provided the relation between the string and the gauge couplings, we can relate these two parameters that define the perturbative regime on each theory,

$$L^4 = \lambda\, l_{\mathrm{s}}^4\,. \tag{2.8}$$

It is clear that both perturbatively valid descriptions are incompatible, but in fact this is good for our purposes. The supergravity approximation is valid when the 't Hooft coupling goes to infinity, when the field theory is strongly coupled, allowing us to get information of the non-perturbative regime of gauge theories that in general cannot be solved otherwise. Infinite 't Hooft coupling is equivalent to infinite number of colors $N \to \infty$. As we saw before, the large N limit also corresponds to the planar limit of the gauge theory and to

the tree-level string theory. It implies that quantum string loops are $1/N$ corrections in the gauge theory. One can also think about stringy corrections coming from the finiteness of the string length. These are corrections in $\alpha' = l_s^2$ and correspond to $1/\sqrt{\lambda}$ corrections in the field theory.

Therefore, in the *Maldacena limit*, i. e. N, $\lambda \to \infty$, classical supergravity on a weakly curved AdS space and a strongly coupled gauge theory describe the same physical setup.

Another interesting remark concerns the holographic interpretation of the AdS/CFT correspondence. Let us forget about the 5-sphere and write the AdS metric in Poincaré coordinates as

$$\mathrm{d}s^2 = \varpi(z)^2 \left(\mathrm{d}z^2 + \mathrm{d}x_\mu \mathrm{d}x^\mu\right) \quad \text{with} \quad \varpi(z) = \frac{1}{z}\,, \tag{2.9}$$

where $z = L^2/r$ is the new radial coordinate and the coordinates x_μ define the brane hyperplane, thus the field theory spacetime. From the AdS metric written in this way, it is easy to see that the gauge theory lives on $z \to 0$ (or $r \to \infty$), that is the conformal boundary of AdS and in Poincaré coordinates is obvious that this boundary is 4-dimensional Minkowski space. Hence, the gauge/gravity duality is *holographic* in the sense that it relates a gravity theory on some spacetime with a field theory living on its boundary. Moreover, the radial coordinate plays the role of the renormalization group scale from the boundary theory point of view. This can be seen from the relation between energies and distances in the bulk (from now on bulk refers to the interior of the AdS space) and in the boundary given by the warp factor,

$$E = \varpi(z)\, E_\mathrm{p} \quad \text{and} \quad l = \frac{1}{\varpi(z)}\, l_\mathrm{p}\,. \tag{2.10}$$

Then, close to the boundary $z \to 0$, large distances (low energy) bulk phenomena corresponds to short distances (high energy) physics in the boundary theory, i. e. ultraviolet physics, while short distance phenomena deeply in the throat $z \to \infty$, map to large distances physics from the field theory point of view, i. e. infrared physics. This implies that different positions in the bulk correspond to different energy scales in the boundary. The RG-flow is parametrized by the radial coordinate: the supersymmetric Yang-Mills theory regularized in the ultraviolet and living on the boundary of the AdS space flows to the infrared fixed-point going down the throat. The fact that ultraviolet effects on the field theory map to infrared effects on the gravity side is known as the *UV/IR duality* [59].

At this point, it is worth to notice that the holographic formulation of the correspondence can be generalized to any dimension provided that the gravity theory lives in an asymptotically AdS $d+1$-dimensional space and the gauge theory lives on its d-dimensional boundary. Nevertheless, the connection with string theory would imply to find a consistent truncation of string theory or M theory yielding to a consistent supergravity in the desired space and this can be a highly non trivial task. We are interested in applications

of the correspondence to plasma physics in $3+1$ dimensional spacetimes, but also to $2+1$ dimensional condensed matter theories. In the latter case, we will assume that the correspondence holds without worrying about the precise string embedding that brings to the four dimensional gravity theory more than saying that it must come from a dimensional reduction of M-theory on an $AdS_4 \times X_7$ spacetime.

The dictionary.

We have presented the basic features of the AdS/CFT correspondence through a mainly qualitative description, but in order to make the duality a powerful tool we need to know how physical observables of the two theories are related and how to obtain quantitative results.

The natural objects to consider in a conformal field theory are operators and the physical observables are expressed as correlation functions of gauge invariant combinations of them, while supergravity and string theory are formulated in terms of fields.

A variation of the field theory coupling constant is related to a variation of the string theory coupling which in turn is related to changing the expectation value of the dilaton field, $g^2_{\rm YM} \propto g_{\rm s} = {\rm e}^{\Phi}$. As the expectation of the dilaton is set by its boundary condition at the AdS boundary, one can infer a connection between operators in the field theory side and excitations of the string fields subject to boundary conditions. In fact, it is possible to establish a one to one field/operator correspondence and to give a precise prescription for computing correlation functions using the duality [45, 46]. A motivation for such connection comes from considering propagating waves in the full ten dimensional spacetime. A wave coming from asymptotic infinity can be absorbed by tunneling into the throat and then propagating through it. This signal may be thought of as a perturbation of the AdS boundary that propagates into the bulk, so correlators of the gauge field must be related with the response of string theory to propagating fields with boundary conditions at the AdS boundary. The field/operator relation can be read off from the brane action, in which gauge theory operators will appear coupled to boundary values of string fields. For instance, the dilaton couples to ${\rm tr}F^2$ and the R-R scalars to ${\rm tr}F\tilde{F}$, where $F_{\mu\nu}$ is the field strength of the gauge field, the graviton couples to the energy-momentum tensor $T_{\mu\nu}$ of the gauge theory and bulk vector (Maxwell) fields couple to global currents in the dual field theory.

In the spirit of that argument it is natural to identify the generating functional of the partition function of the conformal field theory with the partition function of the classical string theory. Withal, in the supergravity approximation the latter can be substituted by its low energy counterpart, leading to a quantitative formulation of the AdS/CFT

correspondence in the regime of interest that in the Euclidean version reads,

$$\left\langle \mathrm{e}^{\int \mathrm{d}^4x\, \phi_0(x)\mathcal{O}(x)} \right\rangle = \mathcal{Z}_{\mathrm{CFT}}\left[\phi_0\right] \equiv \mathcal{Z}_{\mathrm{string}}\left[\phi\right] \approx \mathrm{e}^{-S_{\mathrm{sugra}}[\phi]}\,, \tag{2.11}$$

where the bulk field ϕ is a classical solution for the supergravity action S_{sugra} satisfying the boundary condition $\phi(z,x) = \phi_0(x)$ for $z \to 0$. It is clear from the above expression that the boundary value of the supergravity field can be interpreted as the source for the insertion of an operator in the gauge theory.

The supergravity equations of motion have two linearly independent solutions with different asymptotic behavior close to the AdS boundary,

$$\phi(z,x) = \phi_0(x) z^{\Delta_-} + \phi_1(x) z^{\Delta_+}\,, \tag{2.12}$$

where $\Delta_+ > \Delta_-$ are the characteristic exponents of the equation. These coefficients depend on the character of the field and on its mass. Generically, the first term corresponds to *non-normalizable* fluctuations close to the boundary and the second term corresponds to *normalizable* ones. The scale invariance of the AdS space under $(z,x) \to D\,(z,x)$ transformations, implies that the fields ϕ_0 and ϕ_1 have to rescale in such a way that the bulk field is invariant what turns out to require that the former transforms as a source and the latter as a vev from the conformal field theory point of view. This actually means that the non-normalizable solutions are dual to the insertion of operators in the gauge theory sourced by the boundary value of such modes, while the normalizable modes are understood as the expectation value of the dual operator. Moreover, the characteristic exponent is related to the conformal weight of the operator $\Delta = d - \Delta_-$, where d is the dimensionality of the gauge theory spacetime, leading to a relation between the mass of the supergravity fields and the conformal dimension of their dual operators [1].

Given the relation (2.11), n-point correlation functions in the Euclidean gauge theory are obtained by taking functional derivatives of the supergravity action with respect to the fields that act as sources,

$$\langle \mathcal{O}(x_1)\mathcal{O}(x_2)\ldots\mathcal{O}(x_n)\rangle = \frac{\delta^n S_{\mathrm{sugra}}}{\delta\phi_0(x_1)\delta\phi_0(x_2)\ldots\delta\phi_0(x_n)}\,. \tag{2.13}$$

Although it has been formulated in Euclidean signature, one can in principle make an analytic continuation to Lorentzian signature. However, in the case of finite temperature, this continuation involves the complete discrete Matsubara frequency spectrum of the Euclidean propagator and it can happen that extracting relevant information of the corresponding real frequencies is very hard or even impossible. Then, a prescription to

[1] It can be the case that both fluctuations are normalizable at the boundary, then one can define two different theories depending on which of the modes is interpreted as the source and which as the vev, that in fact corresponds to different dimensions for the dual operator. This will be the case for the model considered in chapter 6.

compute directly Lorentzian correlators will be needed in order to study dynamical properties of the systems. Since Lorentzian Green functions will be the main computational tool used in this thesis, we reserve the next chapter to present the real-time thermal AdS prescription and some of their features.

2.2 Finite Temperature

So far we have described the correspondence for a very peculiar setup that involves an infinitely strongly coupled gauge theory constrained by supersymmetry and conformal invariance, what makes it a nice scenario in order to check the correspondence but that has a very limited phenomenological interest. Fortunately, one can relax such constraints and generalize the correspondence to non-conformal and non-supersymmetric gauge theories by deforming the AdS geometry or by adding new objects to the setup.

One particular property that is shared by all the systems for which we claimed that the AdS/CFT correspondence might be useful is finite temperature. We devote this section to explain how this can be implemented in a holographic frame and some of the most interesting features of this generalization of the gauge/gravity duality.

Adding a black hole.

It is well known that finite temperature and thermodynamics show up naturally in general relativity in the study of black hole physics. In this sense, it is reasonable to expect that the extension to finite temperature of the correspondence is such that the gravity dual of a thermal field theory lives in an anti-de Sitter black hole background.

If we consider the decoupling limit of the *near-extremal* black 3-branes background, the metric in the near-horizon region reduces to

$$\begin{aligned} \mathrm{d}s^2 &= \frac{r^2}{L^2}\left(-f(r)\mathrm{d}t^2+\mathrm{d}\mathbf{x}^2\right)+\frac{L^2}{r^2}\frac{\mathrm{d}r^2}{f(r)}+L^2\mathrm{d}\Omega_5^2\,, \\ f(r) &= 1-r_{\mathrm{H}}^4/r^4\,. \end{aligned} \tag{2.14}$$

The asymptotic behavior is not modified with respect to the zero temperature case (2.7), but the infrared physics must be affected by the presence of the black hole, with regular event horizon at $r = r_{\mathrm{H}}$. Notice that the above metric describes a planar Schwarzschild-AdS black hole since the horizon is flat. The temperature manifests itself as the Hawking temperature of the horizon T_{H} which in turn is identified with the dual field theory temperature. One way to find it passes through Wick rotate to Euclidean signature and demand the absence of conical singularities. This fixes the period of the compact Euclidean time. The temperature is then identified with the inverse of that period, that in fact leads to thermal probability distributions in the field theory.

We can focus on the 2-dimensional part of the Euclidean metric given by the coordinates (τ, r) and look to the region close to the horizon $r \to r_{\rm H}$, so the metric reads

$$\mathrm{d}s^2_{\rm E} \,=\, \frac{r^2_{\rm H} f'(r_{\rm H})}{L^2}\,(r - r_{\rm H})\,\mathrm{d}\tau^2 + \frac{L^2}{r^2_{\rm H} f'(r_{\rm H})}\,\frac{\mathrm{d}r^2}{(r - r_{\rm H})}\,. \tag{2.15}$$

Introducing new coordinates $\rho^2 = 4L^2(r - r_{\rm H})/r^2_{\rm H} f'(r_{\rm H})$ and $\theta = r^2_{\rm H} f'(r_{\rm H})\tau/2L^2$ the metric takes the plane form $\mathrm{d}s^2 = \mathrm{d}\rho^2 + \rho^2 \mathrm{d}\theta^2$, that is free of singularities provided that the angular coordinate has period $\beta_\theta = 2\pi$. We can now read off the field theory temperature as the inverse of the period of the Euclidean time coordinate,

$$T \,\equiv\, T_{\rm H} \,=\, \frac{1}{\beta_\tau} \,=\, \frac{r^2_{\rm H} f'(r_{\rm H})}{4\pi L^2}\,. \tag{2.16}$$

This result is completely general and holds for any kind of black hole [60]. In the concrete case of 5-dimensional AdS-Schwarzschild, with blackening factor $f(r)$ given in (2.14), the temperature is

$$T = r_{\rm H}/(\pi L^2)\,. \tag{2.17}$$

An important remark is that the Euclidean boundary admits two different spin structures depending on the boundary conditions satisfied by fermions on the compact circle. In principle one can either impose periodic (supersymmetric) boundary conditions or anti-periodic (thermal) ones, however, in the presence of a black hole, only anti-periodic boundary conditions are allowed, therefore, supersymmetry will be broken. Also, the presence of the black hole modifies the isometries of the AdS space and the dual gauge theory is not conformal anymore, though it still flows to an ultraviolet fixed point since the bulk space is asymptotically AdS, so only at very high energies the conformal invariance of the field theory will be restored.

This is nice since we are looking for holographic descriptions of 'close to real world' scenarios that in general would not be supersymmetric nor conformal, but on the other hand it makes much more difficult to test the validity of the duality. As we already saw, most of the tests that can be done in the zero temperature case concern quantities protected by the symmetries of the system. The lack of some of them in the finite temperature case of course does not mean that the correspondence does not hold, just that it is harder to check it.

One indication that finite temperature gauge theories are well described by gravity theories in AdS black hole backgrounds comes from the comparison of the entropy of a $\mathcal{N}=4$ $SU(N)$ infinitely strongly coupled theory at finite temperature and the entropy of an ideal Stefan-Boltzmann gas of gluons [61, 62]. In the gravity computation the entropy is given by the Bekenstein-Hawking entropy of the black hole, while for the free gauge theory statistical mechanics fixes the dependence on the number of degrees of freedom

and conformal invariance the scaling with the temperature, giving a final result

$$S_{\rm BH} = \frac{3}{4} S_{\rm SB} = \frac{\pi^2}{2} V N^2 T^3 \,. \tag{2.18}$$

The appearance of a relative factor between both of them is not surprising since the entropy is not protected against running with the coupling constant. In fact, this factor far from contradicting the duality must be regarded as a holographic prediction about the strongly coupled gauge theory. Notice that the gravity result captures the scaling with the number of colors, which indicates the presence of N^2 unconfined gluons, thus the gravity background must be interpreted as the dual of the deconfined (plasma) phase of finite temperature $\mathcal{N} = 4$ Yang-Mills theory. Moreover, coming back to the discussion about plasmas in the previous chapter, results at RHIC and lattice simulations in conjunction with this holographic relation between infinitely coupled and free gauge theories supports the picture of a strongly coupled QGP just above the deconfinement temperature.

Confinement-Deconfinement.

The holographic formulation of the correspondence allows us to construct the conformal field theory dual to a given gravity theory. This is so since we can define local operators of the boundary theory just by considering the boundary behavior of perturbations of the gravity fields. However, the boundary conditions are completely determined by the conformal boundary of the bulk and in principle it is possible to have several bulk geometries with the same boundary, hence satisfying the same boundary conditions. In this case it is necessary to take into account the contributions to the partition function of the boundary theory of all the gravity theories leading to the same boundary theory when evaluating (2.11). In the large N limit, the supergravity action scales with a positive power of N, thus the dominant contribution to the partition function will be given by the configuration with smallest free energy. This provides a natural scenario for a phase transition in the boundary theory, that would happen at the point where two different geometries have the same free energy. Therefore, for each phase of a field theory we can construct its holographic dual and phase transitions correspond to change the geometry of the bulk space in the gravity side [63].

This implies that the AdS/CFT correspondence should be able to reproduce the usual confinement/deconfinement phase transition of finite temperature gauge theories. For the case considered so far, the boundary topology is $S^1 \times \mathbb{R}^3$ in Euclidean signature. The only scale of the field theory is set by the size of the time circle, i. e. the temperature. The absence of dimensionless parameters implies that the temperature can be either zero or different from zero and that all the finite temperatures are equivalent by rescaling. Therefore, no phase transition is possible. One can instead consider a global AdS bulk metric,

whose boundary has topology $S^1 \times S^3$. In this case, two scales are defined on the boundary theory corresponding to the size of the circle and the size of the sphere. A dimensionless parameter can be constructed as the ratio between both of them. Varying this parameter it is possible that the field theory undergoes a phase transition, that in the gravity side must correspond to a 'jump' between two different asymptotically AdS geometries. In fact, for the $\mathcal{N}=4$ case, there exist two solutions to the supergravity equations of motion that share the same asymptotic topology $S^1 \times S^3$ in Euclidean signature, given by

$$\mathrm{d}s^2 = \left(1 + \frac{r^2}{L^2}\right)\mathrm{d}\tau^2 + \left(1 + \frac{r^2}{L^2}\right)^{-1}\mathrm{d}r^2 + r^2\mathrm{d}\Omega_3^2\,, \tag{2.19a}$$

$$\mathrm{d}s^2 = \left(1 + \frac{r^2}{L^2} - \frac{M}{r^2}\right)\mathrm{d}\tau^2 + \left(1 + \frac{r^2}{L^2} - \frac{M}{r^2}\right)^{-1}\mathrm{d}r^2 + r^2\mathrm{d}\Omega_3^2\,, \tag{2.19b}$$

where M is the mass of the black hole. In order to compare the free energy of these two configurations it is necessary to regularize both spacetimes in such a way that they lead to the same boundary geometry. Doing so, one finds that for large temperature in the boundary theory, the AdS black hole metric (2.19b) is favored, while for low temperature the so-called thermal AdS (2.19a) is dominant. This is the well known Hawking-Page transition, where a thermal gas of gravitons eventually collapses forming a black hole when the temperature is increased [64].

This transition is interpreted in the dual large N $\mathcal{N}=4$ gauge theory living on $S^1 \times S^3$ as a confinement/deconfinement phase transition in analogy to QCD. The high temperature phase is analogous to a deconfining phase with free energy of order N^2 that reflects the contribution of gluons and whose gravity dual is given by the AdS black hole metric, whereas the low temperature phase corresponds to a confining phase with free energy of order one (since color singlet hadron contributions are N-independent) whose gravity dual is the thermal AdS background [63].

Finally we can consider the field theory living on $S^1 \times \mathbb{R}^3$. This corresponds to send the radius of the S^3 to infinity and in this case the black hole metric is always favored, so the field theory cannot develop a phase transition but is in the plasma (deconfined) phase. This limit corresponds to the Euclidean version of the metric (2.14) upon redefinition of the variables when only the AdS part is taken into account.

2.3 Finite chemical potential

We have discussed the implementation of finite temperature in the holographic correspondence and found that it is nothing but placing the supergravity theory in a black hole background. This simple deformation allows us to give a holographic dual description of the plasma phase of a Yang-Mills theory in the limit of strong coupling. For the realm

of this thesis this will be enough to illustrate how the AdS/CFT correpondence can be applied to plasma physics, keeping in mind that this gauge theory has to be seen as an oversimplified toy model of real plasmas like those produced at RHIC.

In order to study condensed matter physics at least one supplementary deformation is required: the gauge theory must be placed at finite chemical potential, or finite charge density, thus we need to implement the dual of a $U(1)$ symmetry. Moreover, in the case of superconductors and superfluids, the correspondence should be able to reproduce the phase transition between the normal and the superconducting phases, hence we also need a mechanism for spontaneous symmetry breaking of such symmetry in the bulk.

Adding a global current.

To have a gauge theory at finite charge density means to give a non-zero expectation value to the time component of a global current. The field/operator dictionary tells us that global conserved currents J_μ in the boundary theory couple to bulk massless Maxwell fields A_μ, or equivalently that a global $U(1)$ symmetry of the field theory is dual to a gauge $U(1)$ symmetry of the gravity theory. Therefore, a finite chemical potential is obtained adding a Maxwell term to the Einstein-Hilbert action with a negative cosmological constant, leading to an Einstein-Maxwell theory, that in four dimensions is given by

$$S = \frac{1}{16\pi G}\int \mathrm{d}^4x\sqrt{-g}\left(R + \frac{6}{L^2} - \frac{1}{4}F^2\right) , \tag{2.20}$$

where $F = dA$ is the electromagnetic field strength. We want to consider now four dimensional classical gravity in order to have a holographic description of $2+1$ dimensional strongly coupled condensed matter systems.

Hence, the dual gravitational description of a finite temperature and finite charge density field theory is gravity in an electrically charged black hole background. The unique solution of the above Einstein-Maxwell action describing such gauge theory is the Reissner-Nordstrom AdS black hole [2], whose metric is

$$\begin{aligned} \mathrm{d}s^2 &= \frac{r^2}{L^2}\left(-f(r)\mathrm{d}t^2 + \mathrm{d}x^2 + \mathrm{d}y^2\right) + \frac{L^2}{r^2}\frac{\mathrm{d}r^2}{f(r)} , \\ f(r) &= 1 - \left(1 + \frac{\mu^2 L^2}{4r_{\mathrm{H}}^2}\right)\left(\frac{r_{\mathrm{H}}}{r}\right)^3 + \frac{\mu^2 L^2}{4r_{\mathrm{H}}^2}\left(\frac{r_{\mathrm{H}}}{r}\right)^4 , \end{aligned} \tag{2.21}$$

with a non-zero scalar potential

$$A_t(r) = \mu\left(1 - \frac{r_{\mathrm{H}}}{r}\right) . \tag{2.22}$$

[2] The most general solution is actually a dyonic AdS black hole with both electric and magnetic charge. Since for our purposes it is enough to consider an electrically charged black hole we set the magnetic charge to zero.

The constant term in the scalar potential has been chose such that it vanishes at the black hole horizon, $A_t(r_{\rm H}) = 0$. The parameter μ is then directly identified with the chemical potential of the field theory. The charge density of the field theory is then $n = \mu r_{\rm H}$ and corresponds to the electric field of the black hole. In fact, the scalar potential has to vanish at the horizon in order to have a well defined Maxwell field in the analytic continuation to Euclidean space. One can use the integral Gauss law to compute the charge inside a closed surface at a given r_0, $\oint A = \int_0^\beta \mathrm{d}\tau \int_{r_{\rm H}}^{r_0} \mathrm{d}r r F_{r\tau}$. In the limit $r_0 = r_{\rm H}$, the area of the surface vanishes and since there is no puntual charge located at the origin of the Euclidean space, the integral must vanishes too, what actually implies that $A_t(r_{\rm H}) = 0$.

We can use the definition (2.16) for the Hawking temperature, since the metric used in the previous section to derive it is formally the same as (2.21). The resulting temperature for a charged four dimensional black hole is

$$T = \frac{r_{\rm H}}{4\pi L^2}\left(3 - \frac{\mu^2 L^2}{4 r_{\rm H}^2}\right) . \tag{2.23}$$

In the case of zero chemical potential, the temperature (2.17), that only depends on the horizon radius, introduces a scale in the theory that breaks conformal invariance. The horizon radius $r_{\rm H}$ can be scaled out, thus all the non-zero temperatures are equivalent. Now in the charged black hole we have two scales that parametrize the system: the chemical potential of the field theory and the horizon radius. Again, we can scale out the horizon radius but we are left with the scale set by the chemical potential, so temperatures are not equivalent anymore. Then, the only non trivial dependence on the temperature of any physical quantity will be in the dimensionless ratio T/μ.

Unlike for zero μ where one can have either temperature or not without a smooth connection between both solutions, for finite charge density the temperature can be continuously taken to zero. Then it makes sense to ask what happens when we cool the system down and whether it undergoes a phase transition.

Spontaneous symmetry breaking.

We can probe the above background adding charged matter in the bulk in order to answer this question. Since we are interested in testing whether or not a superconducting phase exist, we will only consider the case of bosonic operators. Spontaneous symmetry breaking occurs when a charged operator condenses, i. e. acquires a vev. In principle the operators that condense do not have to be scalars. Although we will center in the s-wave superconductors for which the order parameter is a scalar operator, one can also talk about p-wave or d-wave superconductors for which the condensate carries angular momentum. In the frame of the AdS/CFT correspondence, the first proposals for a s-wave superconductor

realization were done in [65–67], for the p-wave case in [68–70] and recently for d-wave superconductors in [71].

The presence of a charged scalar operator in the gauge theory is equivalent to consider a charged scalar field propagating in the bulk. This amounts to the addition to (2.20) of an action for the scalar field

$$S = \frac{1}{16\pi G}\int \mathrm{d}^4x\sqrt{-g}\left(|\partial\phi - iqA\phi| + m^2|\phi|^2\right) , \tag{2.24}$$

where q is the charge of the scalar under the $U(1)$ gauge symmetry. The potential for the scalar field has been chosen to be a mass term, though the exact form would be fixed by the string embedding leading to such supergravity action. As mentioned before, we will not care about that issue but rather fix the potential this way and explore the yielding phenomenology. Nevertheless, some proposals of string embeddings with a low energy action compatible with a superconducting phase have been done in [72–74].

An obvius solution to the resulting Abelian-Higgs model coupled to gravity is still a Reissner-Nordstrom AdS black hole (2.21) with scalar potential (2.22) and a trivial expectation value for the charged scalar operator, so a vanishing scalar field in the bulk $\phi = 0$. This solution corresponds to the normal (non-superconducting) phase of the gauge theory. The key observation is that this background can be unstable to the formation of a charged condensate. The finite charge density induces a negative contribution to the effective mass of the scalar field,

$$m^2_{\text{eff}} = m^2 + q^2 g^{tt} A_t^2 = m^2 - \frac{q^2\mu^2 L^2}{r^2 f(r)}\left(1 - \frac{r_{\text{H}}}{r}\right)^2 . \tag{2.25}$$

In anti-de Sitter space, fields with negative squared mass can be stable provided that their mass remains above the Breinthenlohner-Freedman bound, that for d-dimensional AdS is $m^2_{\text{BF}} = -(d-1)^2/4L^2$. The correction to the mass vanishes both at the boundary and at the horizon, but for large enough chemical potential, the effective mass can eventually violate the bound, $m^2_{\text{eff}} < m^2_{\text{BF}}$, at some intermediate point. At high temperature (low μ) we find a Reissner-Nordstrom AdS black hole background solution with zero condensate, that describes the normal phase of the field theory. If we decrease the temperature (increase μ), this solution will become unstable at some critical value T_c and the scalar field will develop a non-trivial profile, what implies a non-zero expectation value for the dual charged operator. This solution of a RN-AdS black hole with a non-zero charged scalar field hovering outside the horizon is an hairy black hole and describes the superconducting phase of the field theory.

In fact, even for a neutral scalar field the described background can become unstable to condensation. It is known that at zero temperature the Reissner-Nordstrom AdS black hole has an $\text{AdS}_2\times\mathbb{R}^2$ geometry close to the horizon, whose size is related to the size of the

four dimensional black hole by $L_2^2 = L^2/6$. So near extremal RN-AdS black holes coupled to a neutral scalar can become unstable too, since stable fields in the asymptotically AdS_4 bulk can be unstable in the AdS_2 near-horizon throat due to the difference in the BF bounds for each part of the space.

Therefore, the minimal content of the gravity dual of an holographic model of superconductivity consists of a charged AdS black hole coupled to a scalar field. Although this model is usually referred to as holographic superconductor it is more proper to speak of an holographic charged superfluid as in [75] since the $U(1)$ symmetry in the boundary field theory is global and there is no clear holographic description of how to add gauge fields. In fact, since superfluidity is associated with the Goldstone mechanism while superconductivity does with the Higgs mechanism, the broken phase of that model actually corresponds to a superfluid in the boundary and a superconductor black hole in the bulk.

In chapter 6 we will come back to the Abelian gauge model introduced in [66] and present some features about the phase transition and the hydrodynamic behavior of the superfluid. A more carefull and extense treatment of holographic superconductivity and superfluidity can be found in the nice reviews [49, 50].

Chapter 3

Thermal correlators and quasinormal modes

We have seen that the AdS/CFT correspondence gives a recipe for computing n-point Euclidean correlators of strongly coupled field theories using the classical gravity dual through the precise relation (2.13). In many cases one is interested in study dynamical properties of the thermal field theory for which real-time correlation functions cannot be obtained by analytic continuation of the Euclidean ones. This is the case of some kinetic coefficients that are obtained as a certain limit of thermal Green functions through Kubo formulas, but also of the hydrodynamic limit (small frequency and momentum). The Euclidean correlator is given in terms of the Matsubara frequencies ($\omega = 2\pi i n$, where $n \geq 1$ is an integer), and the problem relies in doing an analytic continuation of a discrete set of Euclidean frequencies to the real values of ω. Even after doing so it would be very hard to get information about the hydrodynamics of the system, since the lowest Matsubara frequency can be far away from the low frequency limit. On top of that, it is likely to happen that one is not even able to do the analytic continuation due to a lack of an analytic expression for the Euclidean frequencies. All in all, it is clear then that a real-time AdS/CFT prescription for directly compute real-time thermal correlators is needed.

3.1 The Lorentzian propagators

In the Euclidean formulation the correlators where nothing else that the variation of the supergravity on-shell action with respect to the boundary values of the fields. For finite temperature, the solutions to the supergravity equations of motion are completely determined by imposing regularity in the whole bulk, what amounts to give a boundary condition for the field at the boundary and to ensure regularity at the horizon. In the Lorentzian formulation this is not enough since the horizon does not represent the end of the spacetime, fields can cross the horizon, so an additional boundary condition as to be set at $r = r_{\mathrm{H}}$ to fix the solutions to the field equations. This ambiguity in defining the bulk solutions is related to the multiple Green functions that one can define for a thermal field theory. Selecting a concrete boundary condition will then correspond to fix which thermal correlators are going to be computed.

As an example, let us consider a massless scalar in an AdS black hole background, that for convenience we can write as

$$\mathrm{d}s^2 = \frac{\mathrm{d}r^2}{f(r)} + r^2\mathrm{d}\mathbf{x}^2 \pm f(r)\mathrm{d}t^2\,, \tag{3.1}$$

for which the horizon is located at $r = r_{\mathrm{H}}$ and the boundary at $r = \infty$. Notice that the plus or minus sign corresponds to Euclidean or Lorentzian signature, respectively, and that for both of them we are calling t the time coordinate. The equation of motion for the scalar propagating in this space is

$$\frac{1}{r^3}\partial_r\left(r^3 f(r)\partial_r\phi\right) + \frac{1}{r^2}\partial_i^2\phi \pm \frac{1}{f(r)}\partial_t^2\phi = 0\,. \tag{3.2}$$

We can Fourier transform the field

$$\phi(r,t,\mathbf{x}) = \int \frac{\mathrm{d}^4k}{(2\pi)^4}\mathrm{e}^{\pm i\omega t + i\mathbf{k}\mathbf{x}} f_k(r)\phi_0(k)\,, \tag{3.3}$$

where $f_k(r\to\infty) := 1$ in order to satisfy the boundary condition $\phi|_\partial = \phi_0(x^\mu)$. The equation of motion in terms of the mode function $f_k(r)$ reads

$$\frac{1}{r^3}\partial_r\left(r^3 f(r)\partial_r f_k(r)\right) - \left(\frac{\mathbf{k}^2}{r^2} \pm \frac{\omega^2}{f(r)}\right) f_k(r) = 0\,. \tag{3.4}$$

Near the boundary at $r\to\infty$ the two solutions of the equation behave as ~ 1 and $\sim r^{-4}$ for both signatures. Near the horizon we have a different situation for each frame. For the Euclidean version, the two asymptotic behaviors close to the horizon go like $\sim (r-r_{\mathrm{H}})^{\pm\omega}$ and imposing regularity corresponds to pick the minus sign solution, that will correspond to a particular linear combination of the two asymptotic solutions close to the boundary. Thus fixing the boundary condition at the boundary and imposing regularity at $r = r_{\mathrm{H}}$ completely determines the bulk solution in the Euclidean formulation. In Minkowski space, one finds the same behavior close to the boundary, but close to the horizon the two possible solutions go like $\sim (r-r_{\mathrm{H}})^{\pm i\omega}$ that of course are both stable solutions: they oscillate very rapidly close to the horizon but with a constant amplitude. So now regularity is not enough to uniquely determine the solution in the bulk. As we already pointed out, this is not bad by itself, different boundary conditions will lead to different thermal propagators, what implies that the AdS/CFT correspondence captures the multiplicity of Green functions that can be defined in a finite temperature field theory. The point is to be able to identify which condition corresponds to which correlation function. But even after doing that and obtaining the bulk solution to be fed back into the supergravity action, the Euclidean prescription (2.11) cannot be directly extended to the Lorentzian case.

This can be easily seen if we write the classical action for the bulk field solution and integrate the radial coordinate, obtaining a boundary term that in principle gets

contributions from both the horizon and the boundary,

$$S_{\text{sugra}} = K \int \frac{\mathrm{d}^4k}{(2\pi)^4} \sqrt{-g} g^{rr} \phi(-k,r) \partial_r \phi(k,r) \,, \tag{3.5}$$

with K a normalization constant. If we were in the Euclidean case there would not be any contribution from the horizon and the Green function would reduce to

$$G_{\text{E}}(k) = -2K\sqrt{g} f_{-k}(r) \partial_r f_k(r)|_{r\to\infty} \,, \tag{3.6}$$

throwing away the contact terms when taking the limit [76]. But if one extends the recipe to the Lorentzian case in a straightforward manner,

$$\left\langle \mathrm{e}^{i\int \mathrm{d}^4x \phi_0(x)\mathcal{O}(x)} \right\rangle = \mathrm{e}^{iS_{\text{sugra}}[\phi]} \,, \tag{3.7}$$

and tries to compute the two point function related to the chosen boundary condition, one ends up with

$$G(k) = -\mathcal{F}(r,k)\Big|_{r=r_{\text{H}}}^{r\to\infty} - \mathcal{F}(r,-k)\Big|_{r=r_{\text{H}}}^{r\to\infty} \,, \tag{3.8}$$

where $\mathcal{F}(k,r) = K\sqrt{-g} g^{rr} f_{-k}(r) \partial_r f_k(r)$. However, this result can not be correct: Green functions are in general expected to be complex quantities, like for instance the retarded one, and the above quantity is not. The mode function satisfies $f_k^*(r) = f_{-k}(r)$, so the imaginary part of $\mathcal{F}(r,k)$ can be shown to have no dependence on r, so contributions from the boundary and from the horizon will cancel each other leading to a real correlator. Even keeping only the contributions to the boundary term at $r \to \infty$, the imaginary parts cancel since reality of the field equation implies $\mathcal{F}(r,-k) = \mathcal{F}^*(r,k)$. Therefore, we cannot obtain the thermal Green functions by direct variation of the action.

Retarded two-point function prescription.

The first proposal that overcame these problems was made by Son and Starinets in [77], and though it was an *ad hoc* proposal for computing retarded or advanced two-point functions supported on the matching with the zero temperature result, it has been proven to be valid by the more rigorous prescription made in [78], based on the Schwinger-Keldish formalism, that we will later briefly review.

The first problem to solve in a Lorentzian formulation of the correspondence is the identification of boundary conditions in the bulk as different kinds of correlators in the boundary theory. If we come back to the behavior of the solutions to (3.4) close to the horizon and we also recover the time dependent phase $\mathrm{e}^{-i\omega t}$ in the wave function, we can write the solutions as

$$\phi_- \sim \mathrm{e}^{-i\omega t} f_k(r) \sim \mathrm{e}^{-i\omega t}(r-r_{\text{H}})^{-i\omega/4\pi T} \sim \mathrm{e}^{-i\omega(t+r_*)} \,, \tag{3.9a}$$

$$\phi_+ \sim \mathrm{e}^{-i\omega t} f_k^*(r) \sim \mathrm{e}^{-i\omega t}(r-r_{\text{H}})^{i\omega/4\pi T} \sim \mathrm{e}^{-i\omega(t-r_*)} \,, \tag{3.9b}$$

where we have defined the coordinate $r_* = (\ln(r - r_{\rm H}))/(4\pi T)$, for which the horizon sits at $r_* = -\infty$. It is clear that these plane wave solutions represent two different directions of motion. The solution (3.9a) corresponds to a left moving wave front in r_*, thus a wave that moves towards the horizon, i. e. infalling, whereas solution (3.9b) represents a right moving wave front in r_*, thus a wave that moves away from the horizon, i. e. outgoing. In the former case, the oscillating field travels from the boundary all the way through the bulk up to the horizon and then disappears, being absorbed by the black hole. In the latter case, the field is emitted by the black hole and then travels forward from the horizon until it reaches the boundary. Since classical black holes do not radiate, the infalling solutions satisfy causality and it seems natural to associate them with retarded correlators on the field theory, on the other hand the outgoing solutions satisfy anti-causal conditions so they should be associated with the advanced correlators on the boundary theory.

We are interested in studying the reaction of strongly coupled systems to small perturbations and their relaxation back to equilibrium, so the physical boundary condition to impose on the bulk fields is therefore that the solutions have to be *infalling* at the black hole horizon. This implies that the response will be given by the retarded propagators of the field theory operators, in agreement with the knowledge from linear response theory.

The second problem is the reality of the propagator found by direct variation of the action, that cannot be interpreted as the retarded Green function. The authors of [77] proposed that the Lorentzian retarded two-point correlator should by defined as

$$G_{\rm R}(k) = -2\mathcal{F}(r,k)\Big|_{r\to\infty} \tag{3.10}$$

in analogy to the zero temperature and the Euclidean cases, but with no direct proof. It is surprising that the boundary term coming from the horizon must be thrown away during the computation and that only the solution at the boundary is involved in the final prescription for the retarded correlator taking into account that it existence relies on the presence of the black hole horizon and on the boundary conditions imposed there. Nevertheless, this definition was proven to work in all the cases for which independent verification was possible, and later on it was shown to be a particular case of the general real-time formulations made by [78, 79]. In many cases, this simple prescription is enough to get physically interesting results and it can be generalized to the case of more than one field. In particular, in chapter 6 we will show how it works for a system of coupled fields. Note that the advanced correlators corresponds to pick the *outgoing* boundary condition for the bulk field, that translates in changing $f_k \to f_k^*$, thus the prescription reproduces the well-known relation $G_{\rm A}(k) = G_{\rm R}^*(k)$.

Even if the formula (3.10) works fairly well, it is still a postulate and cannot be generalized to n-point Green functions. We will now briefly comment the general formulation of AdS Lorentzian correlators to avoid the feeling that this prescription is imposed *ad hoc*.

Schwinger-Keldish propagators.

The analytic extension of the AdS black hole, the 'eternal black hole', has two disconnected boundaries, see the left side of figure 3.1 below. This has been interpreted as having two independent copies of the field theory each one living in one of the two boundaries [80–83], based on the original ideas of Israel [84]. In Schwarzschild time, that is identified with the time in the dual field theory, the second boundary corresponds to the extension to complex values $t \to t - i\beta/2$, where β is the inverse of the temperature. This suggested to the authors of [78] a natural identification in the field theory with the Schwinger-Keldysh formalism[1] , where the description of the thermal field theory in Lorentzian signature needs to double the degrees of freedom and extend time to complex values. The corresponding Schwinger-Keldysh path starts at some time t_i, extends along the real axis to a time t_f and then moves in the imaginary direction to $t_f - i\beta/2$. Then it comes back in the real direction to $t_i - i\beta/2$ and finally it goes to $t_i - i\beta$. The second set of field operators live on the $t - i\beta/2$ piece. In the right side of figure 3.1, a general Schwinger-Keldish path is shown. The parameter σ is arbitrary, but the symmetric path corresponding to the value $\sigma = \beta/2$ appears naturally in the gravity computation. The general case can also be reproduced introducing a rescaling in the boundary values of fields living in the second boundary.

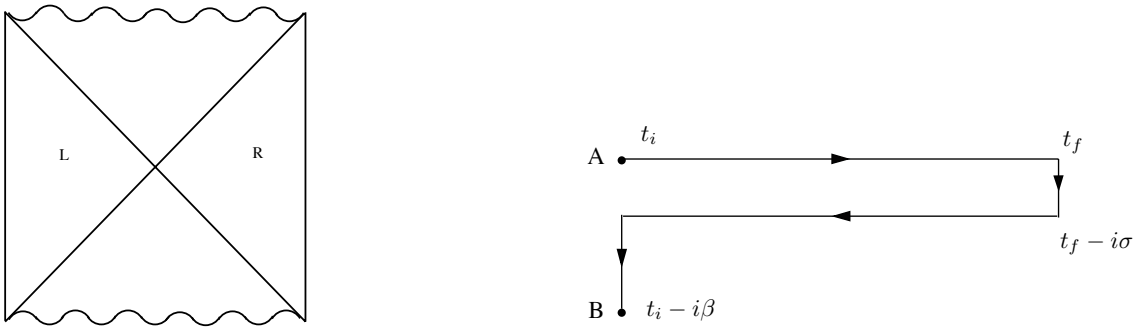

Figure 3.1: *(Left) Full Penrose diagram of an eternal AdS black hole. (Right) The general Schwinger-Keldish contour.*

If we consider a massless scalar propagating in the extended AdS space of (3.1), the equations of motion can be solved independently in the left (L) and the right (R) quadrants of the above diagram. Near the horizons the solutions will behave like (3.9a) or (3.9b) in both of them. We can label the solutions attending to their near-horizon behavior as $\phi_{\pm,\mathrm{R}}$ and $\phi_{\pm,\mathrm{L}}$ if they live in the R quadrant or in the L one, respectively. Of course R fields vanish in the L quadrant and vice versa.

[1] A description of the Schwinger-Keldysh formalism can be found in Thermal Field Theory books, like [85].

The Schwarzschild coordinates do not cover the whole space. In order to have a general prescription we need first a frame in which we can describe all the Penrose diagram. It is achieved by using the Kruskal coordinates for the AdS black hole case, which cover the entire spacetime of the maximally extended Schwarzschild-AdS black hole and that are well behaved everywhere outside the singularity,

$$U = -\mathrm{e}^{-2\pi T(t-r_*)} \quad , \quad V = \mathrm{e}^{2\pi T(t+r_*)} \, . \tag{3.11}$$

The R quadrant corresponds to $U < 0$ and $V > 0$, while the L quadrant corresponds to $U > 0$ and $V < 0$. The future horizon sits at $U = 0$ whereas the past horizon sits at $V = 0$ in the complete space, since in the left quadrant the Schwarzschild time runs backwards. In Kruskal coordinates the horizons are regular surfaces. We can again solve the equations of motion close to the horizons, and we find that the normal Kruskal modes are

$$\phi_{\mathrm{out}} \sim \mathrm{e}^{-i\tilde{\omega}U} \sim \mathrm{e}^{-i\tilde{\omega}(t_{\mathrm{K}}-x_{\mathrm{K}})/2} \, , \tag{3.12a}$$

$$\phi_{\mathrm{in}} \sim \mathrm{e}^{-i\tilde{\omega}V} \sim \mathrm{e}^{-i\tilde{\omega}(t_{\mathrm{K}}+x_{\mathrm{K}})/2} \, , \tag{3.12b}$$

where the Kruskal time and radial coordinate are $t_{\mathrm{K}} \equiv U + V$ and $x_{\mathrm{K}} \equiv V - U$, so it is clear that the first solution is outgoing in R, while the second one is ingoing in this quadrant.

Notice that $\omega \neq \tilde{\omega}$, modes of definite frequency in the Schwarzschild sense mix positive and negative frequency modes in the Kruskal sense, since as it is well known positive and negative frequency modes are defined in a different way in different vacua. Following Unruh [86], we take the Kruskal vacuum to be the sensible vacuum in the near horizon region, since fields arbitrarily close to the black hole horizon still have well-defined finite energy. On the other hand, asymptotic observers experience a thermal bath. The meaningful states close to the horizon should have well-defined frequency in the Kruskal sense. We can construct positive or negative frequency Kruskal modes out of Schwarzschild modes with arbitrary frequency by demanding that the combinations have the appropriate analytic properties that the Kruskal modes have, i. e. positive frequency solutions are analytic in the lower-half complex U and V planes and negative frequency solutions are analytic in the upper-half complex planes.

In this way it is possible to construct four different solutions by connecting L and R solutions smoothly through the horizons, but one is still forced to choose some boundary conditions at the black hole horizons. However, we want to reproduce the Schwinger-Keldish propagators, thus the boundary conditions are now given in a natural way by the contour time ordering in the SK path. It turns out that it picks two out of the four solutions: positive frequency and ingoing in the future horizon and negative frequency and outgoing in the past horizon, from the R quadrant point of view. So the final physical solution is a linear combination of this two modes satisfying boundary conditions at both

of the boundaries of the extended AdS black hole. If we impose that at the R boundary it takes the value $\phi_1(k)$ and at the L boundary $\phi_2(k)$, the bulk field can be written as

$$\begin{aligned}\Phi(r,k) &= \left[(n+1)f^*_{k,\mathrm{R}}(r) - n f_{k,\mathrm{R}}(r)\right]\phi_1(k) + \sqrt{n(n+1)}\left[f_{k,\mathrm{R}}(r) - f^*_{k,\mathrm{R}}(r)\right]\phi_2(k)\\ &+ \sqrt{n(n+1)}\left[f^*_{k,\mathrm{L}}(r) - f_{k,\mathrm{L}}(r)\right]\phi_1(k) + \left[(n+1)f_{k,\mathrm{L}}(r) - n f^*_{k,\mathrm{L}}(r)\right]\phi_2(k)\\ &= \Phi_{\mathrm{R}}(r,k) + \Phi_{\mathrm{L}}(r,k)\,, \end{aligned} \tag{3.13}$$

where $n = 1/(\mathrm{e}^{\omega/T} - 1)$. Feeding back the action (3.5) with this field and taking into account that it will split in two terms, one for the R quadrant and one for the L quadrant, we can get the SK matrix of propagators G_{ab} with $a, b = 1, 2$ by taking functional derivatives of the action, but more generally we can compute any n-point correlator. If one does the computation for the two-point functions and substitutes the conjectured prescription (3.10) for the retarded correlator and the analogous for the advanced one, the result is

$$\begin{aligned} G_{11}(k) = -G^*_{22}(k) &= (n+1)G_{\mathrm{R}}(k) - nG_{\mathrm{A}}(k) = \mathrm{Re}\, G_{\mathrm{R}}(k) + i\coth\frac{\beta}{2T}\,\mathrm{Im}\, G_{\mathrm{R}}(k)\,,\\ G_{12}(k) = G_{21}(k) &= \sqrt{n(n+1)}(G_{\mathrm{A}}(k) - G_{\mathrm{R}}(k)) = \frac{2\,i\,\mathrm{e}^{-\beta\omega/2}}{1-\mathrm{e}^{-\beta\omega}}\,\mathrm{Im}\, G_{\mathrm{R}}(k)\,, \end{aligned} \tag{3.14}$$

that exactly corresponds to the SK propagator of a thermal field theory in the symmetric path case $\sigma = \beta/2$. The arbitrary σ propagator can also be reproduced if one rescales the boundary condition on the second boundary a factor $\mathrm{e}^{(\sigma-\beta/2)\omega}$.

This general formulation reproduces the Schwinger-Keldish formalism for thermal field theories by taking the maximal extension of the AdS space and imposing boundary conditions at both boundaries. From the R quadrant perspective, bulk fields are combinations of infalling positive frequency and outgoing negative frequency eigenmodes of the Kruskal vacuum close to the event horizons. The prescription of [77] for retarded correlators is then recovered when only the infalling modes are considered.

3.2 Quasinormal modes

We have seen that the retarded propagators of the field theory correspond to imposing *infalling* boundary conditions at the black hole horizon for fields in the gravity dual. On the other hand, infalling boundary conditions are also the constitutive ingredient for the calculation of the quasinormal modes of black holes. These modes are solutions to the linearized equations of motion with complex frequency, whose imaginary part represents the damping in time of the field on the background. Perturbed black holes are intrinsically dissipative systems. If a field is excited in the presence of a black hole, the energy of the fluctuation will be lost inside the horizon or spread out to infinite and eventually the final state will be a larger black hole with no fluctuations. This process is described by the quasinormal spectrum, that was first studied in the context of asymptotically flat space

(for a review see [87,88]). In an AdS geometry, fluctuations cannot escape to infinit since it acts effectively as a box, thus all the energy is dissipated by the black hole horizon. The spectrum of quasinormal excitations was first computed for black holes in asymptotically anti de Sitter spacetimes in [89] and afterwards they have been exhaustively studied in different AdS black hole backgrounds and in various dimensions [90–100] (for a recent review see [101]).

The authors of [91] observed that the quasinormal frequencies of BTZ black holes coincide with the poles of the retarded two-point functions in the dual two-dimensional conformal field theory. In [94,95] it was shown that this observation extends generally to the Lorentzian AdS/CFT correspondence when one imposes infalling boundary conditions at the horizon, i. e. quasinormal frequencies in AdS can be interpreted as the poles of the retarded Green functions or resonances in the dual field theory. The direct implication of this fact is that the inverse of the imaginary part of quasinormal modes give the relaxation time back to equilibrium of the plasma under small perturbations.

The analysis of the quasinormal spectrum requires solving an eigenvalue problem subject to boundary conditions for the corresponding linear differential equations. At the horizon we impose infalling boundary conditions to the fluctuations to ensure that they are absorbed by the black hole, but at the boundary of AdS various boundary conditions can be imposed. Regularity of the solutions imply that scalar and gauge invariant fields satisfy Dirichlet boundary conditions at the AdS boundary, whereas for gauge dependent fields the situation is more subtle, in principle there is no compelling reason that selects a preferred boundary condition. The procedure in that case will pass through first find the gauge invariant combinations and then see which boundary conditions have to be satisfied in order to match the poles of the corresponding retarded Green functions.

To examine how the identification of quasinormal modes of black holes and poles of retarded Green functions arise, let us consider a generic gauge invariant perturbation Z_k that satisfies infalling boundary conditions at the horizon. We can write this solution as a linear combination of the local solutions close to the boundary,

$$Z_k(z) = \mathcal{A}(\omega, \mathbf{k}) y_1(z) + \mathcal{B}(\omega, \mathbf{k}) y_2(z)\,, \tag{3.15}$$

where $\mathcal{A}(\omega, \mathbf{k})$ and $\mathcal{B}(\omega, \mathbf{k})$ are the *connection coefficients* of the differential equation. Near the boundary the solution becomes

$$Z_k(z \approx 0) = \mathcal{A}(\omega, \mathbf{k})\, z^{\Delta_-}(1 + \dots) + \mathcal{B}(\omega, \mathbf{k})\, z^{\Delta_+}(1 + \dots)\,, \tag{3.16}$$

where again $\Delta_+ > \Delta_-$ are the characteristic exponents close to the boundary. In general, fields can be redefined such that $\Delta_+ > 0$ and $\Delta_- = 0$. Imposing Dirichlet boundary conditions correspond to impose $\mathcal{A}(\omega, \mathbf{k}) = 0$. In fact this equation establishes the relation between frequencies and momenta that has to be satisfied in order to ensure that the

solution is normalizable at the boundary. Thus the eigenvalue equation $\mathcal{A} = 0$ defines the quasinormal mode spectrum of black hole fluctuations.

On the other hand, the on-shell action in terms of the gauge-invariant fields to quadratic order in perturbations reduces to a boundary term plus contact terms that do not contain derivatives of the field,

$$S = \lim_{z\to 0} \int \mathrm{d}^4 k F(\omega, \mathbf{k}) g(z)\, Z'(z) Z(z) + \dots \,, \tag{3.17}$$

where $F(\omega, \mathbf{k})$ contains the normalization of the action and the dependence on the parameters ω and $\mathbf{k}$, and $g(z)$ contains the dependence in the radial coordinate. Applying the prescription (3.10) for computing retarded correlators, we find that the two-point function for the dual operator of the bulk field $Z(z)$ is

$$G_{\mathrm{R}}(\omega, \mathbf{k}) = 2\,(\Delta_+ - \Delta_-)\, F(\omega, \mathbf{k}) \frac{\mathcal{B}(\omega, \mathbf{k})}{\mathcal{A}(\omega, \mathbf{k})} \lim_{z\to 0} \left(g(z) z^{\Delta_+ - \Delta_- - 1} \right) , \tag{3.18}$$

provided that $\Delta_+ - \Delta_- \notin \mathbb{Z}$. When the difference between characteristic exponents is an integer, one of the two asymptotic boundary solutions can get a logarithmic contribution and this relation would be modified. Anyway, if the resultant radial dependence has a well-defined limit at the boundary, as it will be in the cases considered later on, for any value of the characteristic exponents the retarded correlator will be proportional to the ratio of connection coefficients,

$$G_{\mathrm{R}}(\omega, \mathbf{k}) \propto \frac{\mathcal{B}(\omega, \mathbf{k})}{\mathcal{A}(\omega, \mathbf{k})} + \dots \,, \tag{3.19}$$

thus the poles of the propagator will be given by the zeros of $\mathcal{A}(\omega, \mathbf{k})$. As we already said, the condition that the connection coefficient $\mathcal{A}$ vanishes is equivalent to impose that the solutions are just made of normalizable modes, hence the fields correspond to states of the gauge theory and not to the insertion of operators. In this sense, the quasinormal modes can be viewed holographically as the response of the medium in the absence of sources.

By comparison between the gravity point of view and the field theory point of view, one can state that all the information about the poles of the retarded Green functions or resonances of a quantum field theory is encoded in the quasinormal mode spectrum of the dual gravity theory. This identification allows us to get relevant information about transport properties and excitation spectra of the near-equilibrium strongly coupled plasma using classical supergravity computations.

In the holographic dual gauge theory, the plasma tries to restore thermal equilibrium in the presence of small perturbations. That involves *dissipation* in the case of perturbations localized in time or *absorption* it they are localized in space. Quasinormal modes are complex frequency eigenvalues that describe how small perturbations fall through the

horizon of the black hole after traveling a finite time in the background. They are interpreted as the inverse of relaxation times of excitations on the plasma, hence quasinormal modes give a dual description of dissipation processes in the field theory. For periodic perturbations localized in space, relaxation back to equilibrium will be measured in terms of *absorption lengths* in the plasma. They will correspond in the gravity dual to the inverse of *complex momentum* eigenvalues that describe the falling through the horizon of small perturbations after traveling a finite distance in the background. Both the QNM and the CMM are solutions to the same linearized equations of motion satisfying the same boundary conditions. The difference is that quasinormal modes decay exponentially in time, while complex momentum modes decay along the direction of propagation. The complex momentum spectrum has been computed in the frame of AdS black holes in [102], but it was considered before for horizons of compact spatial geometry, where such modes are interpreted as Regge poles [103] of the S-matrix. In chapter 5 we will consider both type of solutions in order to study the response of the plasma to different kind of perturbations.

3.3 Stability issues

We will now show how the pole structure of the retarded Green functions is restricted by stability considerations. This of course does not fix the precise location of the poles in the complex frequency or complex momentum planes, but allows us to identify the instabilities of the system, hence the breakdown of the description signaling possible phase transitions in the dual gauge theory. In fact, in chapter 6 we will use the appearance of tachyonic excitations as a signal of the system entering a superconducting phase.

Instabilities appear as exponentially growing modes, i. e. modes that are not absorbed by the black hole after traveling a finite time or distance. The time and space dependence of bulk fields is given simply by exponentials of the form

$$\phi \sim \mathrm{e}^{-i\omega t}\mathrm{e}^{ikx}\,, \tag{3.20}$$

where we are considering that the perturbation propagates in the x direction. Stability demands that the solutions are exponentially decaying. Since we want to ensure causality, in the case of quasinormal modes we impose $t > 0$, thus instabilities will appear as quasinormal modes with positive imaginary part $\mathrm{Im}\,\omega > 0$ and we should expect all the poles of the retarded Green function lying in the lower-half of the complex frequency plane. In the case of complex momentum modes we want to impose that they are outgoing from the origin of the perturbation. For $x > 0$ this implies that $\mathrm{sign}\,\omega = \mathrm{sign}\,\mathrm{Re}\,k$, while stability demands that $\mathrm{Im}\,k > 0$. On the other hand, for $x < 0$ the outgoing condition translates to $\mathrm{sign}\,\omega = -\mathrm{sign}\,\mathrm{Re}\,k$ and the stability condition to $\mathrm{Im}\,k < 0$. These two conditions imply that complex momentum poles of the retarded Green function lie in the first and third quadrants of the complex momentum plane.

All these conditions summarizes to the following stability criteria

$$\begin{aligned} \text{QNM} \quad &: \quad \operatorname{Im}\omega < 0\,, \\ \text{CMM} \quad &: \quad \operatorname{sign}\left(\frac{\omega}{\operatorname{Re} k}\right) = \operatorname{sign}\operatorname{Im} k\,. \end{aligned} \tag{3.21}$$

The above requirement has been proved to hold in the case of a Schwarzschild-AdS background by studying the behavior of the Schrödinger-like equations of motion of quasinormal modes in [89] and analogously for complex momentum modes in [102].

We can also adopt the field theory perspective. As we saw in section 1.3, to study the effect of small external perturbations it is enough to use linear response theory when the energy of the perturbation is negligible compared to the total energy of the system. In this linear approximation, the response of a field Φ to a perturbation represented by an external source $j(t,\mathbf{x})$ is given by the convolution of the retarded Green function $G_{\mathrm{R}}(t-\tau,\mathbf{x}-\boldsymbol{\xi})$ with the source,

$$\langle\Phi(t,\mathbf{x})\rangle = -\int \mathrm{d}\tau\,\mathrm{d}^3\boldsymbol{\xi}\, G_{\mathrm{R}}(t-\tau,\mathbf{x}-\boldsymbol{\xi})\, j(\tau,\boldsymbol{\xi})\ , \tag{3.22}$$

where the retarded two-point correlation function is

$$G_{\mathrm{R}}(t-\tau,\mathbf{x}-\boldsymbol{\xi}) = -i\,\Theta(t-\tau)\,\langle[\Phi(t,\mathbf{x}),\Phi(\tau,\boldsymbol{\xi})]\rangle\ . \tag{3.23}$$

Using Fourier transforms, the response can be written as

$$\langle\Phi(t,\mathbf{x})\rangle = -\int \frac{\mathrm{d}\omega}{2\pi}\frac{\mathrm{d}^3\mathbf{k}}{(2\pi)^3}\,\mathrm{e}^{-i\omega t+i\mathbf{k}\mathbf{x}}\,\widetilde{G}_{\mathrm{R}}(\omega,\mathbf{k})\,\tilde{\jmath}(\omega,\mathbf{k})\ . \tag{3.24}$$

We can now choose to make an analytical continuation either to the complex ω-plane or to the complex $\mathbf{k}$-plane.

Let us first consider that we choose to analytically continue to the complex frequency plane. We can then use Cauchy's theorem to evaluate this integral by closing the contour on the lower half of the complex ω plane for $t > 0$, thus picking up the contributions from the poles of the retarded propagator, i.e. the frequencies of the quasinormal modes in the AdS/CFT correspondence. At this point we assume that the only singularities of the retarded Green function are single poles in the lower half complex frequency plane. This is indeed the case for the holographic retarded two-point functions. In principle one could think that for $t < 0$ the integration contour should be closed on the upper half plane picking contributions from non-analyticities there, but causality (encoded on the Heaviside function in (3.23)) ensures that the retarded propagator vanishes for $t < 0$, thus there should be no poles in the upper half plane. Therefore all the poles of the retarded Green function should lie in the lower-half complex frequency plane. The retarded propagator can be written as

$$\widetilde{G}_{\mathrm{R}}(\omega,\mathbf{k}) \simeq \sum_{\text{poles}} \frac{R_n(\omega,\mathbf{k})}{\omega-\omega_n(\mathbf{k})}\ , \tag{3.25}$$

where $\omega_n := \Omega_n - i\Gamma_n$ and R_n are the residues of the retarded propagator evaluated at the poles. We should emphasize that this is a formal expression since the infinite sum does not necessarily converge; we will come back to this issue in section 5.2. Doing a partial Fourier transform in space, the response of the system to a perturbation is now expressed by a sum over the poles

$$\langle \Phi(t,\mathbf{k})\rangle = i\theta(t)\sum_n R_n(\omega_n(k),\mathbf{q})\,\tilde{j}(\omega_n(\mathbf{k}),\mathbf{k})\,\mathrm{e}^{-i\Omega_n(\mathbf{k})t-\Gamma_n(\mathbf{k})t}\ , \tag{3.26}$$

where we have assumed that the source does not introduce new non-analyticities in the lower half plane. This will be the case, for example, if we consider that the perturbation is localized in time, i. e. we strike the medium once at $t = 0$, so the source will be $j(t,\mathbf{x}) \propto \delta(t)$. A constrain in the location of the poles comes both from the reality of the response (3.26) and from the time reversal symmetry $\rho(\omega,\mathbf{k}) = \rho(-\omega,\mathbf{k})$ of the spectral function $\rho(\omega,\mathbf{k}) = -2\mathrm{Im}\,G_{\mathrm{R}}(\omega,\mathbf{k})$. These conditions yield to the poles coming in pairs. The relation between the partners and their residues is such that if ω_n is a pole with associated residue R_n then $\widetilde{\omega}_n = -\omega_n^*$ is also a pole with residue $\widetilde{R}_n = -R_n^*$. Unpaired poles can also be present if they lie on the imaginary axis and their residues are purely imaginary.

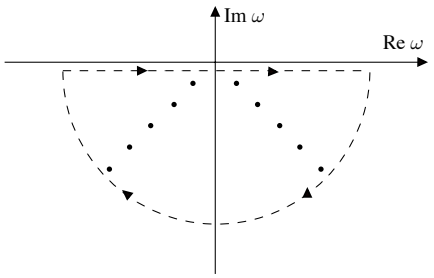

Figure 3.2: *Relevant integration contour for the poles in the complex ω-plane. All the poles are in the lower-half plane, corresponding to the interpretation of quasinormal modes as the poles of the retarded Green function.*

Therefore, from the field theory we find that that the complex frequency poles not only have to be in the lower half plane, but they also have to come in pairs. The presence of a pole in the upper half plane will correspond to a tachyonic mode traveling backwards in time, thus to an instability. This is consistent with the result found from the gravity theory, where exponentially growing modes, identified as instabilities, lie in the upper half complex ω plane. In figure 3.2 is depicted the typical arrangement of quasinormal modes appearing in the study of small perturbations of black holes in AdS backgrounds.

Now we switch the roles of time and one spatial coordinate and analytically continue to the complex k plane. We consider again that the only singularities of the retarded

propagator are single poles in the complex momentum plane, so

$$\widetilde{G}_{\mathrm{R}}(\omega,k) \simeq \sum_{\text{poles}} \frac{R_n(\omega,k)}{k-k_n(\omega)} \ , \tag{3.27}$$

where $k_n = k_n^R + ik_n^I$. We can choose a periodic perturbation localized in space, so we assume a source of the form $j(t,\mathbf{x}) = \delta(x)\exp[-i(\omega t - \mathbf{k}_\perp \mathbf{x}_\perp)]$. From (3.22), the response of the system takes the form

$$\langle \Phi(t,\mathbf{x})\rangle = -\frac{1}{2\pi}\, \mathrm{e}^{-i(\omega t - \mathbf{k}_\perp \mathbf{x}_\perp)} \int \mathrm{d}q k\, \mathrm{e}^{iqx}\, \widetilde{G}_{\mathrm{R}}(\omega, \mathbf{k}_\perp, k) \ . \tag{3.28}$$

Such a perturbation has the form of a plane wave in the perpendicular directions $\mathbf{x}_\perp$. We have assumed that the perturbation started far in the past such that the system has reached a stationary state. We will also assume that it is no further modulated in the $\mathbf{x}_\perp$-directions, i.e. we set $\mathbf{k}_\perp = 0$. By Cauchy's theorem we can evaluate this integral by closing the contour on the upper half of the complex k plane for $x > 0$ or on the lower-half complex k plane for $x < 0$. The response of the system to a perturbation localized in space as a sum over the poles reads

$$\langle \Phi(t,\mathbf{x})\rangle = -i\ \mathrm{sign}(x)\, \mathrm{e}^{-i\omega t} \sum_n R_n(\omega, k_n(\omega))\, \mathrm{e}^{ik_n^R(\omega)x - k_n^I(\omega)x} \ . \tag{3.29}$$

By parity symmetry $x \to -x$, if k_n is a pole, then also $\tilde{k}_n = -k_n$ has to be a pole. The expectation is that the fluctuation creates damped waves that move away from the origin of the perturbation, so we want that our modes move to the left for $x < 0$ and to the right for $x > 0$. It implies that the poles of the retarded Green function have to lie in the first and third quadrants of the complex k plane for $x > 0$ and $x < 0$, respectively. A typical arrangement of complex momentum poles and the corresponding integration contours is depicted in figure 3.3.

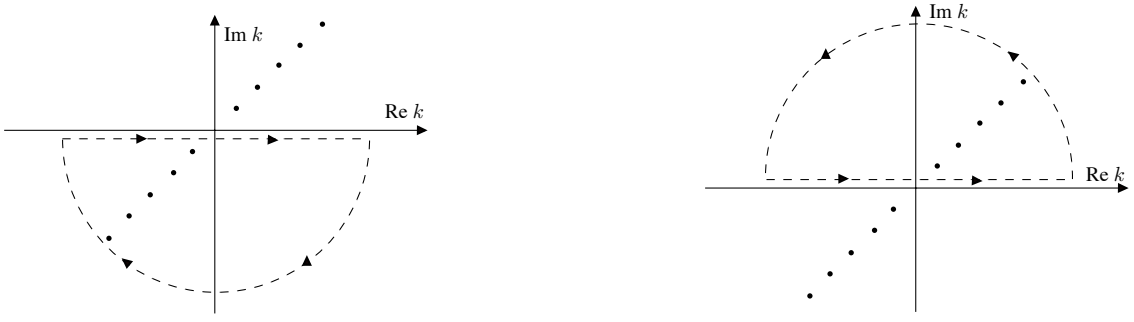

Figure 3.3: *Relevant integration contours for the poles in the complex momentum plane. (Left) Contour for $x < 0$. (Right) Contour for $x > 0$. To obtain exponentially decaying waves traveling away from the origin of the perturbation it is necessary that poles lie in the first and third quadrants.*

Part II

Applications of the AdS/CFT correspondence

Chapter 4

AdS black holes as reflecting cavities

In section 3.1 we have reviewed how thermal propagators can be computed holographically from classical solutions propagating in an asymptotically AdS black hole background. In section 3.2 we have presented a very interesting result of the correspondence, the relation between the quasinormal mode spectrum that describes the decay of perturbations in black holes and the singularities in the complex frequency plane of two-point functions in the holographic dual. Semiclassical computations suggest that both could be simply related to geometric properties of the bulk, in particular to its causal structure [104–109]. Very massive fields, corresponding to operators of large conformal dimension, can be studied using a WKB approximation where the field propagates along geodesics. We have seen that in the black hole background, the space has an analytic extension through the horizon to another asymptotically AdS region. Spacelike geodesics can explore both regions and give information about the thermal state where the field theory is defined. It is also possible to relate different geodesics with the frequency in the field theory, in such a way that in the large frequency limit the geodesic approaches a null ray. The geodesic approximation has been used to compute the asymptotic position of quasinormal modes in the large mass limit, although it has been argued that the results should be generalizable to the case of fields with small mass [107].

In this chapter we show that null geodesics in the bulk give useful information about the singularities of the dual correlators even for fields with small mass. In the large frequency limit, that we can associate to the ultraviolet behavior of the field theory, the classical solutions to the equations of motion can be described in terms of the eikonal approximation. Therefore, the propagation of fields in the bulk is well approximated by null rays and it reduces to a problem of geometric optics in the curved spacetime. We first illustrate this by introducing a mirror in AdS and studying the spectrum of the dual theory and we then proceed in section 4.2 to find the eikonal approximation for a scalar field in AdS_{d+1} black hole backgrounds and show how the solution bouncing on the singularity can be extended to the asymptotic region behind the horizon. In section 4.3 we explain the asymptotic location of the singularities of field theory correlators and hence the quasinormal mode spectrum of the black hole in simple terms of the geometric shape of the black hole, seen as a reflecting cavity with the asymptotically AdS boundaries and

the future and past singularities as walls. Finally, we discuss possible applications of the high frequency-null ray identification and the interpretation in thermal field theories.

4.1 AdS with a mirror

To illustrate that null geodesics in AdS contain the relevant information about the singularities of the dual two-point correlators let us pick up a very simple example, a scalar field in AdS_{d+1} spacetime. We work with the metric

$$\mathrm{d}s^2 = \frac{1}{z^2}\left(-\mathrm{d}t^2 + \mathrm{d}z^2 + \mathrm{d}\mathbf{x}^2\right) , \tag{4.1}$$

where $z = 0$ is the boundary of AdS and we introduce a mirror at a finite value of the radial coordinate $z = z_0$. This translates into Dirichlet boundary conditions for the fields at this surface.

A scalar field ϕ with mass $m^2 = \Delta(\Delta - d)$ is dual to a scalar operator $\mathcal{O}$ of conformal dimension Δ. The source $j(t)$ of the operator in the field theory corresponds to a boundary condition for the dual field in the bulk. Consider a spatially homogeneous source localized in time $j(t) = \delta(t)$. Then, the expectation value (vev) of the operator will be given by the two-point correlator $G(t, x)$ as

$$\langle \mathcal{O}(t) \rangle \sim \int \mathrm{d}t' \int \mathrm{d}\mathbf{x} \int \mathrm{d}\mathbf{x}' G(\mathbf{x} - \mathbf{x}', t - t')\delta(t') = VG(t, \mathbf{q} = 0) , \tag{4.2}$$

where V is the volume of the space and $\mathbf{q}$ is the spatial momentum. The singularities of the vev are thus related to singularities of the correlator. In the holographic description, the expectation value is implicit in the asymptotic behavior of the field, that we can compute using Witten diagrams [63]. We are interested in the propagation from points $(z = 0, t_0, \mathbf{x}_0)$ at the boundary, to the bulk at $(z, t', \mathbf{x}')$ and back to the boundary at $(z = 0, t, \mathbf{x})$. The value of the field at the boundary can be computed using the convolution of two bulk-to-boundary propagators

$$\phi_0(t) \sim \int_0^{z_0} \frac{\mathrm{d}z}{z^{d+1}} \int \frac{\mathrm{d}\mathbf{x}\, \mathrm{d}\mathbf{x}_0\, \mathrm{d}\mathbf{x}'\, \mathrm{d}t_0\, \mathrm{d}t'\, z^{2\Delta}\, \delta(t_0)}{|z^2 + (\mathbf{x} - \mathbf{x}')^2 - (t - t')^2|^{\Delta}\, |z^2 + (\mathbf{x}' - \mathbf{x}_0)^2 - (t' - t_0)^2|^{\Delta}} . \tag{4.3}$$

After integrating over the spatial directions and t_0 and introducing Schwinger parameters w_1 and w_2, we find

$$\phi_0(t) \sim \int \mathrm{d}t' \int_0^{z_0} \mathrm{d}z z^{2\Delta - d - 1} \int_0^{\infty} \mathrm{d}w_1 \int_0^{\infty} \mathrm{d}w_2\, (w_1 w_2)^{\Delta - (d+1)/2} \mathrm{e}^{-w_1 \left| z^2 - (t - t')^2 \right|} \mathrm{e}^{-w_2 \left| z^2 - t'^2 \right|} \tag{4.4}$$

The ultraviolet limit corresponds to $w_1 \to \infty$, $w_2 \to \infty$. The integral is dominated in this case by null trajectories $z = \pm t'$ and $z = \pm(t - t')$. If $t = 0$, the two classes of null trajectories become degenerate and there is a singularity. In the presence of a mirror, we

can consider a null ray going from the boundary to the mirror and back as part of a single trajectory, so in some heuristic sense the two null trajectories also become degenerate when $t = 2z_0$. In the following we will show that this intuitive picture gives the correct answer by computing explicitly two-point Green functions in the field theory.

Using the prescription given in section 3.1, the field theory correlator $G(k)$ can be computed from the on-shell action for classical solutions of the bulk field $\phi_k(z)$. The result is a boundary term given by relation (3.10). For simplicity, we will consider zero spatial momentum and modes with fixed frequency $\phi(t,z) = \mathrm{e}^{-i\omega t}\varphi(z)$. The equation of motion for the field is

$$(\Box - m^2)\,\phi = 0 \quad \Rightarrow \quad z^{d+1}\partial_z\left(z^{1-d}\varphi'(z)\right) + (z^2\omega^2 - \Delta(\Delta - d))\varphi(z) = 0\,. \tag{4.5}$$

In order to regularize, we introduce a cutoff at $z = \epsilon$, $\epsilon \to 0$, such that $\varphi(\epsilon) = \epsilon^{\Delta_-}$, where Δ_- is the smallest characteristic exponent of the equation of motion. The solution is given in terms of Bessel functions. Imposing Dirichlet boundary conditions on the field at $z = z_0$ and using $\nu^2 = m^2 + \frac{d^2}{4} = \left(\Delta - \frac{d}{2}\right)^2$,

$$\varphi(z) = \frac{z^{d/2}\left(Y_\nu(\omega z_0)J_\nu(\omega z) - J_\nu(\omega z_0)Y_\nu(\omega z)\right)}{\epsilon^{d/2-\Delta_-}\left(Y_\nu(\omega z_0)J_\nu(\omega\epsilon) - J_\nu(\omega z_0)Y_\nu(\omega\epsilon)\right)}\,. \tag{4.6}$$

Taking the limit $\epsilon \to 0$, up to contact terms, the holographic Green function is given by

$$G_\Delta(\omega) = c_\Delta\omega^{2\nu}\frac{Y_\nu(\omega z_0)}{J_\nu(\omega z_0)}\,. \tag{4.7}$$

If ν is an integer, there are extra logarithmic terms that cancel the branch cut in $Y_\nu(\omega z_0)$ when $\omega \to 0$. As an example, in AdS_5 a massless scalar field gives

$$G_4(\omega) = c_4\omega^4\left(\frac{\pi Y_2(\omega z_0)}{J_2(\omega z_0)} - \log\left[(\omega z_0)^2\right]\right)\,. \tag{4.8}$$

Apart from a possible branch cut coming from the $\omega^{2\nu}$ factor, the only singularities of the Green function are poles ω_n on the real frequency axis, associated to the zeros of the Bessel function

$$J_\nu(\omega_n z_0) = 0, \quad n = 1, 2, 3\ldots \tag{4.9}$$

Since $J_\nu(-x) = (-1)^\nu J_\nu(x)$, the poles are paired ω_n and $-\omega_n$.

We are interested in the ultraviolet behavior of the correlator and how it is related to light-like propagation in the bulk, so we take the $\omega \to \infty$ limit. Then, (4.7) can be approximated by

$$G_\Delta(\omega) \simeq c_\Delta\omega^{2\nu}\tan\left[\omega z_0 - \left(\nu - \frac{1}{2}\right)\frac{\pi}{2}\right]\,. \tag{4.10}$$

The asymptotic position of the poles is therefore

$$\omega_n z_0 = (2n+1)\frac{\pi}{2} + \left(\nu - \frac{1}{2}\right)\frac{\pi}{2} \equiv n\pi + \omega_0 z_0, \quad n \in \mathbf{Z}\,. \tag{4.11}$$

To show explicitly the relation with null trajectories is more convenient to look at the time-dependent propagator.

$$G_\Delta(t) = \int_{\mathcal{C}} \mathrm{d}\omega \mathrm{e}^{-i\omega t} G_\Delta(\omega)\,. \tag{4.12}$$

For the Feynman propagator, the contour $\mathcal{C}$ in the complex frequency plane is defined in such a way that it picks up all the positive frequencies for $t \geq 0$ and the negative frequencies for $t < 0$, so it passes slightly above the real axis for $\omega > 0$ and slightly below for $\omega < 0$. Above some frequency ω_k, the position of the poles will be well approximated by the asymptotic expression (4.11), so the propagator would have a piece coming form the lowest modes plus the contribution from the infinite high-frequency modes. For $t \geq 0$, we find

$$\begin{aligned} G^+_{\Delta,F}(t) &\simeq G^+_{F,\mathrm{IR}}(t) + 2\pi i c_\Delta (i\partial_t)^{2\nu} \mathrm{e}^{-i\omega_0 t} \sum_{n=k}^{\infty} \mathrm{e}^{-i\pi n t/z_0} = \\ &= G^+_{F,\mathrm{IR}}(t) + 2\pi i c_\Delta (i\partial_t)^{2\nu} \mathrm{e}^{-i\omega_0 t} \frac{\mathrm{e}^{-i(k-1)\pi t/z_0}}{\mathrm{e}^{i\pi t/z_0} - 1}\,. \end{aligned} \tag{4.13}$$

We can understand this expression as being defined using the usual prescription for spacetime-dependent correlators $t \to t - i0^+$. Strictly speaking, the expression above is well defined only when 2ν is an integer ($\nu \geq 0$ by unitarity). When this is not the case, there will be a branch cut that must be taken properly into account. This will introduce power-like corrections, but the location of the singularities of the propagator in time is determined by the sum over high-frequency poles. For $t < 0$

$$G^-_{\Delta,F}(t) \simeq G^-_{F,\mathrm{IR}}(t) - 2\pi i c_\Delta (-i\partial_t)^{2\nu} \mathrm{e}^{i\omega_0 t} \frac{\mathrm{e}^{-i(k-1)\pi t/z_0}}{\mathrm{e}^{i\pi t/z_0} - 1}\,. \tag{4.14}$$

We can see now that the singularities associated to the ultraviolet behavior of the Feynman propagator appear at regular intervals of time

$$t = 2nz_0, \quad n \in \mathbf{Z}\,. \tag{4.15}$$

The identification of these singularities with the singularities on the null trajectories of the bulk propagator leads to the geometric interpretation of a light ray bouncing on and off from the boundary at $z = 0$ and the mirror at $z = z_0$, if we take $t = 0$ as the 'initial point'. The points where the ray reaches the boundary coincide with the singularities in the time-dependent Green function, see figure 4.1.

4.2 The eikonal approximation in AdS black holes

In black hole backgrounds, the absorption of classical fluctuations of the fields is described by an infinite set of modes with complex frequencies, known as the quasinormal modes.

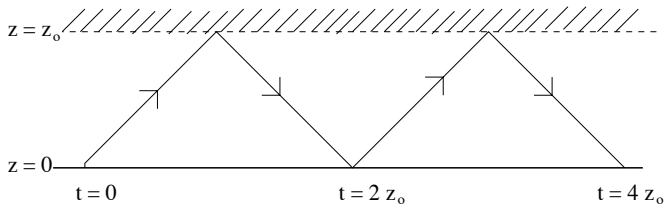

Figure 4.1: *Null geodesic bouncing on and off from the boundary at $z = 0$ and the mirror surface at $z = z_0$.*

In the holographic dual the frequencies of these modes correspond to singularities of the two-point correlators, that are in last instance responsible for the dissipative behavior of the thermal theory. The relation between null trajectories ending on the boundary and the high frequency behavior of the correlators strongly suggests that the analytic continuation of the space behind the horizon can explain the asymptotic location of quasinormal frequencies or equivalently, the singularities of the dual correlators in complex frequency and time.

The eikonal approximation is a high frequency limit where $\omega \gg R$ and R is the typical curvature of the spacetime. This approximation leads to the classical limit of geometric optics in the curved spacetime, similar to ray optics in ordinary electromagnetism. The null trajectories we want to describe start at the AdS boundary and propagate into the interior until they hit the singularity. Presumably it should be possible to extend the geodesic to the asymptotically AdS region behind the horizon by joining it to a null ray that starts at the singularity and continues towards the second boundary. However, the eikonal approximation is expected to fail at the singularity, so it is a matter of concern what is the fate of solutions there. In the following, we construct the classical solutions in the eikonal approximation in the two asymptotically AdS regions and find the matching conditions at the future and past singularities.

In the eikonal approximation, an ansatz for the field is

$$\phi(x) = A(x)e^{i\theta(x)}\,, \tag{4.16}$$

where the eikonal phase $\theta(x)$ is $O(\omega)$ and the amplitude $A(x)$ is $O(1)$. We consider a scalar field with the Klein-Gordon equation of motion

$$(\Box - m^2)\,\phi = 0 \Rightarrow \frac{1}{\sqrt{-g}}\partial_\mu\left(\sqrt{-g}g^{\mu\nu}\partial_\nu\phi\right) - m^2\phi = 0\,. \tag{4.17}$$

Expanding this equation in ω, we find that the leading order gives the eikonal equation

$$g^{\mu\nu}\partial_\mu\theta\partial_\nu\theta = 0\,, \tag{4.18}$$

so $k^\mu = \partial^\mu\theta$ is a null vector field. It defines a family of null geodesics tangent to the field and in electromagnetism it can also be identified with the four-momentum of the photons.

Notice that the mass is neglected in this approximation, it will appear as a lower energy effect, while the leading behavior is universal. The next orders give the equations

$$\begin{aligned} k^\mu \partial_\mu A &= -\frac{1}{2}\partial_\mu k^\mu A\,, \\ (\Box - m^2)\, A &= 0\,. \end{aligned} \tag{4.19}$$

The first equation describes the evolution of the amplitude along the geodesic, while the last start to take into account subleading effects like the mass.

To work out the eikonal approximation we will use the Rosen coordinate system, that is better adapted to null geodesics. A nice explanation of coordinate systems adapted to the Penrose limit can be found in [110] and an example of its application to the eikonal expansion in [111]. The AdS_{d+1} black hole metric is $(d \geq 2)$ [1]

$$\mathrm{d}s^2 = -f(r)\mathrm{d}t^2 + \frac{\mathrm{d}r^2}{f(r)} + r^2 \mathrm{d}\mathbf{x}^2, \quad f(r) = r^2 - \frac{1}{r^{d-2}}\,. \tag{4.20}$$

We will consider only geodesics at a fixed point in the spatial directions $\mathbf{x}$, so in terms of the affine parameter u they are determined by two functions $(t(u), r(u))$. These functions can be found by solving the variational problem with Lagrangian

$$\mathcal{L} = \frac{1}{2}\left(-f(r)\,\dot{t}^2 + \frac{\dot{r}^2}{f(r)}\right) \tag{4.21}$$

where $\dot{t}$, $\dot{r}$ are the first derivatives with respect to u. The variation with respect to t introduces a conserved quantity E, so that

$$\dot{t} = \frac{E}{f(r)}\,. \tag{4.22}$$

For null geodesics we can further impose the condition $\mathcal{L} = 0$, so we find

$$\dot{r}^2 = f(r)^2 \dot{t}^2 = E^2\,. \tag{4.23}$$

This also implies that $\ddot{r} = 0$. In the Rosen coordinate system we take the affine parameter of the null geodesics u to be one of the coordinates, while we introduce another coordinate v satisfying the null condition $g^{\mu\nu}\partial_\mu v \partial_\nu v = 0$ and that corresponds to the Hamilton-Jacobi function of the variational problem. We have several possibilities

$$\begin{array}{llll} 1) & E>0,\ \dot{r} = -E & u = -r & v = -t - \int \frac{\mathrm{d}r}{f(r)} \\ 2) & E>0,\ \dot{r} = E & u = r & v = -t + \int \frac{\mathrm{d}r}{f(r)} \\ 3) & E<0,\ \dot{r} = -E & u = r & v = t + \int \frac{\mathrm{d}r}{f(r)} \\ 4) & E<0,\ \dot{r} = E & u = -r & v = t - \int \frac{\mathrm{d}r}{f(r)} \end{array} \tag{4.24}$$

[1] We have taken the AdS radius $R = 1$, and the coordinates are rescaled as $(t, r, \mathbf{x}) \to (t/r_{\mathrm{H}}, r_{\mathrm{H}} r, \mathbf{x}/r_{\mathrm{H}})$. Restoring the units, the Hawking temperature of the black hole is $T = d r_{\mathrm{H}}/4\pi R^2$.

The choices of coordinates 1) and 4) correspond to geodesics starting at the boundary $u = -\infty$ and reaching the singularity at $u = 0$. On the other hand, 2) and 3) correspond to geodesics that go from the singularity at $u = 0$ to the boundary at $u = \infty$. Geodesics described by 1) and 2) go forwards in time while the ones described by 3) and 4) go backwards. The metric in Rosen coordinates is

$$\mathrm{d}s^2 = 2\mathrm{d}u\mathrm{d}v - f_\pm(u)\mathrm{d}v^2 + u^2\mathrm{d}\mathbf{x}^2\,, \quad f_\pm(u) = u^2 - \frac{(\pm 1)^{d-2}}{u^{d-2}}\,, \tag{4.25}$$

where $f_+(u) = f(u)$ is valid for 2) and 4), while for 1) and 3) we have $f_-(u)$, instead. This distinction is important only when d is odd, since when d is even $f_-(u) = f_+(u) = f(u)$.

We can now write the eikonal ansatz (4.16) as $\phi(u, v) = A(u)\mathrm{e}^{i\omega v}$ and expand in inverse powers of the frequency

$$\phi(u, v) = A_0(u)\mathrm{e}^{i\omega v}\left(1 + \frac{A_1(u)}{i\omega} + \frac{A_2(u)}{(i\omega)^2} + \dots\right)\,. \tag{4.26}$$

Plugging back in the equation of motion (4.17), we see that the eikonal equation (4.18) is automatically satisfied by our choice of v. The next orders in the expansion (4.19) have the following solution to $O(1/\omega)$

$$\begin{aligned} A_0(u) &= (-g)^{-1/4} = u^{(1-d)/2}\,, \\ A_1(u) &= \frac{1}{8}(d^2 - 1 + 4m^2)u - (\pm 1)^{d-2}\frac{d-1}{8}u^{1-d}\,, \end{aligned} \tag{4.27}$$

where the + solution applies for geodesics 2) and 4), while the − is valid for 1) and 3). Then, choosing the correct definition of v and the correct sign in $A_1(u)$, the solution (4.26) describes the four possible geodesics given by (4.24).

This solution is valid as long as $u^{d-1}\omega \gg 1$ and $u/\omega \ll 1$, so it will stop to be trustable when we get close to the singularity $u = 0$ or the boundary $u \to \infty$. There is an extra issue concerning the definition of v in (4.24). The function $f(r)$ has a pole at $r = 1$, so in general v will be shifted by a complex value for $r < 1$. This could be compensated by defining v differently for $r > 1$ and $r < 1$ with a compensating constant in this region. The right treatment pass by using Kruskal coordinates, we will analyze this more thoroughly in section 4.3.

Matching of eikonal solutions and bouncing rays.

There are two possible descriptions of a ray bouncing on the boundary, one joining the geodesics associated to 2) with 1) in (4.24) or the time reversed process joining 3) with 4). In terms of the eikonal approximation we should find a matching when we continue the solutions close to the boundary.

At large values of the radial coordinate r the black hole factor can be neglected $f(r) \simeq 1$ and it is better to switch to the coordinate system focused on the boundary (4.1). In this case, the right identification of eikonal phases will be

$$\begin{aligned} &1) \quad e^{i\omega v} \sim e^{-i\omega(t+r)} \sim e^{-i\omega(t-z)} \\ &2) \quad e^{i\omega v} \sim e^{-i\omega(t-r)} \sim e^{-i\omega(t+z)} \\ &3) \quad e^{i\omega v} \sim e^{i\omega(t+r)} \sim e^{i\omega(t-z)} \\ &4) \quad e^{i\omega v} \sim e^{i\omega(t-r)} \sim e^{i\omega(t+z)} \end{aligned}$$

From section 4.1 we know that the solutions close to the boundary are Bessel functions. To match with the plane wave behavior of 2), we take the combination that gives the second Hankel function

$$\phi_{(2)} \simeq e^{-i\omega t} H_\nu^{(2)}(\omega z) \sim e^{-i\omega(t+z)}, \quad \omega z \gg 1\,. \tag{4.28}$$

We can treat the bouncing on the boundary as the continuation of this solution to negative values of z, $z \to -z$, that we should interpret as a parity transformation of the solutions in the z direction. Under this transformation, the solution changes to the first Hankel function, that shows the right asymptotic behavior to match with the eikonal solution of 1)

$$\phi_{(1)} \simeq e^{-i\omega t} H_\nu^{(1)}(\omega z) \sim e^{-i\omega(t-z)}. \tag{4.29}$$

The time reversed process can be found using the transformation $t \to -t$, so it works in the same way, the initial solution is

$$\phi_{(3)} \simeq e^{i\omega t} H_\nu^{(2)}(\omega z) \sim e^{i\omega(t-z)}, \tag{4.30}$$

while the reflected one is found again by analytic continuation $z \to -z$

$$\phi_{(4)} \simeq e^{i\omega t} H_\nu^{(1)}(\omega z) \sim e^{i\omega(t+z)}. \tag{4.31}$$

We are interested now in rays coming from the boundary that bounce on the future singularity and rays coming from the region behind the horizon that bounce on the past singularity. The expansion of the amplitude (4.26) fails close to the singularity $u^{d-1}\omega < 1$. However, the ansatz (4.16) in the form $\phi = A(u)e^{i\omega v}$ gives still valid solutions to the equations of motion. We can solve the Klein-Gordon equation as a Frobenius expansion, being the general solution of the form

$$A(u) = C_1 y_1(u) + C_2 \left[y_2(u) + \log u\, y_1(u)\right], \tag{4.32}$$

where $y_1(u)$ and $y_2(u)$ are series expansions in the u coordinate. For $d \geq 2$ we find

$$\begin{aligned} y_1(u) &= 1 + \frac{i\omega}{d-1}u^{d-1} - \frac{m^2}{d^2}u^d - \frac{3\omega^2}{4(d-1)^2}u^{2(d-1)} + \dots \\ y_2(u) &= 1 + \frac{i\omega}{d-1}u^{d-1} + \frac{d^2-(d-2)m^2}{d^3}u^d + \frac{(4-3d)\omega^2}{4(d-1)^3}u^{2(d-1)} + \dots \end{aligned} \tag{4.33}$$

To describe the bouncing on the singularity we need to extend the geodesic associated to 1) and defined for $u < 0$ to positive values of the affine parameter. In the original coordinates, r is extended to negative values. The eikonal phase does not change, but the branch cut appearing in (4.32) implies that the amplitude will in general pick up a non-trivial phase factor. In order to understand the extended solution from the point of view of an observer in the second boundary, we must change $r \to -r$ keeping $u > 0$. The time runs forwards for an observer in the second boundary, so there is no time reversal. The solution is then of the type 2), so we come to a situation analogous to the starting one and we can use the results we have already obtained to describe the bouncing on the second boundary and on the past singularity, that from this perspective looks like a future singularity.

4.3 Black holes as reflecting cavities

We have shown that in the high frequency limit, the eikonal approximation provides a good description of classical solutions in the bulk, and that the matching conditions at the boundary and singularities are consistent with a limit where a geometric description can be given in terms of null rays bouncing on the boundaries and singularities, so the black hole looks effectively as a box. We have also related null geodesics reaching the boundary with ultraviolet singularities in the time-dependent correlators of the dual field theory and hence with the asymptotic location of singularities in the high frequency limit.

A similar light-cone singularity in *real time* was found in [107] from the limit of space-like geodesics. It was shown that in the WKB computation there are three possible geodesics in the Euclidean geometry, associated to different branches of the correlator. The singularity belongs to an unphysical branch, while the physical result is given by a combination of two complex branches with no singularities. Therefore, the singularities associated to null geodesics should appear at complex values of time. Indeed, it was shown that for complex values with $\mathrm{Im}\, t \sim \beta/2$, the two extra branches disappear. In terms of the eikonal approximation, the extension to complex values of time will follow from the extension of the solution beyond the horizon. We will now proceed to study null geodesics in the black hole in order to extract information about the singularity structure of the correlators in the thermal field theory.

Consider a geodesic starting at the AdS boundary, bouncing on the singularity and reaching the AdS boundary behind the horizon. This corresponds to the analytic extension to positive values of u for the case 1) in (4.24). Notice that v will be shifted in general due to the contribution from $\int \mathrm{d}r/f(r)$. In order to keep a constant eikonal phase, the value

of t has to be shifted as well as part of the analytic continuation. We find then

$$\Delta t = \int_{-\infty}^{\infty} \frac{\mathrm{d}u}{f(u)} \,. \tag{4.34}$$

The function $f(u)$ has two poles at the horizon $u = \pm 1$, since for d odd we must switch between $f_-(u)$ and $f_+(u)$. The contour we pick pass above the first pole at $u = -1$ and below the second pole at $u = 1$. Then, using the expression

$$\frac{1}{x \mp i\epsilon} = \mathcal{P}\frac{1}{x} \pm i\pi\delta(x) \,, \tag{4.35}$$

the shift in time on the AdS boundary behind the horizon is

$$\Delta t = \frac{2\pi}{d}\left(\cot\frac{\pi}{d} - i\right) . \tag{4.36}$$

We have seen that the geodesic coming from the region behind the horizon after bouncing on the past singularity is equivalent to the one we have just described. We can also consider geodesics going backwards in time using the analytic extension of 3), as well as a contour that surrounds the poles at the horizon in the opposite way. We can then identify the complex values of time where the geodesics hit one of the AdS boundaries with the location of singularities of field theory correlators in the complex time plane. The time coordinate is given in dimensionless units, in order to restore the temperature dependence $\beta = 1/T$, we must divide by the radius of the horizon $r_H = 4\pi/d\beta$. For the lowest dimensional AdS_{d+1} spaces, the singularities t_n, $n \in \mathbf{Z}$ are at

$$\begin{array}{ll} AdS_{2+1} & t_n = i\frac{n\beta}{2} \\ AdS_{3+1} & t_n = \frac{n\beta}{2}\left(\frac{1}{\sqrt{3}} \pm i\right) \\ AdS_{4+1} & t_n = \frac{n\beta}{2}(1 \pm i) \end{array} \tag{4.37}$$

The value of the imaginary part can be understood in terms of the Wick rotation of the metric to Euclidean time (c.f. [80]), where it can be seen that the second boundary of AdS corresponds to the antipodal point in the thermal circle, with β being the full period. The value of the real part can also be understood in simple geometric terms. For this purpose, the best suited coordinate system are Kruskal coordinates

$$U = \mathrm{e}^{2(t+r_*)}, \quad V = -\mathrm{e}^{-2(t-r_*)}, \quad r_* = \int \frac{\mathrm{d}r}{f(r)} \,. \tag{4.38}$$

with a metric

$$\mathrm{d}s^2 = \frac{-f(UV)\mathrm{d}U\mathrm{d}V}{4UV} + r^2(UV)\mathrm{d}\mathbf{x}^2 \tag{4.39}$$

In AdS_3, the metric takes the particularly simple form

$$\mathrm{d}s^2 = \frac{-\mathrm{d}U\mathrm{d}V}{4(1+UV)^2} + \left(\frac{1-UV}{1+UV}\right)^2 \mathrm{d}x^2 \,. \tag{4.40}$$

The black hole does not cover the entire (U, V) plane, but it is limited by the asymptotic AdS boundary and by the singularity. They can be deduced from the conditions $r^2(UV) \to \infty$ and $r^2(UV) \to 0$, using the relation

$$UV = -\mathrm{e}^{4r_*(r)} \,. \tag{4.41}$$

For instance,

$$\begin{array}{lll} AdS_{d+1} & \text{singularity} & \text{boundary} \\ d=2 & UV=1 & UV=-1 \\ d=3 & UV=\mathrm{e}^{\frac{2\pi}{3\sqrt{3}}} & UV=-\mathrm{e}^{\frac{2\pi}{\sqrt{3}}} \\ d=4 & UV=1 & UV=-\mathrm{e}^{\pi} \end{array} \tag{4.42}$$

The real value of the position of the singularities t_n in the complex time plane can be found following the path of null geodesics in the Kruskal diagram, and using that $t = \log(-U/V)/4$. The null geodesics bounce on the boundaries and the singularities, giving the picture of a reflecting cavity. Following figure 4.2, the points where the singularities are located are

$$\begin{array}{lcll} AdS_{d+1} & (U,V):\ t=0 \to \text{ singularity } \to \text{ boundary} & & \\ d=2 & (1,-1) \to (1,1) \to (-1,1) & \Rightarrow & \mathrm{Re}\, t = 0 \\ d=3 & (\mathrm{e}^{\frac{\pi}{\sqrt{3}}}, -\mathrm{e}^{\frac{\pi}{\sqrt{3}}}) \to (\mathrm{e}^{\frac{\pi}{\sqrt{3}}}, \mathrm{e}^{-\frac{\pi}{3\sqrt{3}}}) \to (-\mathrm{e}^{\frac{7\pi}{\sqrt{3}}}, \mathrm{e}^{-\frac{\pi}{3\sqrt{3}}}) & \Rightarrow & \mathrm{Re}\, t = \frac{2\pi}{3\sqrt{3}} \\ d=4 & (\mathrm{e}^{\frac{\pi}{2}}, -\mathrm{e}^{\frac{\pi}{2}}) \to (\mathrm{e}^{\frac{\pi}{2}}, \mathrm{e}^{-\frac{\pi}{2}}) \to (-\mathrm{e}^{\frac{3\pi}{2}}, \mathrm{e}^{-\frac{\pi}{2}}) & \Rightarrow & \mathrm{Re}\, t = \frac{\pi}{2} \end{array} \tag{4.43}$$

In agreement with eq. (4.36). From this formula we can also do a Fourier transformation to deduce the asymptotic quasinormal frequencies, up to a shift that depends on the mass of the field considered. The general formula is

$$\omega_n \simeq 4\pi T n \left(\cot\frac{\pi}{d} \pm i\right) \sin^2\frac{\pi}{d} \ , \tag{4.44}$$

that coincides with the results found in [97, 112] using a WKB approximation to the equations of motion in the AdS black hole backgrounds.

4.4 Conclusions

Using the eikonal approximation, we have seen that the asymptotic formula for the quasinormal spectrum of fields with large mass in AdS black holes is also valid for fields with small mass in the large frequency limit. The analytic formula derived for the the asymptotic value of quasinormal frequencies (4.44), agrees with the expressions found in [97,112] using a WKB analysis, and with expressions derived for fields with large mass [107–109] and for fields with small mass in AdS_{2+1} $\omega_n \simeq 4\pi i T n$ [91], the numerical results in AdS_{3+1} $\omega_n \simeq (\sqrt{3} \pm 3i)\pi T n = \frac{3}{4}(\sqrt{3} \pm 3i) n\, r_{\mathrm{H}}$ [96] and AdS_{4+1} $\omega_n \simeq 2\pi i T n(1 \pm i)$ [89].

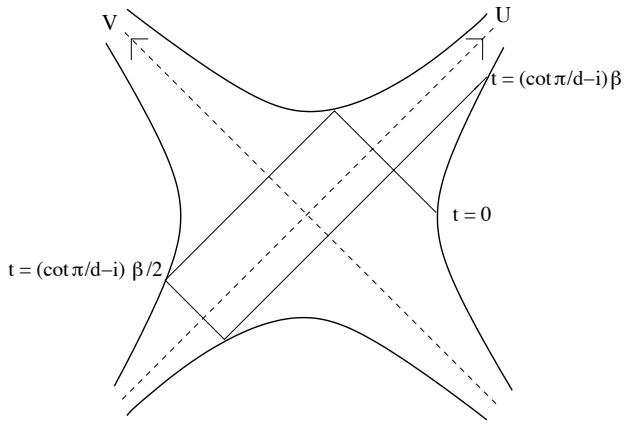

Figure 4.2: *Kruskal diagram of a eternal black hole in AdS space. The light solid line represents a null geodesic starting on the boundary at $t = 0$ bouncing on the future singularity, on the second AdS boundary, on the past singularity and back to the boundary at $t = (\cot \frac{\pi}{d} - i)\beta$.*

An interesting question is whether a geometric analysis of null geodesics in the analytic extension of the black hole could be applied to more general cases, like charged or rotating black holes or black holes with different asymptotics. A simple example is the topological AdS_{4+1} black hole of [113], where the (t, r) part of the metric is the same as AdS_{2+1}, so the zero-momentum quasinormal spectrum will have the same asymptotic behavior. In the dual theory, the correlators are then similar to a free theory, in contrast with the non-extremal black hole. This could be related to the fact that the topological black hole corresponds to D3 branes in the Milne universe, so non-renormalization theorems could still hold. The non-extremal black hole, on the other hand, corresponds to a high temperature phase of the theory.

In this analysis the AdS boundary has played a crucial role since it is there where the value of the quasinormal modes is determined. Other geometries, like asymptotically flat spacetimes, do not have a similar boundary, making it more difficult to find a similar prescription. Although in principle there could be a description of extended null geodesics bouncing on the singularities, it is not clear that they can return in the way they do in AdS spacetimes. Nevertheless addressing this issues could give interesting results.

The relation between null geodesics and the high-frequency singularities of the dual correlators also gives a good starting point to solve the inverse holographic problem: how to construct a gravitational background from the field theory. The information contained in the location of the singularities in time is quite topological, it only knows about the causal structure of the space-time. Interesting ideas related to the emergence of the causal structure of the bulk from the field theory can also be found in [114, 115]. For operators with large conformal dimension, the geodesic approximation could be used to gather more information, see [116] for instance.

Let us now discuss the holographic interpretation of the black hole computation for Green functions in the thermal field theory. In section 3.1 we explained the holographic prescriptions for computing Lorentzian correlators. Concretely, the relation between the Schwinger-Keldysh path and the second boundary of the eternal black hole that was pointed out in [78], whose analysis shows that there is only one SK path consistent with the prescription of [77] to compute the retarded Green function, corresponding to the symmetric choice $\sigma = \beta/2$ in the Schwinger-Keldish contour, see figure 3.1 (right). In the thermal field theory, the SK correlator is built introducing insertions of operators at $\mathrm{Im}\, t = 0$ or $\mathrm{Im}\, t = -i\beta/2$, so it is a matrix with components

$$G_{SK}(t) = \begin{pmatrix} G_F(t) & G^<(t+i\beta/2) \\ G^>(t-i\beta/2) & G_F(t)^\dagger \end{pmatrix},$$

where $G^>(t)$, $G^<(t)$ are the Wightman Green functions and $G_F(t)$ is the time-ordered (Feynman) correlator. The relation between the Feynman and the Wightman Green functions, together with the KMS relation[2]

$$\begin{aligned} G_F(t) &= \theta(t)\left(G^>(t) - G^<(t)\right) + G^<(t)\,, \\ G^>(t) &= G^<(t+i\beta)\,, \end{aligned}$$

imply that the SK correlator should have singularities on the imaginary time axis. All these correlators can be written in terms of the spectral function, $\rho(t) = G^>(t) - G^<(t)$. The Fourier transforms read

$$G^>(\omega) = \mathrm{e}^{\omega\beta} G^<(\omega) = \frac{\mathrm{e}^{\omega\beta}}{\mathrm{e}^{\omega\beta}-1}\rho(\omega)\ ; \quad G_F(\omega) = \left(\theta(t) + \frac{1}{\mathrm{e}^{\omega\beta}-1}\right)\rho(\omega)\,.$$

Notice that all of them at least have poles at $\omega_n = 2\pi i n/\beta$, thus singularities at $t = i\beta n$ appear from the ultraviolet contribution of that poles to the time dependent correlators in the same way they did at the end of section 4.1. Since for $d > 2$ we find no such singularities, this means that the singularities associated to null rays should correspond to the commutator, that is the spectral function, since it is the combination for which such ultraviolet contribution vanishes. This is consistent with the identification of the singularities of frequency-dependent correlators with quasinormal modes.

The singularities of frequency-dependent thermal correlators computed from holography turn out to be poles, indicating that there is always an exponential decay with time. For fields with larger conformal dimensions the location of the poles is modified due to the shift of the quasinormal spectrum. Also notice that all this analysis has been made at zero momentum. At non-zero momentum the singularities of the spectral function move in the complex frequency plane, but they remain as poles, in contrast with Green functions at

[2]Which can be derived from the periodicity in imaginary time of Euclidean correlators.

weak coupling where poles open up in branch singularities. Also in [117] it was argued that higher curvature corrections in the bulk, that correspond to quantum corrections in the field theory, do not change the nature of the singularities. On the other hand the analysis of [118] shows that subleading corrections in the large-N expansion can introduce power-like tails in time. These corrections correspond to quantum corrections in the bulk, so it would be interesting to analyze Green functions in the black hole background beyond the classical approximation.

Chapter 5

Beyond hydrodynamics in the sQGP

In recent years a new paradigm concerning the high temperature behavior of QCD has been established: the strongly coupled Quark-Gluon Plasma (sQGP). Experimental results from heavy ion collisions at RHIC indicate that QCD at temperatures around $2T_c$ is strongly interacting, in spite of being in a deconfined phase, and thus rendering perturbative computations not suitable for describing it. In the previous chapters, we have seen how holography can be a useful tool to understand analytically the dynamics of non-Abelian gauge theories in the strongly coupled plasma phase by performing classical computations in the asymptotically AdS black hole gravity duals. In this chapter we apply the holographic techniques explained before in order to study the response of the plasma to small external perturbations, paying special attention to the hydrodynamic regime and its domain of validity. Our gravity background is given by (2.14), thus our dual field theory is the plasma phase of the strongly coupled $\mathcal{N}=4$ gauge theory. Nevertheless, the results might be relevant also for RHIC physics.

Hydrodynamic modes like diffusion, shear or sound modes are also described by quasinormal modes in the gravity dual. They are special cases of quasinormal modes whose frequencies vanish in the zero momentum limit [92,93]. One of the most interesting results of this AdS black hole hydrodynamics has been the derivation of a universal bound for the shear viscosity to entropy ratio $\frac{\eta}{s} \geq \frac{\hbar}{4\pi k_B}$ [119, 120] for field theories that admit a supergravity dual description[1]. It has also been argued that this value is relevant to the description of heavy ion phenomenology at RHIC [125]. The shear viscosity is a hydrodynamic transport coefficient governing the momentum diffusion through the medium. One way to derive it is to compute the lowest quasinormal frequency in the retarded two-point correlator in the vector channel of the stress tensor.

The hydrodynamic approximation can be interpreted as a low energy effective theory where all the degrees of freedom except the hydrodynamic modes have been integrated out. It is then possible to make a systematic expansion in higher derivative terms, whose coefficients depend on the microscopic physics. The first order terms correspond to the usual hydrodynamic equations, while second order terms take into account the finite de-

[1] It has been shown that this bound can be violated in effective theories of higher derivative gravity, like Gauss-Bonnet theories [121–123], or in gauge theories that have different central charges [124].

lay in the response of the system. Second order hydrodynamics is important since the relativistic first order formalism leads to the well-known problem of acausal signal propagation. As it is reviewed in appendix A.3, the speed of signal propagation is determined by the so called front velocity $v = \lim_{\omega\to\infty} \frac{\omega}{q^R}$, with q^R the real part of the complex momentum mode. Diffusion equations as they arise typically in first order hydrodynamics do not have a finite front velocity and therefore allow acausal behavior. In second order hydrodynamics the non-zero delay of the response is encoded in a relaxation time constant and can restore causality [126–129]. The latter have been recently computed for conformal theories using the AdS/CFT correspondence [130–133]. However, even second order hydrodynamics cannot simply be extended to arbitrary short wavelengths or high frequencies and thus a front velocity smaller than the speed of light in second order hydrodynamics is not guaranteed, since inevitably the hydrodynamic description breaks down at small wavelengths. Thus the question arises how causal signal propagation is guaranteed in the $\mathcal{N}=4$ plasma at strong coupling. We will show numerically that the hydrodynamic mode approaches the front velocity $v_{\mathrm{F}} = 1$ and argue that this is indeed the exact value for all quasinormal modes including the hydrodynamic diffusion modes.

As an effective theory, the hydrodynamic approximation will be valid up to energies of the order of the microscopic scale, in this case given by the temperature T. At weak coupling hydrodynamic modes are collective excitations made up by the collective motion of the hard particles. Therefore they actually should decouple at short wavelengths. In standard perturbative finite temperature field theory and in the HTL approximation collective excitations do indeed appear already in the two-point correlators of the fundamental fermion and gauge fields. At weak coupling one distinguishes a soft scale of order gT from a hard scale T. Above T the hard partons are the quarks and gluons of the elementary fields, at the soft scale there are quasiparticles, dressed quarks and gluons and collective excitations, i.e. the plasmon and plasmino modes [85,134,135]. They show up as poles in the retarded two-point functions but can be distinguished by the behaviour of the residues at momenta at or above the hard scale T: the residues of the collective excitations decay exponentially signaling their decoupling at short wavelengths. What can we expect then for the quasinormal modes? In fact the high frequency and short wavelength limit can be interchanged with the $T \to 0$ limit [94]. Going to zero temperature an infinite number of quasinormal modes come together and open up a branch cut, characteristic for the $T = 0$ retarded correlators. Therefore, the residues of almost all quasinormal modes should not decay in this limit. However, a finite number might still decouple, and indeed this is what we find for the residues of quasinormal modes representing diffusive behaviour at long wavelengths.

In what follows we present an analysis of the residues of the quasinormal modes and complex momentum modes of R-current and energy-momentum tensor correlators. In

section 5.1 we recall how linear response theory is related to hydrodynamic behaviour. We study the regime of validity of the hydrodynamic approximation and define a lower bound in length and time scales. Since hydrodynamic simulations of the QGP evolution are a key point in the paradigm of the sQGP, it is of utmost importance to be able to define hydrodynamic time scales from when on such approximation is valid. In section 5.2 we discuss how the retarded Green function can be expressed as infinite sums over the poles at the quasinormal frequencies or complex momenta. We point out that these sums do not converge and analytic terms are needed to regularize the sums. These analytic terms should not be confused with contact terms arising from the action.

In sections 5.3 and 5.4 we study quasinormal frequencies and complex momentum modes and their residues for R-charge correlators and stress tensor correlators respectively. We find that the behaviour of the hydrodynamic mode in the shear channel is very similar to the one in the diffusion channel for the R-charge correlators. Both of them decouple for short wavelengths, signaling a breakdown of the effective field theory based on the hydrodynamic mode alone. This is not the case in the sound channel: the lowest mode, the sound mode, does not decouple at short wavelengths. It becomes similar to a higher quasinormal mode. We also study how well the spectral functions can be approximated by summing only over the contributions of the lowest quasinormal modes. Knowledge about the complex momentum eigenvalues for fixed real frequencies allows us to compute (numerically) the front velocity. We find that the front velocity for all modes, even the hydrodynamic one, is in agreement with causal signal propagation.

5.1 Hydrodynamic scales and linear response theory

We consider a medium in thermal equilibrium. By now we know that linear response theory is enough to study the effect of small external perturbations when their energy is negligible compared to the total energy of the system. The response of a field Φ to a perturbation represented by an external source $j(t, \mathbf{x})$ is given by (3.22). We saw in section 3.3 that if we make an analytic continuation to the complex ω plane the retarded Green function is of the form (3.23) and assuming that the source does not introduce new non-analyticities, the response is given by (3.26) as a sum over complex frequency poles. Therefore, the location of the quasinormal modes determine their frequency and damping and their residues determine how much each mode contributes to the response. For each channel corresponding to a gauge invariant operator in the dual gauge theory there is an infinite tower of quasinormal modes. Since for holographic duals of gauge theories there exist infinitely many quasinormal modes the precise form of the response also depends on the form of the source. There is however an exception to this: the extreme long-wavelength modes of conserved charges such as energy and momentum. Perturbations that induce a

change in the overall charge have to excite the special hydrodynamic modes. These are modes whose quasinormal frequencies obey $\lim_{\mathbf{q}\to 0}\omega_{\mathrm{H}}(\mathbf{q}) = 0$. This behaviour guarantees that the integrated response $\int \mathrm{d}^3\mathbf{x}\,\langle\Phi(t,\mathbf{x})\rangle$ is time independent, as it has to be for a conserved charge. Notice however that there is no fundamental reason that would forbid neutral perturbations to dissipate away primarily in the higher quasinormal modes, i.e. the infinite tower of modes with non vanishing zero momentum limit. It is also interesting to think about what the presence of the infinitely many quasinormal modes mean for the formulation of an initial value problem. Let us assume for the moment that there would be only one quasinormal mode, e.g. a diffusion mode in a conserved charge. The time development for $t > 0$ would then be completely determined by specifying the expectation value of the field at $t = 0$, i.e. $\langle\Phi(0,\mathbf{x})\rangle = \Phi_0(\mathbf{x})$. Indeed, cutting the sum in (3.26) after the first term, the hydrodynamic term in this case, leaves us with a one-to-one relationship between the initial value and the source $\widetilde{\Phi}_0(\mathbf{q}) = R(\mathbf{q})\,\tilde{\jmath}(\mathbf{q})$. However, in our case there are infinitely many quasinormal modes and therefore one has to specify not only the field at $t = 0$ but also an infinite number of its time derivatives in order to be able to compute the source from the initial condition. Strictly speaking the system becomes non-Markovian due to the presence of the infinitely many quasinormal modes: it remembers (at least for short times) the history of how it reached a certain state. Putting it another way, we can define a system to be in local thermal equilibrium if it has no memory, i.e. the response is completely dominated by the hydrodynamic mode.

We will concentrate on simple forms of source perturbations. We imagine that the source acts only over a time interval Δt. Such a perturbation will excite a significant number of quasinormal modes for small Δt and in the limit where $\Delta t \to 0$ it will excite all quasinormal modes with equal weight. We can then assume a source of the form $j(t,\mathbf{x}) = \delta(t)\cos(\mathbf{q}\mathbf{x})$.

At small values of the momentum, the hydrodynamic mode dominates the long time behaviour since it has the smallest imaginary part. In fact, we can define the hydrodynamic time scale, from which on the hydrodynamic mode dominates and the hydrodynamic approximation is good, by demanding that the response in the hydrodynamic mode equals the response in the first quasinormal mode at the time τ_{H}. We can estimate this time scale using (3.26)

$$\tau_{\mathrm{H}} = \frac{\log|R_{\mathrm{H}}\,\tilde{\jmath}_{\mathrm{H}}| - \log|R_1\,\tilde{\jmath}_1|}{\Gamma_{\mathrm{H}} - \Gamma_1}\,, \tag{5.1}$$

where we have written $\tilde{\jmath}_n = \tilde{\jmath}(\omega_n(\mathbf{q}),\mathbf{q})$. The hydrodynamic description will be trustable for times larger than τ_{H}, whereas for shorter times the contribution of higher modes must be taken into account.

In the same way we did in section 3.3, we can again switch the roles of time and space and consider periodic perturbations localized in space, over an interval Δx in the x

direction. In the limit $\Delta x \to 0$ the source as the form $j(t, \mathbf{x}) \propto \delta(x)$. The response of the system is then given by (3.29) as a sum over complex momentum poles. Analogously to what we did before, we can define a hydrodynamic length scale. From (3.29) we find

$$\ell_{\mathrm{H}} = \frac{\log|R_{\mathrm{H}}| - \log|R_1|}{\mathrm{Im}\, q_{\mathrm{H}} - \mathrm{Im}\, q_1} \ . \tag{5.2}$$

For distances from the origin of the perturbation larger than ℓ_{H}, the hydrodynamic mode will dominate the response of the system. We emphasize that the definition of the hydrodynamic length scale (5.2) applies only if the sources are localized in space. For a more general source, the Fourier transform evaluated at the complex momentum mode $\tilde{\jmath}(\omega, \mathbf{q}_n(\omega))$ will enter in the definition of ℓ_{H} in an analogous way to (5.1).

As we have seen the response and the hydrodynamic scales depend crucially on the knowledge of the residues of the retarded correlators. In the following we will determine them numerically and study such hydrodynamic scales.

5.2 Including higher thermal resonances

The hydrodynamic mode provides a good description of the system at very long wavelengths $\omega, q \ll T$. As we have argued, for shorter times or distances the holographic computation shows that higher modes start to be relevant. It is an interesting question to see if a description in terms of the hydrodynamic mode plus a few thermal resonances gives a reasonable good model of the plasma up to frequencies of the order of the temperature $\omega \sim T$. What we mean by thermal resonances are the quasinormal modes found in the holographic dual, that describe the dissipation of gauge-invariant configurations.

Due to conformality, the properties of the $\mathcal{N} = 4$ plasma rescale trivially with the temperature T. A possible way to introduce a non-trivial temperature dependence would be to compactify the theory in a three sphere of radius R. The compactification breaks conformal invariance, so there is a non-trivial dependence on RT. Then, the physics of the plasma in flat space $R \to \infty$ can also be recovered in the infinite temperature limit $T \to \infty$ [63]. Computations of the quasinormal mode spectrum at lower temperatures $RT \geq 1$ [89, 136] show that the lowest modes are long lived enough to have a good quasiparticle interpretation. Other computations in the context of flavor branes, where high and low temperature is given in terms of the quark mass m_q/T, also show similar results for the quasinormal spectrum of mesons [137–140]. This suggests that for more realistic plasmas, e.g. non-conformal and maybe closer to the intermediate temperature regime between the deconfinement transition and the free gas limit than the simpler models just mentioned, a description in terms of bound states could be appropriate, although usually colored bound states are considered [141–143]. In spirit, this approach is similar

to the description of QCD correlators at low energies using the lowest states of the meson spectrum.

From the linearized AdS/CFT computation, we know that the retarded correlators of channels with hydrodynamic modes have the general form

$$\widetilde{G}_{\mathrm{R}}(\omega,q)=\sum_{i=1}^{n_{\mathrm{H}}}\frac{R_{\mathrm{H}}^{(i)}}{\omega-\Omega_{\mathrm{H}}^{(i)}}+\sum_{n=1}^{\infty}\frac{R_n}{\omega-\omega_n}+\frac{-R_n^*}{\omega+\omega_n^*}+\mathcal{A}(\omega,q)\ , \tag{5.3}$$

where Ω_{H}, ω_n are the hydrodynamic and quasinormal poles, R_{H}, R_n their residues and n_{H} is the number of hydrodynamic modes. For the shear and diffusive channels $n_{\mathrm{H}}=1$, while for the sound channel $n_{\mathrm{H}}=2$ and $\Omega_{\mathrm{H}}^{(2)}=-\Omega_{\mathrm{H}}^{(1)\,*}$, $R_{\mathrm{H}}^{(2)}=-R_{\mathrm{H}}^{(1)\,*}$.[2] The term $\mathcal{A}$ denotes possible terms analytic in frequency and momentum. In principle they look like the contact terms that can arise from Ward identities or some choice of renormalization scheme, in which case they could be absorbed by a finite number of counterterms. However, their origin is different and we will see that they are necessary in order to give a consistent Green function, the main reason being the infinite sum over quasinormal modes.

Let us concentrate on a particular example, the density-density correlator of the R-current. In [139] the explicit form of the current-current correlator at zero momentum was found ($\mathfrak{w}:=\omega/(2\pi T)$),

$$G_{ij}(\mathfrak{w})=\delta_{ij}\frac{N^2T^2}{8}\left\{i\mathfrak{w}+\mathfrak{w}^2\left[\psi\left(\frac{(1-i)}{2}\mathfrak{w}\right)+\psi\left(\frac{-(1+i)}{2}\mathfrak{w}\right)\right]\right\}\sim\sum_n\frac{\widetilde{R}_n}{\mathfrak{w}-\mathfrak{w}_n}\ . \tag{5.4}$$

The poles and its residues can be extracted from the following representation of the digamma function

$$\psi(x)=-\gamma_{\mathrm{E}}-\sum_{n=1}^{\infty}\left(\frac{1}{x-1+n}-\frac{1}{n}\right)\ , \tag{5.5}$$

so the residues will scale as $\widetilde{R}_n\sim\mathfrak{w}^2\,r_n$, with $r_n\sim 1$ and the frequencies $\mathfrak{w}_n\sim n$. Evaluated at the pole this gives $\widetilde{R}_n\sim\mathfrak{w}_n^2\,r_n\sim n^2$, as was confirmed numerically in [2]. Using current conservation, the density-density correlator is related to the longitudinal current-current correlator through $G_{tt}=\frac{q^2}{\omega^2}G^L_{ii}$, so the residues of the density-density correlator go as $R_n\sim q^2\,r_n\sim q^2$.

The imaginary part of the retarded correlator receives a contribution from the quasinormal modes

$$\mathrm{Im}\,\widetilde{G}_{\mathrm{R}}\sim\omega\sum_n\frac{\mathrm{Im}\,\left(\omega_n^2R_n\right)}{\left(\omega^2-\mathrm{Re}\,\omega_n^2\right)^2+\left(\mathrm{Im}\,\omega_n^2\right)^2}\sim q^2\omega\sum_n\frac{1}{n^2}\ . \tag{5.6}$$

[2]There exist of course also channels without any hydrodynamic behaviour $n_H=0$, such as scalar field perturbations. We will not consider these channels.

The sum over the quasinormal modes is convergent in this case. On the other hand the real part goes as

$$\mathrm{Re}\,\widetilde{G}_{\mathrm{R}} \sim \sum_n \frac{|\omega_n|^2 \mathrm{Re}\ (\omega_n^* R_n)}{(\omega^2 - \mathrm{Re}\,\omega_n^2)^2 + (\mathrm{Im}\,\omega_n^2)^2} \sim q^2 \sum_n \frac{1}{n}\ . \tag{5.7}$$

In this case the sum is not convergent, although the Green function is finite. The divergence of the sum over quasinormal modes can be cured by subtracting a divergent analytic part, or in a better defined way, subtracting order by order a small analytic part. The analytic term would look

$$\mathcal{A} = \sum_n \mathcal{A}_n \sim -q^2 \sum_n \frac{1}{n}\ . \tag{5.8}$$

In order to give a consistent approximation to the retarded correlator, the analytic term must be properly taken into account. For the first m modes

$$\widetilde{G}_{\mathrm{R}}(\omega, q) \simeq \frac{-iq^2\sigma_{\mathrm{H}}(q)}{\omega + iq^2 D_{\mathrm{H}}(q)} + q^2 \sum_{n=1}^{m} \left(\frac{r_n(q)}{\omega - \omega_n(q)} + \frac{-r_n^*(q)}{\omega + \omega_n^*(q)} \right) - C_m q^2, \quad \omega, q < T\ , \tag{5.9}$$

where we have defined the hydrodynamic pole and residue in terms of a q-dependent 'conductivity' and 'diffusion coefficient' $R_{\mathrm{H}} = -i\,q^2\sigma_{\mathrm{H}}(q)$ and $\Omega_{\mathrm{H}} = -i\,q^2 D_{\mathrm{H}}(q)$. In the zero momentum limit, they take the value of the known constant transport coefficients $D = 1/(2\pi T)$, $\sigma = N^2 T/16\pi$. The coefficient of the analytic term C_m depends on the number of modes and diverges when $m \to \infty$. The exact Green function including all the modes would differ by a small amount from this approximation at small enough frequencies.

In the hydrodynamic approximation only the mode associated to diffusion would be considered, adding higher derivative corrections to the effective description as momentum increases. It is then interesting to find out its exact behaviour beyond the hydrodynamic limit from the holographic dual.

5.3 R-charge current correlators

We now consider the conserved current J_μ associated to the global R-symmetry in the $\mathcal{N}=4$ theory

$$\partial^\mu J_\mu = 0\ . \tag{5.10}$$

The diffusion of the R-charge $Q = \int \mathrm{d}^3\mathbf{x}\, J_0$ is described by a hydrodynamic mode, that at low frequencies and momenta dominates the response of the system to small perturbations j_μ

$$\langle \delta J_\mu(t, \mathbf{x}) \rangle = -\int \mathrm{d}t'\, \mathrm{d}^3\mathbf{x}'\, G_{\mu\alpha}(t - t', \mathbf{x} - \mathbf{x}')\, j^\alpha(t', \mathbf{x}')\ . \tag{5.11}$$

The global current J_μ is dual to a five-dimensional gauge field A_M.[3] We work in the gauge $A_r = 0$. The gauge invariant quantities are the longitudinal and transverse electric fields

[3] That is actually a component of the metric with the group index associated to an internal space.

$E_L = qA_0 + \omega\,\mathbf{q}\cdot\mathbf{A}/q$, $\mathbf{E}_T = \omega\mathbf{A}_T$, where $\mathbf{q}\cdot\mathbf{A}_T = 0$. We describe the method to find the quasinormal modes in the appendix A.1.

The retarded two-point functions can be expressed in terms of two scalar functions Π_T and Π_L corresponding to transverse and longitudinal polarizations, assuming $\mathbf{q} = (0, 0, q)$

$$\widetilde{G}_{TT} = \Pi_T \ , \qquad \widetilde{G}_{tt} = \frac{q^2}{\omega^2 - q^2}\,\Pi_L \ , \tag{5.12}$$

$$\widetilde{G}_{tz}(\omega, q) = \frac{\omega}{q}\,\widetilde{G}_{tt}(\omega, q) \ , \qquad \widetilde{G}_{zz}(\omega, q) = \frac{\omega^2}{q^2}\,\widetilde{G}_{tt}(\omega, q) \ . \tag{5.13}$$

The results for residues $R_n^{T,L}$ of the quasinormal modes of the scalar functions $\Pi_{T,L}$ are plotted in figure 5.1. We have also computed the quantities $\sigma_{\rm H}(q)$ and $D_{\rm H}(q)$ and they are shown in figure 5.2. We remark that the residues of the density-density correlator are actually

$$R_n^{(tt)} = \frac{q^2}{\omega_n^2(q) - q^2}\,R_n^{(L)}(q) \ . \tag{5.14}$$

The longitudinal fluctuations show interesting behaviour related to the diffusion mode. The peaks and dips in Figure 5.1 appear roughly at the locations where the hydrodynamic mode [4] crosses the imaginary part of the quasinormal frequency.

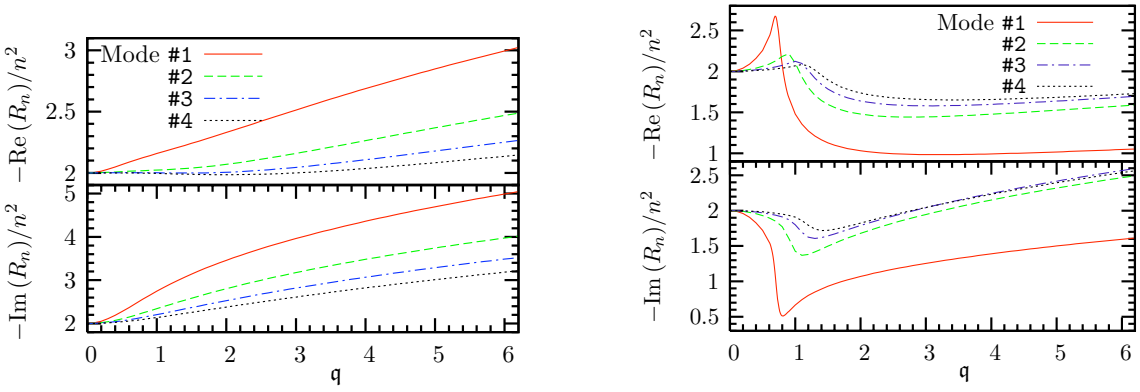

Figure 5.1: *(Left) Real and imaginary parts of the residues for the first four quasinormal modes in the transverse component E_T. (Right) Idem for longitudinal component E_L. The n^2 scaling is necessary to recover the asymptotic behaviour of the spectral function at large frequencies. Close to the crossing with the diffusion mode $\mathfrak{q} \sim 1$, the residues of the longitudinal component present peaks. The residues grow with momentum, this is also reflected in the growth of the spectral function. All the numerical values of residues are normalized by a factor $N^2T^2/8$ in what follows.*

The hydrodynamic mode behaves in a very different way. The diffusion pole quickly moves towards negative imaginary frequencies, while the residue first grows according to hydrodynamics and later goes over into a damped oscillation with the momentum, as shown in figure 5.2. Such oscillatory behavior the residue of the diffusion mode, implies

[4] We continue calling it like this even outside the regime of validity of the hydrodynamic approximation.

that for a finite value of $q < 2\pi T$ the q-dependent conductivity we have defined becomes zero and then negative. Notice that the analytic corrections that can come from higher modes would not solve this problem, so clearly the diffusion mode does not have a good hydrodynamical interpretation anymore. Furthermore, the residue vanishes exponentially with increasing momentum, so this mode decouples and the system leaves the hydrodynamic regime. The zeros appear when the diffusion pole reaches the value of the imaginary part of the quasinormal frequencies at zero momentum. The values of the momentum when this happens can be found analytically (appendix A.2). At a slightly smaller value of the momentum the imaginary part of the n^{th} higher quasinormal mode becomes smaller than the value for the hydrodynamic mode, i.e. the diffusion mode crosses the n^{th} quasinormal mode. This first happens at around $\mathfrak{q} = 0.68$. The time development is then dominated by the contribution of the lowest quasinormal modes instead of the hydrodynamic mode. In the section 5.4 we will find an analogous behaviour in the shear diffusion mode of the stress tensor two-point function.

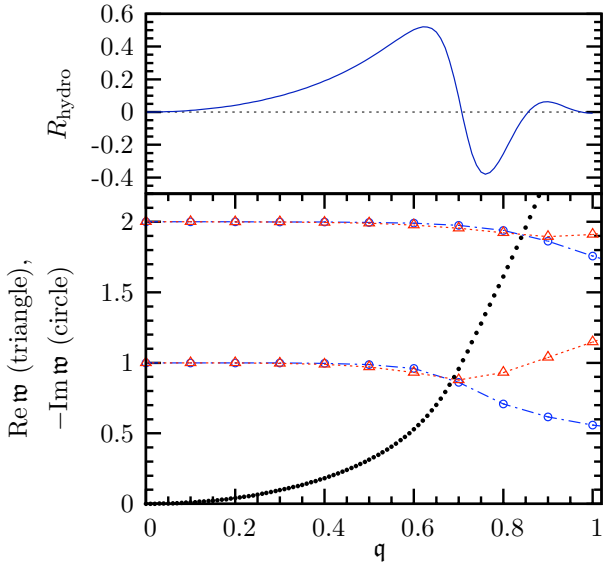

Figure 5.2: *In the lower figure, we show the real and imaginary parts of the quasinormal frequencies in the longitudinal channel and the value of the frequency for the diffusion mode. The quasinormal frequencies remain fairly stable as momentum increases, until there is a 'crossing' with the diffusion mode (it reaches a special value $\mathfrak{w} = -in$). From there on the quasinormal frequencies start approaching the real axis. The residue of the diffusion mode, in the upper figure, behaves according to hydrodynamics $\sim q^2$ for small momentum. For larger momentum, it shows an oscillatory decaying behaviour. The zeros of the residue coincide with the 'crossing' values.*

A way to estimate the regime of validity of the hydrodynamic approximation is to introduce an external perturbation, localized in time or space and compute the hydrodynamic time (5.1) or length (5.2) scales. In the first case we consider the evolution of the charge density (given by G_{tt}), while in the second case we do it for the longitudinal component of

the current (given by G_{zz}). The time-localized source is a plane wave of fixed momentum q that begins at $t = 0$ and last some time Δt. The perturbation creates inhomogeneities that start to relax to equilibrium after it is switched off. The late time relaxation will be dominated by the diffusion mode. If the perturbation lasts for a long time, it is possible for the system to reach a steady state already dominated by the diffusion mode. This seems to be the case as long as Δt is a few times the inverse temperature. If the perturbation is short lived, then we find that the minimal time to enter the diffusion dominated regime is $2\pi T\tau_{\rm H} \sim 0.35$. We also find that for short wavelengths, when q approaches the value of the zero of the hydro residue, $\tau_{\rm H}$ grows unbounded. So for wavelengths of the order of the inverse temperature or higher, the relaxation to equilibrium is never dominated by the diffusion mode, but by higher modes.

The space-localized source is a pulse constant on x and y directions and localized in the z direction with size Δz. The pulse is oscillating with some fixed frequency ω. The perturbation will be screened as we move in the z direction far from the plane where the pulse is localized. At large enough distances, the diffusion complex momentum mode would dominate the decay of the perturbation. We find that if the size of the pulse is larger than the scale given by the temperature $\Delta z > 1/T$ and the frequency is low enough $\omega < 2\pi T$, the screening is dominated by the hydro mode at any distance. However, at higher frequencies the diffusion mode starts dominating at larger distances from the source, so $\ell_{\rm H} > 0$. When the size of the source is of the order of the inverse temperature, finite size effects like the shape of the perturbation start to be important to determine the hydrodynamic length scale. In our definition of hydrodynamic time and length scales there is an explicit dependence on the source,

$$\tilde{j} = \begin{cases} \frac{\sin(\omega\Delta t)}{\omega} & \text{localized in time} \\ \\ \frac{\sin(q\Delta x)}{q} & \text{localized in space} \end{cases} \tag{5.15}$$

The source is evaluated at the value of the of the mode $\omega_n(q)$ or $q_n(\omega)$. For large values of the frequency or the momentum, the $\sim 1/\omega$, $1/q$ scaling determines the response, while for very low values it is constant. For intermediate values however, the sine function introduces an oscillatory behaviour. In general, we will find different answers for different kind of perturbations, depending on their shape.

In summary, no matter the value of q for the time-dependent source there is a minimal hydrodynamic time scale $\tau_{\rm H}$ if the duration of the perturbation is short enough. However, for the space-localized source one can always lower the frequency to a value where the length $\ell_{\rm H}$ becomes zero, no matter how small the source is.

The validity of the hydrodynamic regime can also be studied through the spectral function. As a first approximation we could pick only the diffusion mode. However, the

spectral function and the residue have the same sign, so the approximation would clearly fail at the first zero. This means that in order to have a sensible approximation for larger values of the momentum, we must take into account higher modes. We will see that this solves the problem.

Following the discussion in section 5.2, we can compare the results from the exact retarded density-density correlator $\widetilde{G}_{tt}$ with the approximation taking the first four quasinormal modes or just the hydrodynamic mode. In order to fix the analytic term C_4 in (5.9), we equate the values of the exact and the approximate Green functions at zero frequency and $\mathfrak{q} = 0.2$, giving $C_4 \simeq 3.9$. In figure 5.3 we can see that the approximation for fixed momentum is very good in the interval $\mathfrak{w} < 1$, even for larger values of the momentum.

Figure 5.3: *Imaginary (left) and real (right) parts of the retarded G_{tt} correlator as a function of the frequency at $\mathfrak{q} = 0.2$ (black) and $\mathfrak{q} = 0.4$ (grey). The dotted line is the hydrodynamic mode contribution, the solid line is the exact solution and the dashed line is the four-mode approximation.*

We also present the residues of complex momentum modes in figures 5.4 and 5.5. Again these are the residues of the scalar functions $\Pi_{T,L}$. We find that contrary to the quasinormal modes, the hydrodynamic mode does not decay at high frequencies.

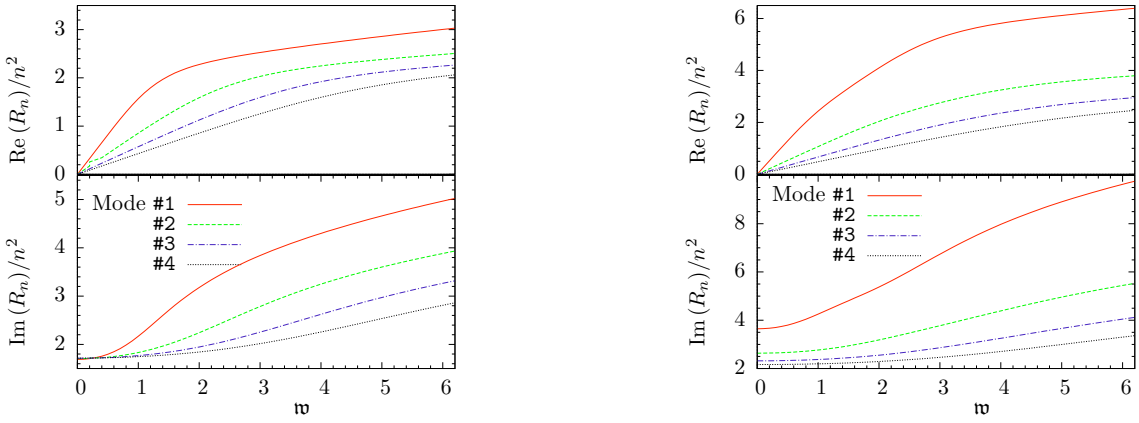

Figure 5.4: *(Left) Real and imaginary parts of the residues for the first four complex momentum modes in the transverse component Π_T. (Right) Idem for longitudinal component Π_L.*

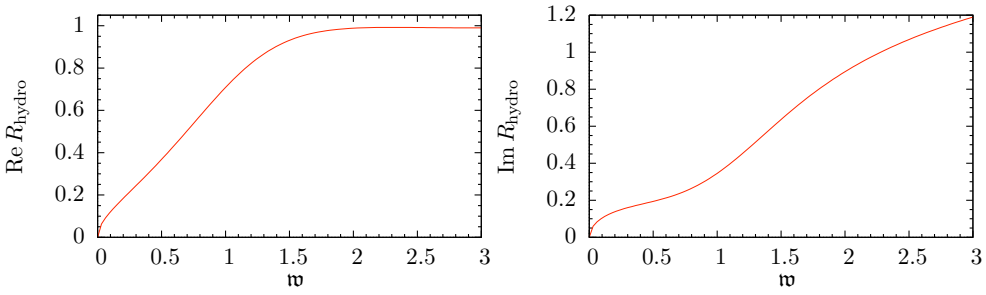

Figure 5.5: *Real and imaginary parts of the residues for the diffusion complex momentum mode.*

In [102] the locations of the complex momentum modes in the R-charge diffusion channel have been studied. It was found numerically that the real part of the complex momentum approaches ω whereas the imaginary part becomes smaller and smaller at high frequency for all the modes. Furthermore we argued in the introduction that the high frequency and momentum limit can be exchanged with the zero temperature limit $T \to 0$. The theory at $T = 0$ recovers Lorentz symmetry and in the case at hand even conformal symmetry. This restricts all signal propagation at $T = 0$ automatically to the light cone, showing that indeed $v_F = 1$.

5.4 Energy-momentum tensor correlators

The energy-momentum tensor is a conserved quantity

$$\partial^\mu T_{\mu\nu} = 0 \ , \tag{5.16}$$

we can identify $E = \int \mathrm{d}^3\mathbf{x}\, T_{00}$ and $P_i = \int \mathrm{d}^3\mathbf{x}\, T_{0i}$ as the conserved energy and momentum. Since they are conserved and cannot be dissipated away, they will slowly spread through the plasma or they will be displaced between different regions. This is described by the hydrodynamic shear and sound modes. The response to an external perturbation represented by the source $j_{\mu\nu}(t, \mathbf{x})$ is given by

$$\langle \delta T_{\mu\nu}(t, \mathbf{x}) \rangle = -\int \mathrm{d}t'\, \mathrm{d}^3\mathbf{x}'\, G_{\mu\nu,\,\alpha\beta}(t - t', \mathbf{x} - \mathbf{x}')\, j^{\alpha\beta}(t', \mathbf{x}') \ , \tag{5.17}$$

where $G_{\rm R}$ is the retarded two-point function. For low frequencies and momentum (large times and distances), the response is dominated by the hydrodynamic modes.

The energy-momentum tensor $T_{\mu\nu}$ in the gauge theory is dual to the five-dimensional metric g_{MN}. We work in the linear approximation, so we will consider small fluctuations h_{MN} on top of the background metric of a planar black hole in AdS_5 space (2.14). We fix the gauge to $h_{rM} = 0$ and expand the metric components in plane waves $h_{\mu\nu}(t, \mathbf{x}, r) = \mathrm{e}^{-i\omega t + i\mathbf{q}\mathbf{x}} h_{\mu\nu}(r)$. It is convenient to use quantities that are gauge-invariant

under the residual diffeomorphism transformations and group them according to their representation under the rotational group. In this way, we can distinguish three different components, scalar, vector and tensor, that correspond to the sound, shear and scalar channels in the dual theory [98]. Assuming that the momentum is along the z direction, and using the dimensionless frequency and momentum $2\pi T(\mathfrak{w},\mathfrak{q}) := (\omega,\mathbf{q})$, the gauge-invariant quantities are

$$\begin{aligned}
&\text{(Shear)} \quad Z_{1i} &&= \mathfrak{q}H_{ti} + \mathfrak{w}H_{zi}, \quad i = x, y \ , \\
&\text{(Sound)} \quad Z_2 &&= \mathfrak{q}^2 H_{tt} + 2\mathfrak{w}\mathfrak{q}H_{tz} + \mathfrak{w}^2 H_{zz} + (\mathfrak{q}^2 - \mathfrak{w}^2 + rf'(r)/2)(H_{xx} + H_{yy}) \ , \\
&\text{(Scalar)} \quad Z_3 &&= H_{xy} \ ,
\end{aligned} \tag{5.18}$$

where $H_{\mu\nu} = h_{\mu\nu}/r^2$. The retarded Green function of the dual gauge theory can then be computed using the Lorentzian prescription (3.10). The method to find the quasinormal modes is explained in appendix A.1. The Green functions G_1, G_2, G_3 found using the Z_1, Z_2, Z_3 components are scalar quantities. They are the coefficients of the tensor projectors depending on ω and q in which energy-momentum correlators can be decomposed once Lorentz invariance is reduced to rotational invariance (c.f. [98]). For instance,

$$G_{tx,\,tx} = \frac{1}{2}\frac{q^2}{\omega^2 - q^2}\, G_1 \ , \tag{5.19}$$

$$G_{tt,\,tt} = \frac{2}{3}\frac{q^4}{(\omega^2 - q^2)^2}\, G_2 \ , \tag{5.20}$$

$$G_{xy,\,xy} = \frac{1}{2}\, G_3 \ . \tag{5.21}$$

We also compute the residues of the different modes. Notice that we are using the functions G_1, G_2 and G_3, so in order to recover the right residue for the different components of the energy-momentum tensor correlators, one should take into account the appropriate factors coming from the tensor projectors.

In the vector and scalar channels, the lowest quasinormal mode shows the right behaviour at low momentum to be identified with the shear ($\omega = -iDq^2$) and sound ($\omega = v_s q - i\Gamma_s q^2$) modes respectively. In figure 5.6 we compare our numerical results with the second order hydrodynamic approximations of [131]. From the Kubo formula of the tensor component $G_{xy,xy}$ the second order corrections including a term $\eta\,\tau_\Pi\,\omega^2$ have been identified with

$$\tau_\Pi = \frac{2 - \log 2}{2\pi T} \ . \tag{5.22}$$

According to the hydrodynamic expansion, the first corrections to the shear and sound poles would be

$$\begin{aligned}
\omega_{\text{shear}} &= -i\frac{\eta}{sT}q^2 - i\left(\frac{\eta}{sT}\right)^2 \tau_\Pi\, q^4 \ , \\
\omega_{\text{sound}} &= v_s q - i\Gamma_s q^2 + \frac{\Gamma_s}{v_s}\left(v_s^2\,\tau_\Pi - \frac{\Gamma_s}{2}\right) q^3 \ .
\end{aligned} \tag{5.23}$$

With η the shear viscosity, s the entropy density and v_s and Γ_s the sound velocity and the sound attenuation. However, in the holographic computation the dispersion relation for the shear mode differs from the second order hydrodynamic result. This discrepancy can be attributed to the necessity of going to third order hydrodynamics to capture the right $O(q^4)$ correction to the shear pole. In terms of the dimensionless variables the holographic theory gives the next to leading order corrections in the dispersion relations

$$\begin{aligned} \mathfrak{w}_{\text{shear}} &= -i\,\frac{\mathfrak{q}^2}{2} - i\frac{(1-\log 2)}{4}\,\mathfrak{q}^4\ , \\ \mathfrak{w}_{\text{sound}} &= \frac{\mathfrak{q}}{\sqrt{3}} - i\,\frac{\mathfrak{q}^2}{3} + \frac{3-2\log 2}{6\sqrt{3}}\,\mathfrak{q}^3\ . \end{aligned} \tag{5.24}$$

When we compare the numerical results with these (fig. 5.6), we find a very good agreement up to $\mathfrak{q} \lesssim 1$. Similar comparisons between the exact values and first order hydrodynamics or the first corrections can be found in [95, 98, 131]. It seems justified then to consider just the first hydrodynamic corrections to describe the properties of the shear and sound modes up to frequencies of the order of the temperature $\omega, q \sim T$. Note however, that the q^4 term that arises from second order hydrodynamics obviously does not approximate the numerical result very well, clearly indicating that second order hydrodynamics is not valid to predict the q^4 terms as already pointed out in [131].

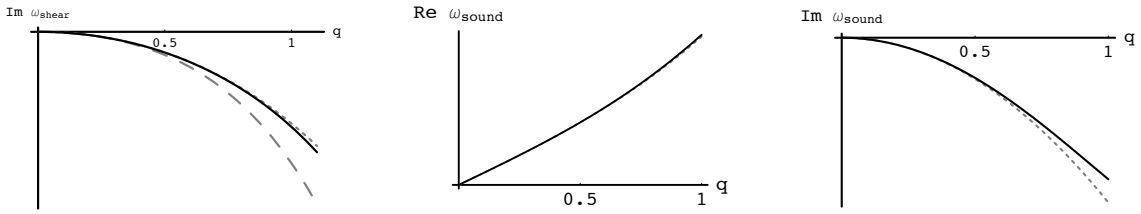

Figure 5.6: *(Left) The numerical value of the shear mode [solid black] compared with the correct expression [dotted gray] and the value from second order hydrodynamics [dashed gray]. (Middle) The numerical value of the real part of the sound mode [solid black] compared with the second order hydrodynamic approximation [dotted gray]. (Right) The numerical value of the imaginary part of the sound mode [solid black] compared with the second order hydrodynamic approximation [dotted gray].*

Again, we have also computed the complex momentum modes that describe the penetration depth of a perturbation inside the plasma as a function of the frequency [102]. Here we show the complex momentum modes for the sound channel in figure 5.7, while for the shear channel can be found in reference above. The results for the residues are displayed in figures 5.8 and 5.9. The zero frequency value corresponds to the inverse of the screening masses in the plasma. Again we find that the imaginary parts become smaller with increasing frequency and that the real parts approach the light cone $\omega/q \to 1$ indicating a front velocity $v_F = 1$ as in the other channels (see Appendix A.3).

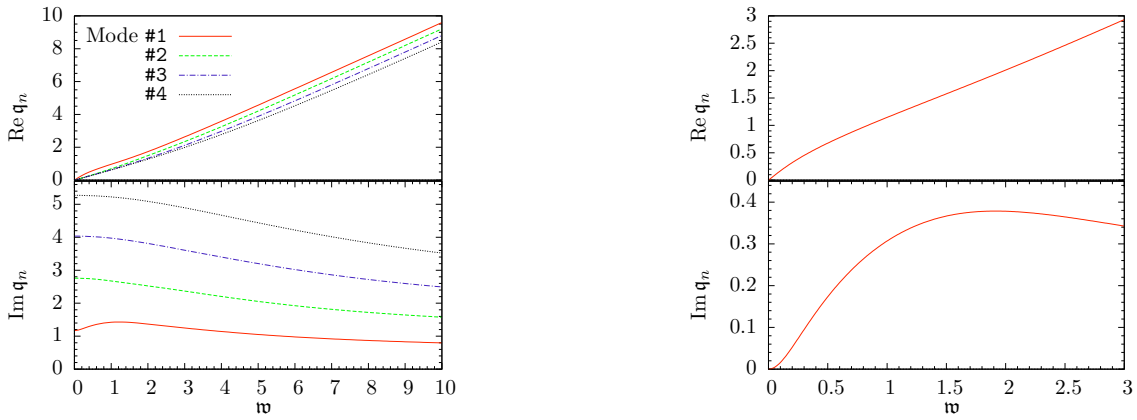

Figure 5.7: *(Left) Real and imaginary parts of the first four complex momentum modes in the sound channel. (Right) Idem for sound mode.*

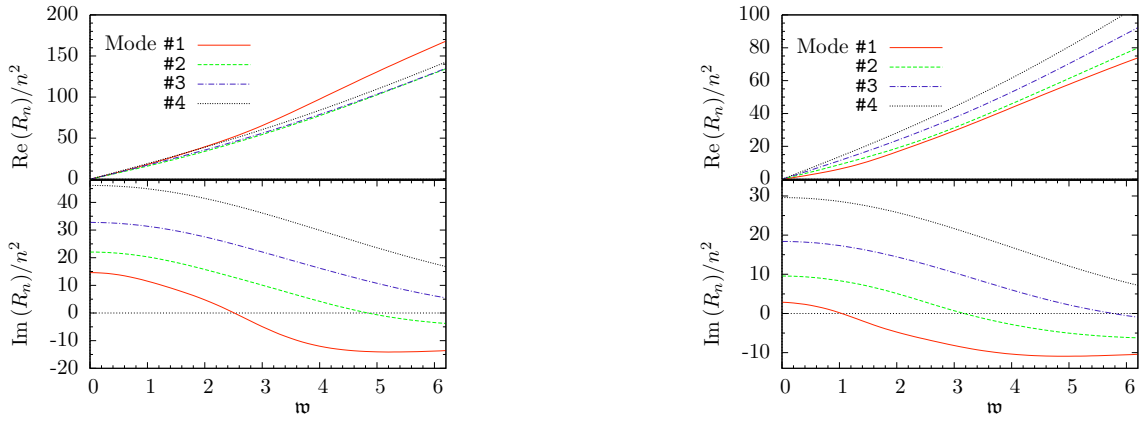

Figure 5.8: *(Left) Real and imaginary parts of the residues for the first four complex momentum modes in the shear channel. (Right) Idem for sound channel.*

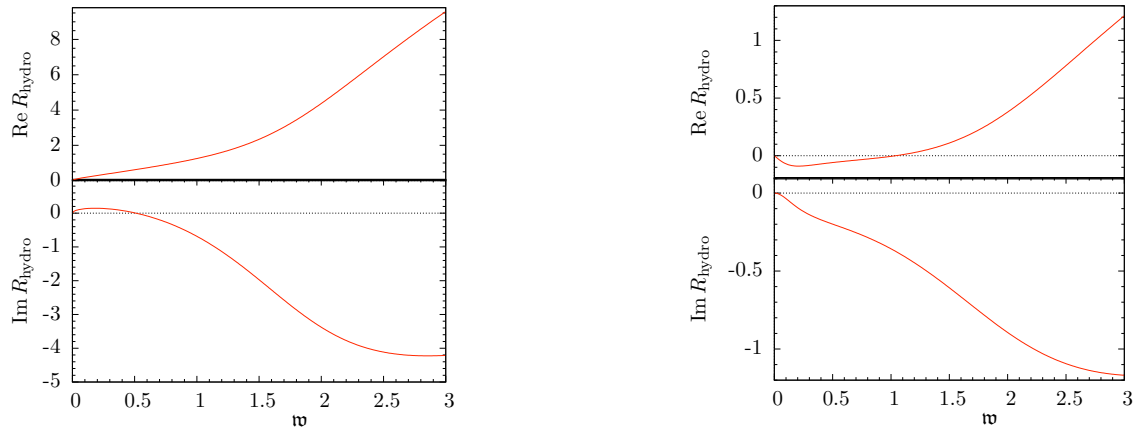

Figure 5.9: *(Left) Real and imaginary parts of the residue for the shear mode. (Right) Idem for the sound mode.*

Residues and higher thermal resonances.

In figures 5.10 and 5.11 we plot the residues of the lowest four quasinormal modes in the shear and sound channels. The residue in the shear mode (figure 5.11) shows a decaying and oscillatory pattern with increasing momentum, similar to the diffusion mode of the R-current. We can apply the same arguments here, at short enough wavelengths the first quasinormal mode will dominate the late time behaviour and the hydrodynamic approximation will not be valid. The sound mode on the other hand has a non-vanishing residue at high momentum, and its pole moves away from the real axis only for low values of the momentum, but then it behaves as an ordinary quasinormal mode, so it always dominates the late time response of the system.

Using the numerical values of the residues, we can study the hydrodynamic time (5.1) and length (5.2) scales for the shear and sound modes. Notice that the residues of the sound channel $R_n^{(2)}(q)$ we have computed are evaluated at the quasinormal frequencies and correspond to the 'scalar' Green function G_2. From (5.19), we can see that in order to expand $G_{tt,\,tt}$ as a sum over quasinormal modes we should use the residues

$$R_n^{(tt,\,tt)} = \frac{2}{3}\frac{q^4}{(\omega_n^2(q)-q^2)^2}\,R_n^{(2)}(q)\ . \tag{5.25}$$

In the shear channel we are computing the residues $R_n^{(1)}(q)$ of the function G_1 evaluated at the quasinormal frequencies. Using (5.19), the residues of $G_{tx,\,tx}$ should be

$$R_n^{(tx,\,tx)} = \frac{1}{2}\frac{q^2}{\omega_n^2(q)-q^2}\,R_n^{(1)}(q)\ . \tag{5.26}$$

However, contrary to the cases of the density-density correlator of the R-current or the $G_{tt,\,tt}$ correlator of the sound channel, the large frequency behaviour does not asymptote to a momentum-dependent constant ($\sim q^2$ or q^4), but to $\sim q^2(\omega^2-q^2)$. This means that there should be an implicit ω^2 dependence in the residues, but this is not shown by our computation. A way to partially recover the right dependence is to use the following definition

$$R_n^{(tx,\,tx)} = \frac{1}{2}\frac{\omega^2-q^2}{(\omega_n^2(q)-q^2)^2}\,q^2\,R_n^{(1)}(q)\ . \tag{5.27}$$

We consider the same kind of perturbations as for the R-current diffusion mode in section 5.3, one is a spatial plane wave of momentum q that is switched on only during a finite amount of time Δt. It sources the transverse and longitudinal momentum densities, whose response is given by $G_{tx,tx}$ and $G_{tt,tt}$. The other perturbation is a pulse of size Δz localized in the z direction that oscillates with frequency ω. We study the response of the transverse and longitudinal momentum currents given by for $G_{zx,zx}$ and $G_{zz,zz}$. The results for the shear mode are qualitatively the same as for the diffusion mode. For a short-lived time-localized source there is a minimal hydrodynamic time $2\pi T\tau_{\rm H} \sim 1.34$. The maximal

value of the momentum beyond which the relaxation to equilibrium is dominated by higher modes at late times is $q \sim 2.6\pi T$. For a space-localized source, for large enough $\Delta z > 1/T$ and small enough frequencies $\omega < 0.6\pi T$, the screening is well described by the complex momentum shear mode. For smaller sizes or higher frequencies in general the shear mode dominates only at a finite distance from the source $\ell_{\rm H} > 0$, unless the frequency is very low.

The sound mode behaves qualitatively different because its residue does not vanish at any value of the momentum. It always dominates the relaxation to equilibrium for long enough times or large enough distances as far as our computation can show. Higher modes dominate the response for a finite time after switching off the source for momenta $q > 1.2\pi T$. There is no minimal time for the sound mode, but since for large frequencies the sound mode behaves as any other mode, the behaviour will not be hydrodynamic until some finite time has passed if the source is very short-lived. If the source is localized in space, higher modes dominate at a finite distance for values of the frequency $\omega > 2.5\pi T$.

We can also study the validity of the hydrodynamic regime through the spectral function. As we found for R-current diffusion, the first zero of the shear residue implies a change of sign for the approximation with the shear mode alone, hence a failure of the hydrodynamic approximation. This happens around $\mathfrak{q} \sim 1.3$. We find that also the spectral function restricted to the sound mode alone changes sign but it is not related to a 'crossing'. It coincides approximately with the change of behaviour of the residues that can be observed in figure 5.10, close to $\mathfrak{q} \sim 1.1$. Therefore, in order to have a consistent description of the system for larger values of momentum, it is necessary to take into account higher modes.

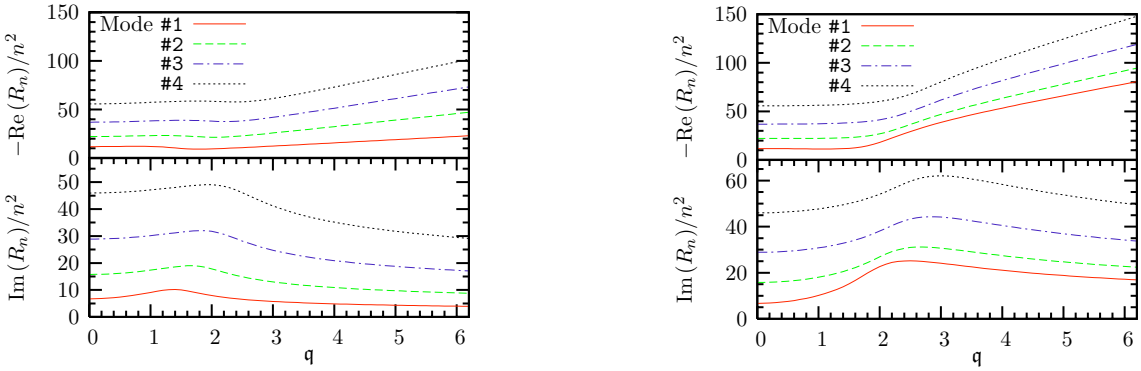

Figure 5.10: *(Left) Real and imaginary parts of the residues for the first four quasinormal modes in the shear channel. (Right) Idem for the sound channel. The numerical values are normalized by $\pi^2 N^2 T^4$ and the square of the mode number.*

Using these results for the residues and the frequencies of the first quasinormal modes we can build an approximation to the retarded correlator as explained in section 5.2. For

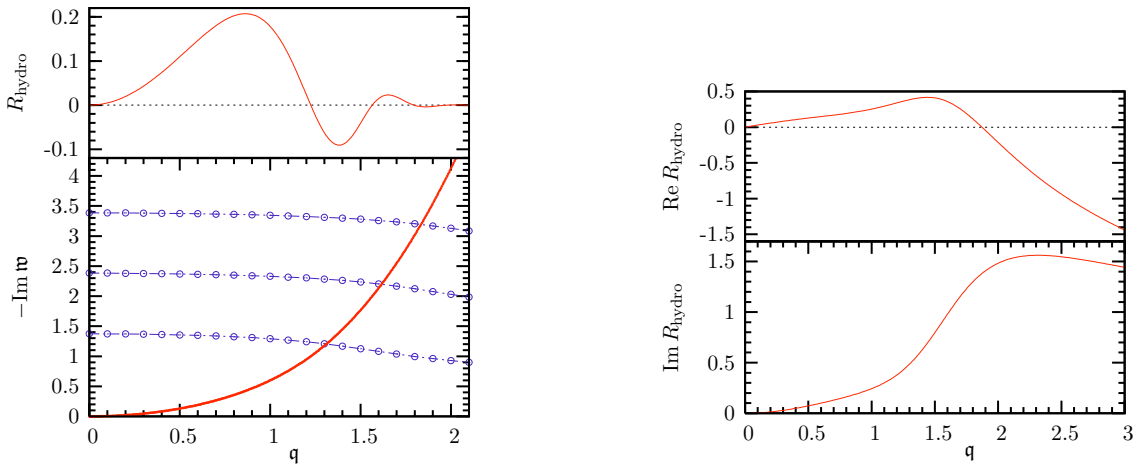

Figure 5.11: *(Left) When the shear mode hits a special value, there is a qualitative change in the behaviour of the quasinormal modes. Zeroes of the residue of the shear mode roughly coincide with the crossing of the shear mode and the quasinormal modes. (Right) The residue of the sound mode behaves as the rest of the quasinormal modes. The numerical values are normalized by* $\pi^2 N^2 T^4$

the sound channel, the properly defined Green function actually includes the boundary terms found in [98] added to the Frobenius series approximation. Otherwise, an unphysical singularity would appear at $\omega = \pm q$. We examine the $G_{tt,\,tt}$ Green function and find that the approximation and the exact function differ by a real constant $C \sim 0.374$. Once this term is included, they agree for a fair interval of frequencies and momenta (fig. 5.12). Even for values of ω, q smaller but comparable to the temperature, the hydrodynamic mode alone gives a remarkable good approximation for the spectral function. We can see that for $\mathfrak{q} = 0.2$, the hydrodynamic approximation and the exact result are virtually indistinguishable for $\mathfrak{w} \lesssim 1$.

Figure 5.12: *Imaginary (left) and real (right) parts of the retarded* $G_{tt,\,tt}$ *correlator as a function of the frequency at* $\mathfrak{q} = 0.2$ *(black) and* $\mathfrak{q} = 0.4$ *(grey) for the real part and* $\mathfrak{q} = 1$ *(grey) for the imaginary part. The dotted line is the hydrodynamic mode contribution, the solid line is the exact solution and the dashed line is the four-mode approximation.*

Other correlators related to the sound channel can be found from $G_{tt,\,tt}$ using the explicit expressions for the tensor projectors [98].

We also examine the $G_{tx,\,tx}$ component of the shear channel, the results are in fig. 5.13. We have to add an analytic piece $\sim 0.9\mathfrak{q}^2\mathfrak{w}$ to the spectral function. To the real part of the correlator we need to add a more complicated term $\sim 1.89\mathfrak{q}^4 - 0.16\mathfrak{q}^2 - 1.77\mathfrak{q}^2\mathfrak{w}^2$. The plots made in figure 5.13 have been done using the definition (5.27), we observe very good agreement for $\mathfrak{w} < 1, \mathfrak{q} \lesssim 0.6$.

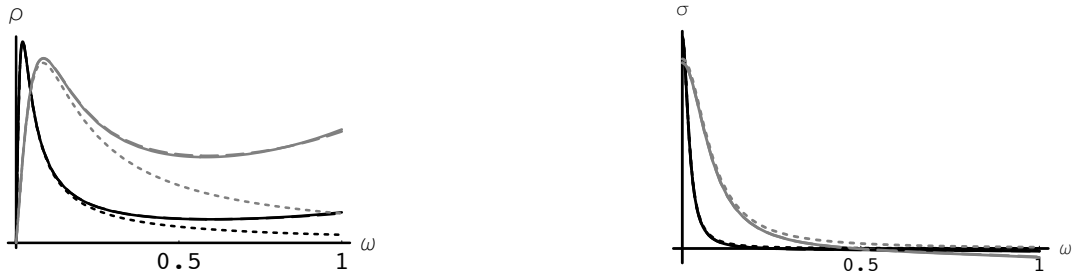

Figure 5.13: *Imaginary (left) and real (right) parts of the retarded $G_{tx,\,tx}$ correlator as a function of the frequency at $\mathfrak{q} = 0.2$ (black) and $\mathfrak{q} = 0.4$ (grey). The dotted line is the hydrodynamic mode contribution, the solid line is the exact solution and the dashed line is the four-mode approximation.*

5.5 Conclusions

We have studied hydrodynamics in the strongly coupled $\mathcal{N}=4$ gauge theory based on linear response theory using the AdS/CFT correspondence. As emphasized we understand hydrodynamics here as the effective theory resulting from integrating out the higher quasinormal modes and keeping only the contribution of the hydrodynamic modes, i.e. those modes whose quasinormal frequency vanishes at zero momentum. We also recall that we can consider this to be a definition of the system being in local thermal equilibrium. One of the important findings is that the hydrodynamic approximation defined in that way has its breakdown built into it: we saw that the diffusion mode in the longitudinal channel of the R-charge crosses the lowest quasinormal mode at around $\mathfrak{q} \approx 0.7$ and that the diffusion mode in the shear channel does it at around $\mathfrak{q} \approx 1.3$. From that value on it is the lowest non hydrodynamic mode that determines the late time behaviour. In fact, already slightly before the spectral function of the hydrodynamic mode ceases to be positive. We interpret this as a signal for the breakdown of the effective theory based on the hydrodynamic mode alone. Similarly, in the sound channel we found that the spectral function of the sound mode switches sign at $\mathfrak{q} \approx 1.1$ and again we take this as a breakdown of a putative effective theory based on the sound channel alone. The full spectral functions (or even the approximation keeping the contributions from only a few quasinormal modes) behave perfectly reasonable at these points.

An important role in our investigations have been played by the residues. We saw

that the shear diffusion mode and the R-charge diffusion are very similar. Both decay in an oscillatory pattern with decreasing frequency and numerically we find that they decouple for momenta $\mathfrak{q} > 1$. As we explain in appendix A.2 this can be understood from the analyzing the in-falling boundary conditions at the special values of the frequency $\mathfrak{w} = -in$ with $n \in \mathbb{N}$. That both diffusion modes show such similarities leads one naturally to suspect that this might be a universal property of holographic hydrodynamic diffusion modes. At the moment it is not clear how such a conjectured universal behaviour could be proved. However it seems doable and an interesting task to generalize the calculations of the residues presented here to other holographic gauge theories and check if the diffusive modes behave in the same way. A clue of why this might happen comes from causality: in order to preserve causality and at the same time reproduce (first order) hydrodynamics in the long wavelength limit some drastic modification at short wavelengths is definitely necessary.

As we have seen, the complex momentum modes needed for the calculation of the front velocity do behave perfectly causal and their residues do not decouple at high frequencies. Although in the small frequency/momentum limit the lowest complex momentum mode can be computed from the analytic continuation of the quasinormal hydrodynamic mode $\mathfrak{w} = -i\mathfrak{q}^2$ this is not so for short wavelengths and high frequencies. This does not come as a surprise, since only rotational invariance is preserved in the finite temperature theory, so non-analyticities between ω and q dependence are expected, like ω/q. An example of this is the fact that the two limits $\omega \to 0$ and $q \to 0$ of the retarded correlator do not commute in general. Also, in order to do the analytic continuation of the Green function properly, all modes must be taken into account, only in the $\omega \to 0, q \to 0$ limit the hydrodynamic mode dominates. It is interesting to consider the hydrodynamic time scale we found in the energy density correlator, $2\pi T\tau_{\mathrm{H}} \approx 1.34$. At RHIC temperatures $T \approx 300$ MeV this translates into a very short time $\tau_{\mathrm{H}} = 0.14\mathrm{fm/c}$. For the R-charge density this is even around four times shorter. One might take this as an indication for an extremely fast thermalization time. Of course, thermalization at RHIC includes processes that are outside the regime of linear response considered here, so the short hydrodynamic scale can at best describe a late stage of thermalization.

Another important point was to see how well the retarded Green's functions can be approximated by keeping only a few quasinormal modes. We found that analytic pieces related to the non-convergence of the sum over quasinormal modes played an important role. Recently, attempts of reconstructing the quasinormal mode spectrum from (much easier to compute) holographic spectral functions have been made in [144]. We think that our observations might also be useful to gain a better control on such procedures.

Chapter 6

Holographic superconductors

The range of physical phenomena to which the AdS/CFT correspondence can be applied is constantly increasing. One of the latest additions is the realization of spontaneous symmetry breaking and the appearance of a superfluid phase at low temperature as explained in 2.3. A model with a charged scalar condensing in the background of a charged AdS black hole has first been introduced in [65]. Shortly afterwards it was realized that a neutral scalar can condense as well and it was shown explicitly that the DC conductivity is infinite in the broken phase [66].

By now there is a large variety of holographic models of superfluidity/superconductivity [70, 72, 73, 145–157]. Specifically hydrodynamical behavior in these models has been addressed before in [75, 158] where the speed of sound has been calculated from derivatives of thermodynamic quantities. The hydrodynamic poles of retarded Green functions have been studied in an analytical approximation for infinitesimal condensate in a p-wave model in [159].

In this chapter we are interested in the hydrodynamics of the holographic superconductor introduced in [66]. In general, hydrodynamic behavior is connected either to the presence of a conserved charge, a spontaneously broken symmetry or a second order phase transition. As we will see in our model all three possibilities are realized. We already know that in holographic models the hydrodynamic modes appear as quasinormal modes in the AdS black hole background whose frequency vanishes in the zero momentum limit and quasinormal modes are identified with the poles of the holographic Green functions. In general, they can be computed using the prescription given in [77] and reviewed in section 3.1. In situations in which there are several fields whose linearized wave equations form a coupled system of differential equations possibly subject to a constraint due to a gauge symmetry the construction of the holographic Green functions is a bit more complicated. We solve this problem in full generality and show that the quasinormal modes defined are the zeros of the determinant spanned by the values at the boundary of a maximal set of linearly independent solutions to the field equations.

Having solved the problem of defining the holographic Green functions we concentrate on finding the lowest quasinormal modes and in particular the ones representing the hydrodynamic behavior of the system. Hydrodynamic modes can be understood as massless

modes in the sense that $\lim_{k\to 0}\omega(k) = 0$. Such modes arise in the presence of a conserved charge. In this case a local charge distribution can not simply dissipate away but has to spread slowly over the medium according to a diffusion process. Other situations in which hydrodynamic modes appear are at a second order phase transition, characterized by the appearance of a new massless mode and spontaneous breaking of a global symmetry where a massless Goldstone boson appears. A discussion of hydrodynamics in systems with spontaneous breaking of global symmetries can be found in [160] and in the relativistic context in [39].

We will consider the abelian gauge model of [66] without backreaction, i.e. assuming that the metric is a simple AdS black hole with flat horizon topology. In [66] it has been established that this model undergoes a second order phase transition towards forming a condensate of the charged scalar field thus spontaneously breaking the $U(1)$ gauge symmetry. The conductivity in the broken phase has a delta function peak at zero frequency and a gap typical of superconductors.

An important particularity of the model is the missing backreaction. Since the metric fluctuations are set to zero this means that effectively there is no energy momentum tensor in the field theory dual. In particular the generators of translations and rotations are missing in the operator algebra. This does of course not mean that the model does not have these symmetries, they are however not realized as inner automorphisms of the operator algebra (they are still outer automorphisms). Besides the space time symmetries being realized as outer automorphisms there is a direct consequence of this in what concerns the hydrodynamics of the model: all hydrodynamic modes related to them are missing. There is no shear mode for the momentum diffusion and no sound mode for the energy transport. The hydrodynamic modes we find in the model are therefore only due to the presence of the $U(1)$ symmetry and its spontaneous breakdown.

Hydrodynamics can be understood as an effective field theory defined by the continuity equations of the conserved currents and so-called constitutive relations which encode the dissipative behavior of the system. The constitutive relations tell us how fast a current is built up due to gradients in the charge density or due to external fields. The constitutive relations depend on transport coefficients such as viscosity or conductivity. Transport coefficients can be divided into absorptive and reactive ones depending on whether they are odd or even under time reversal [160]. A typical example for an absorptive transport coefficient is the diffusion constant, an example for a reactive one is the speed of sound. Reactive transport coefficients such as the speed of sound (the static susceptibility is another example) can often be computed from purely thermodynamic considerations. This has been done for the speed of second sound in this model in [75] and for a variant of fourth sound in [158][1]. As we have argued before, the hydrodynamic modes of en-

[1]Note that in [75] the mode has been called second sound whereas in [158] it was argued that it should

ergy and momentum transport, shear and sound modes are missing. In the broken phase one expects however the appearance of a hydrodynamic mode with approximately linear dispersion relation for small momenta which represents the second sound present in superfluids. Indeed such a mode is bound to appear for each spontaneously broken continuous symmetry [160]. We find (numerically) the second sound mode directly as a pole in the holographic Green functions in the broken phase and read off the speed of sound from its dispersion relation. Our results for the speed of second sound agree (with numerical uncertainties) with the results in [75].

Below the critical temperature one expects actually only a part of the medium to be in the superfluid state whereas another part stays in the normal fluid phase. The fluid is a two component fluid and naively one might expect that this is reflected in the pole structure of the Green functions as the presence of the diffusive pole of the normal fluid component. As we will see, the hydrodynamic character of this diffusive pole is lost however below the critical temperature. We find a pole with purely imaginary frequencies obeying a dispersion relation roughly of the form $\omega = -i\gamma - iDk^2$. The gap γ goes to zero at the T_c such that at the critical temperature this mode goes over into the usual diffusive mode of the normal fluid.

In section 6.1 we introduce the model and describe its properties. We compute the condensate as a function of temperature. This is basically a review of the results of [66] except the fact that we choose to work in the grand canonical ensemble where we hold fixed the value of the chemical potential instead of the value of the charge density.

Afterwards, we compute the quasinormal modes of the complex scalar field in the unbroken phase. As expected we find that at the critical temperature a quasinormal frequency crosses over into the upper half of the complex frequency plane. Since a pole in the upper half plane is interpreted as an instability this is an indication that the scalar field condenses. The quasinormal modes of gauge fields in the four dimensional AdS black hole have been studied before [161]. In particular the longitudinal gauge field channel shows a diffusion pole with diffusion constant $D = 3/(4\pi T)$. The holographic Green functions for gauge fields are often calculated in a formalism that employs gauge invariant variables, i.e. the electric field strengths. For reasons explained in section four we prefer however to work directly with the gauge fields. The longitudinal components obey two coupled differential equations subject to a constraint and we show in full generality how to compute the holographic Green function in such a situation. The quasinormal mode condition boils down to setting a determinant of field values at the boundary of AdS to zero. We find

be rather called fourth sound. There it has been argued that it is the fourth sound that survives the probe limit. In any case working directly in the probe limit we only have one sound mode. For convenience we will refer to it as second sound. Disentangling first, second or fourth sound would need to take into account the backreaction.

that this determinant is proportional to the electric field strength exemplifying that the poles of holographic Green functions are gauge invariant as expected on general grounds.

In section we study the lowest modes of the quasinormal mode spectrum in the superfluid phase. We find that the longitudinal gauge fields at non zero momentum couple to real and imaginary part of the scalar field fluctuations, building up a system of four coupled differential equations subject to one constraint. We solve this system numerically and compute the quasinormal modes from our determinant condition. We find hydrodynamic modes with approximately linear real part of the dispersion relation. We compute the speed of second sound from it and find our results to be in good numerical agreement with what was found in [75] from thermodynamic considerations. The second sound pole has however also an imaginary part and we can fit the dispersion relation (for small momenta) to $\omega = \pm v_s k - i\Gamma_s k^2$ which allows us to read off the attenuation constant Γ_s of second sound. We also find a purely imaginary mode with a dispersion relation of the form $\omega = -i\gamma - iDk^2$ with D the diffusion constant. It is a sort of gapped diffusion mode. The gap γ goes to zero for $T \to T_c$. A simple two fluid model suggests that there is still a normal fluid component and in it charges should diffuse in the usual way right below T_c. Therefore we expect a diffusive pole to show up in the two-point function. The diffusive behavior is modified however at long wavelength by the presence of the gap γ. This mode is therefore not really a hydrodynamic mode.

6.1 The Model

As in [66] we consider a four dimensional planar AdS black hole with line element

$$ds^2 = -f(r)dt^2 + \frac{dr^2}{f(r)} + \frac{r^2}{L^2}(dx^2 + dy^2)\,. \tag{6.1}$$

the blackening factor is $f(r) = \frac{r^2}{L^2} - \frac{M}{r}$. This metric has a horizon at $r_{\rm H} = M^{1/3}L^{2/3}$, the Hawking temperature is $T = \frac{3}{4\pi}\frac{r_{\rm H}}{L^2}$. In the following we will rescale coordinates according to

$$\begin{pmatrix} r \\ t \\ x \\ y \end{pmatrix} \to \begin{pmatrix} r_{\rm H}\rho \\ L^2/r_{\rm H}\,\bar{t} \\ L^2/r_{\rm H}\,\bar{x} \\ L^2/r_{\rm H}\,\bar{y} \end{pmatrix} \tag{6.2}$$

In the new dimensionless coordinates the metric takes the form (6.1) with $M = 1$ times the overall AdS scale L^2.

As explained in section 2.3, we take an abelian gauge model with a massive charged scalar field in order to have a model of superconductivity,

$$\mathcal{L} = -\frac{1}{4}F_{\mu\nu}F^{\mu\nu} - m^2\Psi\bar{\Psi} - (\partial_\mu\Psi - iA_\mu\Psi)(\partial^\mu\bar{\Psi} + iA^\mu\bar{\Psi}) \tag{6.3}$$

and a tachyonic mass $m^2 = -2/L^2$ above the Breitenlohner-Friedmann bound. As in [66] we ignore the backreaction of these fields onto the metric. This so-called probe limit corresponds to case of a scalar field with infinitely large charge. We seek solutions for which the time component of the gauge field vanishes at the horizon and takes a non-zero value μ on the boundary. This value is interpreted as the chemical potential. The boundary condition on the horizon is usually justified by demanding that the gauge field has finite norm there. Here this can be seen as follows: as in [75] we can chose a gauge that removes the phase of the scalar field Ψ from the equations of motion. In this gauge the scalar field current becomes $J_\mu = \psi^2 A_\mu$. Therefore the value of A_μ is directly related to a physical quantity, the current, and it is a well defined physical condition to demand the current to have finite norm at the horizon. This is achieved by taking the scalar field to be regular and the gauge field to vanish at the horizon.

In addition to the gauge field the scalar field might be non trivial as well. In fact we have seen that for high chemical potential (low temperature) the scalar field needs to be switched on in order to have a stable solution. In our study of the quasinormal modes in the next section we will indeed see that a quasinormal mode crosses into the upper half plane at the critical temperature. We denote the temporal component of the gauge field in the dimensionless coordinates by Φ. The field equations for the background fields are

$$\Psi'' + (\frac{f'}{f} + \frac{2}{\rho})\Psi' + \frac{\Phi^2}{f^2}\Psi + \frac{2}{L^2 f}\Psi = 0 \quad , \tag{6.4}$$

$$\Phi'' + \frac{2}{\rho}\Phi' - \frac{2\Psi^2}{f}\Phi = 0 \quad . \tag{6.5}$$

The equations can be solved numerically by integration from the horizon out to the boundary. As we just argued for the current to have finite norm at the horizon we have to chose $\Phi(1) = 0$ and demand the scalar field to be regular at the horizon. These conditions leave two integration constants undetermined. The behavior of the fields at the conformal boundary is

$$\Phi = \bar{\mu} - \frac{\bar{n}}{\rho} + O(\frac{1}{\rho^2}) \,, \tag{6.6}$$

$$\Psi = \frac{\psi_1}{\rho} + \frac{\psi_2}{\rho^2} + O(\frac{1}{\rho^2}) \,. \tag{6.7}$$

The value of the mass of the scalar field chosen allows to define two different theories due to the fact that both terms in the expansion above are normalizable in AdS. The canonical choice of what one considers to be the normalizable mode gives a theory in which ψ_1 is interpreted as a coupling and ψ_2 as expectation value of an operator with mass dimension two. On the other hand one might consider ψ_2 as the coupling and ψ_1 as the expectation value of an operator of dimension one.

All our numerical calculations are done using the dimensionless coordinates. In order

to relate the asymptotic values (6.6), (6.7) to the physical quantities we note that

$$\bar{\mu} = \frac{3L}{4\pi T}\mu\,, \tag{6.8}$$

$$\bar{n} = \frac{9L}{16\pi^2 T^2}n\,, \tag{6.9}$$

$$\psi_1 = \frac{3}{4\pi T L^2}\langle O_1\rangle\,, \tag{6.10}$$

$$\psi_2 = \frac{9}{16\pi^2 T^2 L^4}\langle O_2\rangle\,, \tag{6.11}$$

where μ is the chemical potential, n the charge density and $\langle O_i\rangle$ are the vacuum expectation values of the operators sourced by the scalar field. From now on we will set $L = 1$ and work in the grand canonical ensemble by fixing $\mu = 1$. Different values for $\bar{\mu}$ can now be interpreted as varying the temperature T. For high temperatures the scalar field is trivial and the gauge field equation is solved by $\Phi = \bar{\mu} - \frac{\bar{\mu}}{\rho}$. Spontaneous symmetry breaking means that an operator has a non trivial expectation value even when no source for the operator is switched on. We therefore look for nontrivial solutions of the scalar field with either $\psi_1 = 0$ or $\psi_2 = 0$. Numerically we find that a non-trivial scalar field is switched on at $\bar{\mu} = 1.1204$ corresponding to a critical temperature $T_c = 0.213\mu$ for the operator O_1 and at $\bar{\mu} = 4.0637$ corresponding to a critical temperature of $T_c = 0.0587\mu$ for the operator O_2. We chose to plot the squares of the condensates as a function of reduced temperature.

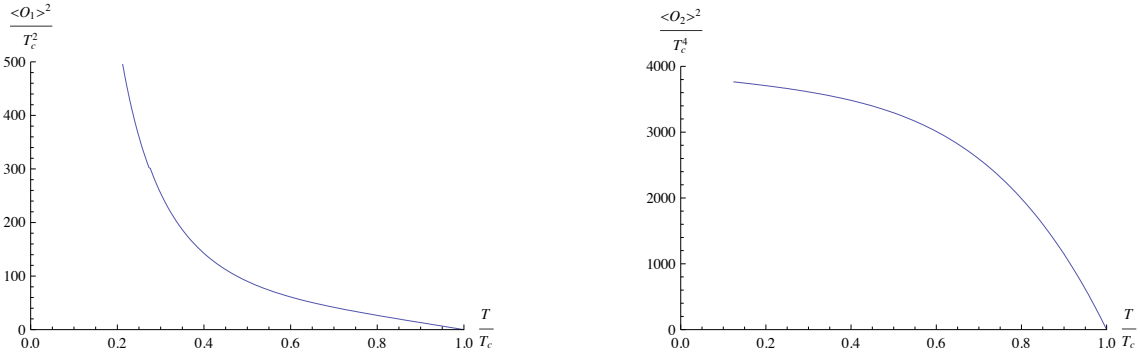

Figure 6.1: *The condensates as function of the temperature in the two possible theories.*

It makes the linear behavior for temperatures just below the critical one manifest,

$$\langle O_i\rangle^2 \propto \left(1 - \frac{T}{T_c}\right)\,. \tag{6.12}$$

Since we want to compute the holographic two point functions we will have to expand the action to second order in field fluctuations around the background. We divide the fields into background plus fluctuations in the following way

$$\Psi = \psi(\rho) + \sigma(\rho, t, x) + i\eta(\rho, t, x)\,, \tag{6.13}$$

$$A_\mu = \mathcal{A}_m(\rho) + a_\mu(\rho, t, x)\,. \tag{6.14}$$

The gauge transformations act only on the fluctuations

$$\begin{aligned} \delta a_\mu &= \partial_\mu \lambda \,, && (6.15)\\ \delta\sigma &= -\lambda\eta \,, && (6.16)\\ \delta\eta &= \lambda\sigma + \lambda\psi \,. && (6.17) \end{aligned}$$

The action expanded out to second order is $S = S^{(0)} + S^{(1)} + S^{(2)}$

$$\begin{aligned} S^{(0)} &= \int \sqrt{-g}\left(-\frac{1}{4}\mathcal{F}_{\mu\nu}\mathcal{F}^{\mu\nu} + \frac{2}{L^2}\psi^2 - (\partial_\mu\psi)(\partial^\mu\psi) - \mathcal{A}_\mu\mathcal{A}^\mu\psi^2\right) ,\\ S^{(1)} &= \int \sqrt{-g}\left(-\frac{1}{2}\mathcal{F}_{\mu\nu}f^{\mu\nu} + \frac{4}{L}^2\psi\sigma - 2\partial_\mu\psi\partial^\mu\sigma - 2\partial_\psi\mathcal{A}^\mu\eta - 2\mathcal{A}^2\psi\sigma \right.\\ &\quad \left. +2\mathcal{A}_\mu\partial^\mu\eta - 2\mathcal{A}_\mu a^\mu\psi^2\right) ,\\ S^{(2)} &= \int \sqrt{-g}\left(-\frac{1}{4}f_{\mu\nu}f^{\mu\nu} - (\partial\sigma)^2 - (\partial\eta)^2 - \mathcal{A}^2\sigma^2 - \mathcal{A}^2\eta^2 + \frac{2}{L}^2\sigma^2 + \frac{2}{L}^2\eta^2 \right.\\ &\quad \left. -2\partial_\mu\psi a^\mu\eta - 2\mathcal{A}^\mu a_\mu\psi\sigma - 2\partial_\mu\sigma\mathcal{A}^\mu\eta + 2\mathcal{A}_\mu\sigma\partial\mu\eta + 2\partial_\mu\eta a^\mu\psi - a^2\psi^2\right) \quad (6.18) \end{aligned}$$

Up to the equations of motion these can be written as boundary terms

$$\begin{aligned} S_B^{(1)} &= \int_B \sqrt{-g}\left(g^{\rho\rho}\mathcal{F}_{\rho\mu}a^\mu - 2g^{\rho\rho}\partial_\rho\psi\sigma + 2A^\rho\psi\eta\right) ,\\ S_B^{(2)} &= -\int_B \sqrt{-g}g^{\rho\rho}\left(\frac{1}{2}g^{\nu\lambda}f_{\rho\nu}a_\lambda + \eta\partial_\rho\eta + \sigma\partial_\rho\sigma + a_\rho\psi\eta\right) . \qquad (6.19) \end{aligned}$$

Note that $S^{(1)}$ is not trivial since according to the holographic dictionary it has to encode the non-vanishing expectation values of the field theory operators.

6.2 Quasinormal Frequencies in the Unbroken Phase

We assume now that the scalar field Ψ has vanishing background value and take the field to depend on t, x, ρ. Frequency ω and momentum k in the dimensionless coordinates are related to the physical ones ω_{ph}, k_{ph} as

$$\omega = \frac{3\omega_{ph}}{4\pi T} \quad , \quad k = \frac{3k_{ph}}{4\pi T} \,. \qquad (6.20)$$

The equations of motion in the unbroken phase are

$$\begin{aligned} 0 &= \Psi'' + (\frac{f'}{f} + \frac{2}{\rho})\Psi' + (\frac{(\Phi+\omega)^2}{f^2} + \frac{2}{f} - \frac{k^2}{f\rho^2})\Psi \,,\\ 0 &= a_t'' + \frac{2}{\rho}a_t' - \frac{k^2}{\rho^2}a_t - \frac{\omega k}{f\rho^2}a_x \,,\\ 0 &= a_x'' + \frac{f'}{f}a_x' + \frac{\omega^2}{f^2}a_x + \frac{\omega k}{f\rho^2}a_t \,,\\ 0 &= \frac{\omega}{f}a_t' + \frac{k}{\rho^2}a_x' \,. \qquad (6.21) \end{aligned}$$

The equation of motion for the complex conjugate scalar $\bar{\Psi}$ can be obtained by changing the sign of the gauge field background Φ in (6.21).

Green Functions.

In order to calculate the quasinormal frequencies we impose ingoing boundary conditions at the horizon. Since the coefficients of the differential equations (6.21) are known analytically and are such that they are of Fuchsian type we can use the Frobenius method to approximate the solutions at the horizon and at the boundary by series expansions. As is well-known the holographic Green functions are proportional to the ratio of the connection coefficients. More precisely we demand

$$\Psi_H = (\rho-1)^{-i\omega/3}(1+O(\rho-1))\,, \tag{6.22}$$

on the horizon and write the local solution at the AdS boundary as

$$\Psi_B = \frac{A}{\rho} + \frac{B}{\rho^2} + \mathrm{O}\left(\frac{1}{\rho^3}\right)\,. \tag{6.23}$$

In the theory with the dimension two operator we take A as the coefficient of the non-normalizable mode and B as the coefficient of the normalizable mode. Writing the local solution on the horizon as a linear combination of normalizable and non-normalizable modes on the boundary fixes the connection coefficient A and B. We have written the boundary action as a functional of real and imaginary part of the scalar field. We will rewrite the boundary action now in terms of the complex scalar Ψ and its conjugate. In addition we introduce a local boundary counterterm to regularize the action.

$$S^B_{\Psi} = \int \left[-\frac{1}{2} f\rho^2(\bar{\Psi}\Psi' + \Psi\bar{\Psi}') - \rho^3\bar{\Psi}\Psi\right]_{\rho=\Lambda}\,. \tag{6.24}$$

This allows to compute the Green functions $G_{\bar{O}O}(q) = \langle\bar{O}(-q)O(q)\rangle$ and $G_{O\bar{O}}(q) = \langle O(-q)\bar{O}(q)\rangle$ fulfilling $G_{O\bar{O}}(-q) = G_{\bar{O}O}(q)$, with q being the four momentum (ω, k). We write $\Psi(q,\rho) = \Psi_0(q)f_q(\rho)$, where we interpret $\Psi_0(q)$ as the source that inserts the operator $O(q)$ in the dual field theory. We introduce a cutoff and normalize the profile function f_q to $1/\Lambda$ at the cutoff. In terms of an arbitrary solution the normalized one is $f_k(\rho) = \Psi_k(\rho)/(\Lambda\Psi(\Lambda))$ where $\Psi_k(\rho)$ has the boundary expansion (6.23). The boundary action is now

$$\begin{aligned} S^B &= -\frac{1}{2}\int \left[\Psi_0(-q)(\rho^2 f f_{-q}\bar{f}'_q + \rho^3 f_q\bar{f}_q)\bar{\Psi}_0(q) + \text{c.c.}\right]_{\rho=\Lambda} \\ &= \int \Psi_0(-q)\mathcal{F}_{\Psi\bar{\Psi}}(\Lambda)\bar{\Psi}_0(q) + \bar{\Psi}_0(-q)\mathcal{F}_{\bar{\Psi}\Psi}(\Lambda)\Psi_0(q)\,. \end{aligned} \tag{6.25}$$

According to the relation (3.10), the renormalized retarded Green functions are given by the limit $\lim_{\Lambda\to\infty} -2\mathcal{F}(\Lambda)$, thus

$$G_{\bar{O}_2O_2} = \frac{B}{A} \quad , \quad G_{O_2\bar{O}_2} = \frac{\bar{B}}{\bar{A}}\,. \tag{6.26}$$

We denote the connection coefficients for the complex conjugate scalar as $\bar{A}$, $\bar{B}$[2]. According to (6.21) they can be obtained by switching the sign of the chemical potential in the expressions for A, B.

The theory with the operator of dimension one can be obtained through a Legendre transform of the theory with dimension two operator. We note that the expectation value of the dimension two operator is $\langle O_2 \rangle = -\rho^2(\rho\Psi(\rho))'\big|_{\rho=\Lambda}$, whereas the source is given by $\Lambda\Psi(\Lambda)$. We therefore add the following terms to the boundary action

$$S^B \to S^B + \int d^4k \left[\rho^3(\bar{\Psi}(\rho\Psi(\rho))' + \Psi(\rho\bar{\Psi}(\rho))'\right]\Big|_{\rho=\Lambda} . \tag{6.27}$$

Now we can evaluate the Green functions as before, the only difference being the normalization of the profile function $f_k(\rho) = \Psi_k(\rho)/[\Lambda\Psi'(\Lambda) + \Psi(\Lambda)]$. This normalization takes care that the term of order $1/\rho^2$ in the boundary expansion couples with unit strength to the source $\Psi_0(q)$. We find finally for the Green functions of the Legendre transformed theory

$$G_{O_1\bar{O}_1} = \frac{A}{B} \quad , \quad G_{\bar{O}_1 O_1} = \frac{\bar{A}}{\bar{B}} , \tag{6.28}$$

as expected. The quasinormal modes in the scalar sector are given by the zeroes of the connection coefficients A and $\bar{A}$ in the theory with operator of dimension two and by the zeroes of B and $\bar{B}$ in the theory with the dimension one operator. In terms of the unnormalized solutions to the field equations we can write the Green functions as

$$G_{\bar{O}_2 O_2} = -\lim_{\Lambda\to\infty}\left(\Lambda^2\frac{\Psi_q'(\Lambda)}{\Psi_q(\Lambda)} + \Lambda\right) , \tag{6.29}$$

$$G_{O_1\bar{O}_1} = \lim_{\Lambda\to\infty}\frac{\Psi_q(\Lambda)}{\Lambda(\Lambda\Psi_q'(\Lambda) + \Psi_q(\Lambda))} . \tag{6.30}$$

Quasinormal Modes from Determinants.

Before presenting the results for the quasinormal modes of the scalar field we would like to outline a method of how to calculate the holographic Green functions for the gauge fields without using gauge invariant variables such as the electric field strength $E = -i(ka_t + \omega a_x)$.

The complicated structure of the gauge symmetry in the broken phase makes it rather difficult to express the boundary action in terms of gauge invariant field combinations. As a warm up for the problem of how to calculate the holographic Green functions in this situation we will consider how we can calculate them in the unbroken phase directly in terms of the gauge fields. We necessarily have to solve a system of coupled differential equations whose solutions are restricted by a constraint.

[2]Note that the infalling boundary condition for the conjugate scalar is $\bar{\Psi} \sim (\rho-1)^{-i\omega/3}$.

The correct boundary conditions for the gauge fields on the horizon are

$$a_t \propto (\rho-1)^{1-i\omega/3}(a_t^0+\dots)\,, \tag{6.31}$$

$$a_x \propto (\rho-1)^{-i\omega/3}(a_x^0+\dots)\,. \tag{6.32}$$

The two coefficients a_x^0 and a_t^0 are not independent but related by the constraint. At this point we have fixed the incoming wave boundary conditions and there seems to be now a unique solution to the field equations. We would expect however two linearly independent solutions with infalling boundary conditions on thehorizon. The constraint reduces this to only one solution. The problem is now that in order to compute the Green function for the charge density and longitudinal current component separately we need solutions that asymptote to $(a_t, a_x) = (1, 0)$ and $(a_t, a_x) = (0, 1)$ respectively. This is of course not possible with only one available solution at the horizon. Because of the gauge symmetry the gauge field system (6.21) allows for an algebraic solution

$$a_t = -\omega\lambda\,, \tag{6.33}$$

$$a_t = k\lambda\,, \tag{6.34}$$

with $\lambda' = 0$, i.e. λ being independent of ρ. This is of course nothing but a gauge transformation of the trivial solution. Remember that even after fixing the radial gauge $a_\rho = 0$, gauge transformations with gauge parameters independent of ρ are still possible. These gauge transformations appear as algebraic solutions to the field equations. We also stress that the infalling boundary conditions really have to be imposed only on physical fields, i.e. the electric field strength. Having therefore an arbitrary non trivial gauge field solution corresponding to an electric field with infalling boundary conditions we can add to it the gauge mode (6.33).

We can use this to construct a basis of solutions that allows the calculation of the holographic Green functions. Let us now assume that there is a solution that takes the values $(a_t, a_x) = (1, 0)$ at the boundary. We will call this solution from now on α_i^t for $i \in t, x$. Analogously we define the solution α_i^x. According to the holographic dictionary the solution α_i^t couples to the boundary value $\lim_{\rho\to\infty} a_t(q,\rho) = \mathcal{A}_t(q)$, i.e. the source of the field theory operator J_t (the time component of the conserved current J_μ). In parallel α_i^x couples to the boundary value $\mathcal{A}_x(q)$. A generic solution of the gauge field equations can now be written in terms of the boundary fields as

$$a_i(q,\rho) = \mathcal{A}_x(q)\alpha_i^x(\rho) + \mathcal{A}_t(q)\alpha_i^t(\rho)\,. \tag{6.35}$$

Using this expansion the boundary action can be written as

$$S_B = \frac{1}{2}\int_B \mathcal{A}_i(-q)\left[\left(\rho^2\alpha_t^i(-q,\rho)\frac{d}{d\rho}(\alpha_t^j(q,\rho)) - f(\rho)\alpha_x^i(-q,\rho)\frac{d}{d\rho}(\alpha_x^j(q,\rho))\right)\right]_{\rho=\Lambda}\mathcal{A}_j(q)\,, \tag{6.36}$$

where again we have introduced a cutoff at $\rho = \Lambda$. From this it follows that the holographic Green functions are given by

$$2\mathcal{F}^{ij}(\rho) = \rho^2 \alpha_t^i(-k,\rho)\frac{d}{d\rho}(\alpha_t^j(k,\rho)) - f(\rho)\alpha_x^i(-k,\rho)\frac{d}{d\rho}(\alpha_x^j(k,\rho))\,, \tag{6.37}$$

in the limit

$$G^{ij} = \lim_{\Lambda\to\infty} -2\mathcal{F}^{ij}(\Lambda)\,. \tag{6.38}$$

Notice also that $\frac{d}{d\rho}[\mathcal{F}^{ij}(\rho) - \mathcal{F}^{*ji}(\rho)] = 0$ by the field equations.

Although there are no terms of the form $a_t' a_x$ in the boundary action this formalism gives automatically expressions for the mixed Green functions G_{tx} and G_{xt}! But we still have to construct the solutions $\alpha_j^i(\rho)$. This can be done in the following way: suppose we have an arbitrary solution $(a_t(\rho), a_x(\rho))$ obeying the infalling boundary conditions (6.31). We can add to this now an appropriate gauge mode, such that at the cutoff the solution takes the form $(1,0)$ or $(0,1)$ in terms of $a_t(\Lambda), a_x(\Lambda)$. This is easily achieved by solving

$$\begin{pmatrix} c_t^t & c_x^t \\ c_t^x & c_x^x \end{pmatrix}\begin{pmatrix} a_t(\Lambda) & a_z(\Lambda) \\ -\omega\lambda & k\lambda \end{pmatrix} = \begin{pmatrix} 1 & 0 \\ 0 & 1 \end{pmatrix}. \tag{6.39}$$

The linear combinations formed with coefficients c_j^i give now new solutions $(\alpha_t^t(\rho), \alpha_x^t(\rho))$ and $(\alpha_t^x(\rho), \alpha_x^x(\rho)))$ obeying the correct boundary conditions on the AdS boundary. Using the general expression for the Green function (6.38) we get explicitly in terms of solutions obeying the infalling boundary conditions

$$G_{tt} = \lim_{\Lambda\to\infty} \Lambda^2 \frac{k a_t'(\Lambda)}{k a_t(\Lambda) + \omega a_x(\Lambda)}\,, \tag{6.40}$$

$$G_{tx} = \lim_{\Lambda\to\infty} \Lambda^2 \frac{\omega a_t'(\Lambda)}{k a_t(\Lambda) + \omega a_x(\Lambda)}\,, \tag{6.41}$$

$$G_{xt} = -\lim_{\Lambda\to\infty} \Lambda^2 \frac{k a_x'(\Lambda)}{k a_t(\Lambda) + \omega a_x(\Lambda)}\,, \tag{6.42}$$

$$G_{xx} = -\lim_{\Lambda\to\infty} \Lambda^2 \frac{\omega a_x'(\Lambda)}{k a_t(\Lambda) + \omega a_x(\Lambda)}\,. \tag{6.43}$$

Note that the denominator for all is given by $k a_t(\Lambda) + \omega a_x(\Lambda)$ which is up to an irrelevant constant nothing but the gauge invariant electric field E_x. Therefore we see immediately that the poles of these Green function are gauge invariant and coincide of course with the poles of the Green function in the gauge invariant formalism where $G \propto \frac{E_x'}{E_x}$. Indeed using the constraint on the boundary we find the well known expressions [98]

$$\begin{aligned} G_{tt} &= \frac{k^2}{k^2-\omega^2}\lim_{\Lambda\to\infty}\Lambda^2\frac{E_x'}{E_x} \quad , \quad G_{tx} = \frac{k\omega}{k^2-\omega^2}\lim_{\Lambda\to\infty}\Lambda^2\frac{E_x'}{E_x}\,, \\ G_{xx} &= \frac{\omega^2}{k^2-\omega^2}\lim_{\Lambda\to\infty}\Lambda^2\frac{E_x'}{E_x}\,. \end{aligned} \tag{6.44}$$

On general grounds one expects indeed that the poles of the holographic Green functions for gauge fields are gauge independent.

If we are interested only in the location of quasinormal frequencies we do not even have to construct the holographic Green functions explicitly. From the linear system in (6.39) we infer that the quasinormal frequencies coincide with the zeroes of the determinant of the field values at the boundary. Indeed vanishing determinant means that there is a nontrivial zero mode solution to (6.39) such that the boundary values of the fields are $(0, 0)$ which in turn means that the coefficient in the solution of the non-normalizable mode vanishes. The determinant is $\lambda(ka_t + \omega a_x)$ and again given by the electric field strength. In fact these remarks apply to systems of coupled differential equations in AdS black hole metric in general: the quasinormal frequencies corresponding to the poles of the holographic Green functions are the zeroes of the determinant of the field values on the boundary for a maximal set of linearly independent solutions obeying infalling boundary conditions on the horizon. The fact that the differential equations are coupled is the holographic manifestation of mixing of operators under the RG flow. Therefore one has to specify at which scale one is defining the operators. The scheme outlined above is dual to define the operators at the cutoff Λ.

Hydrodynamic and higher QNMs.

We have numerically computed the quasinormal frequencies for the fluctuations satisfying the equations of motion (6.21) for both the O_2 and the O_1 theories. The quasinormal modes of the scalar field correspond to zeroes of A in the theory of dimension two operator and to zeroes of B in the dimension one operator theory, where A and B are the connection coefficients of the boundary solution (6.23). Results for the lowest three poles of the scalar field at zero momentum are shown in Figure 6.2.

The poles with positive real part correspond to the quasinormal modes of the complex scalar Ψ, while those with negative real part are the quasinormal modes of $\bar{\Psi}$, obtained by changing the overall sign of the gauge field background Φ. As the temperature is decreased, the poles get closer to the real axis, until at the critical temperature T_c the lowest mode crosses into the upper half of the complex frequency plane. It happens at $T_c = 4.0637$ for the theory of dimension two operator and at $T_c = 1.1204$ in the case of the dimension one operator theory. For $T < T_c$ the mode would become tachyonic, i. e. unstable. This instability indicates that the scalar field condenses and the system undergoes a phase transition at $T = T_c$. At the critical point, the lowest scalar quasinormal mode is a hydrodynamic mode in the sense that it is massless, $\lim_{k\to 0}\omega(k) = 0$. This mode is identified with the Goldstone boson that appears after the spontaneous breaking of the global $U(1)$ symmetry and in the next section we will see that it evolves into the second

sound mode characteristic of superfluid models.

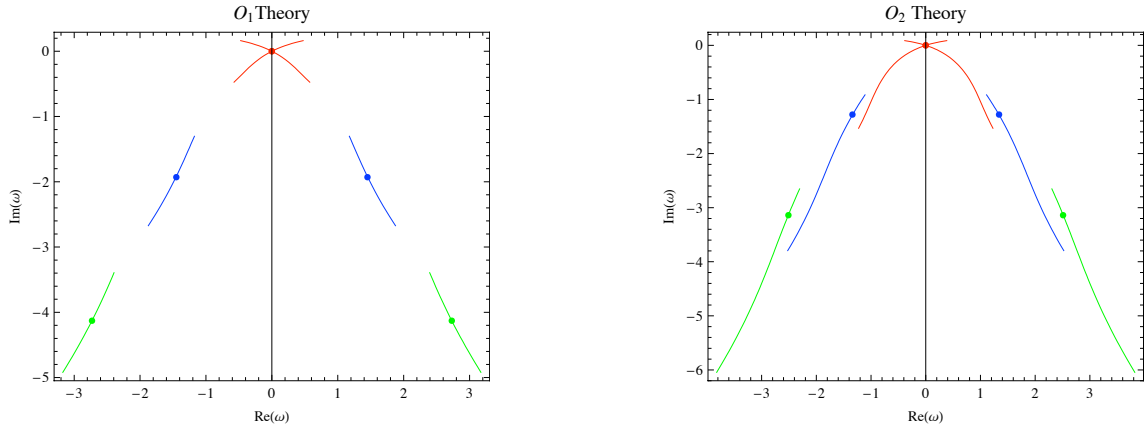

Figure 6.2: *Lowest scalar quasinormal frequencies as a function of the temperature and at momentum $k = 0$, from $T/T_c = \infty$ to $T/T_c = 0.81$ in the O_2 theory (right) and to $T/T_c = 0.56$ in the O_1 theory (left). The dots correspond to the critical point $T/T_c = 1$ where the phase transition takes place. Red, blue and green correspond to first, second and third mode respectively.*

The quasinormal modes correspond to simple poles of the retarded Green function, so close to the nth pole the Green function can be approximated by $G(\omega, k, T) \sim \frac{R_n(\omega,k,T)}{\omega - \omega_n(k,T)}$. Knowing the connection coefficients we can compute the Green functions and therefore the residue for each quasinormal mode as explained in appendix A.1. For the lowest quasinormal mode at $k = 0$ and at the critical temperature, the residue takes the value $R_2(T_c) = -2.545 + 0.825i$ in the O_2 theory and $R_1(T_c) = 0.686 - 0.348i$ in the O_1 theory. In general, one expects the residues of hydrodynamic modes that correspond to conserved quantities of the system to vanish in the limit of zero momentum, since its susceptibility remains constant. Consider for instance the diffusion mode associated to conserved density. The susceptibility is defined through the two point correlation function as

$$\chi = \lim_{k,\omega\to 0} \langle \rho\rho \rangle = \lim_{k,\omega\to 0} \frac{i\sigma k^2}{\omega + iDk^2} = \frac{\sigma}{D}\,, \tag{6.45}$$

where D is the diffusion constant and σ is the conductivity. The residue, $i\sigma k^2$, vanishes and one recovers the well-known Einstein relation $\sigma = D\chi$. However, for hydrodynamic modes appearing at second order phase transitions the order parameter susceptibility should diverge at the critical point. This order parameter susceptibility is given in our case by the correlator of the boundary operator sourced by the scalar field. At the critical temperature it is

$$\chi_{\bar{O}_i O_i} = \lim_{k,\omega\to 0} \langle \bar{O}_i O_i \rangle = \lim_{k,\omega\to 0} \frac{R_i(k, T_c)}{\omega - \omega_H(k, T_c)} \to \infty \tag{6.46}$$

since $\omega_H(0, T_c) = 0$ while the residue remains finite. This result allows us to identify the lowest scalar quasinormal mode in the unbroken phase with the Goldstone boson appearing at the critical point.

In the model under consideration one can also compute the gauge field fluctuations in the normal phase. Nevertheless, as the model does not include the backreaction of the metric, the computation is not sensitive to temperature anymore. This can be seen from the equations of motion (6.21) of the gauge fluctuations, that do not depend on the background solutions thus are independent of the temperature. Hence we recover the results for the quasinormal modes of vector field perturbations in the AdS_4 black hole background computed by [161]. For our purposes the most important fact is the presence of a hydrodynamic mode corresponding to diffusion. For small momenta that mode has dispersion relation $\omega = -iDk^2$ with $D = 1$ (which is $D = 3/(4\pi T)$ in physical units). In order to study the behavior of the diffusion pole in the unbroken phase as a function of the temperature one has to consider the backreacted model described in [67].

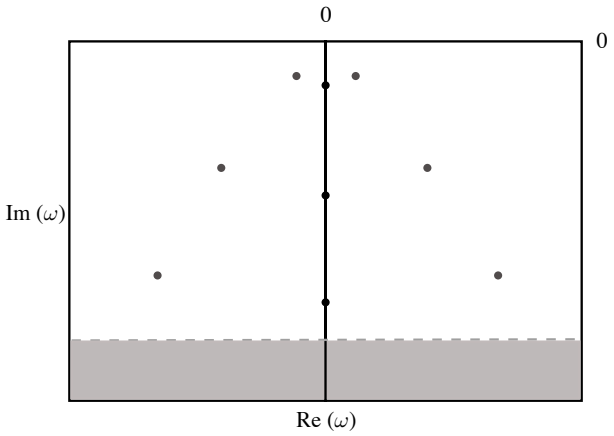

Figure 6.3: *Schematic plot of the poles in the coupled system, i.e. in the broken phase at small finite momentum right below T_c. These poles are present in each retarded correlation function for the coupled fields η, σ, A_t, A_x, while their residues might vanish for specific fields. Close to the origin we find the (pseudo)diffusion mode and two hydrodynamic second sound modes. In addition two sets of higher quasinormal modes are shown. In the unbroken phase these poles originate from the scalar (grey dots). We also expect a tower of purely imaginary poles stemming from the longitudinal vector channel (black dots). The grey area indicates where our numerical methods break down.*

6.3 Quasinormal Frequencies in the Broken Phase

In this section we will apply our determinant method for finding quasinormal modes of a coupled system of field equations. With this technique we follow the model analyzed in the previous section into its broken phase. Figure 6.3 schematically summarizes our analysis. The two formerly separate sets of scalar (grey dots) and longitudinal vector poles (black dots) present in the unbroken phase where the scalars and vectors decouple, are now unified into one inseparable pole structure in the coupled system. This is in

analogy to a coupled system of two harmonic oscillators in which it makes no sense to ask for the eigenfrequencies of the single oscillators. One could of course try to diagonalize the system of differential equations, in our case however this looks rather complicated and we prefer to work directly with the coupled system and with the gauge fields instead of gauge invariant variables. The lowest modes (see figure 6.3) are two hydrodynamic second sound modes originating from the two lowest scalar quasinormal modes in the unbroken phase. In addition we will find a non-hydrodynamic pseudodiffusion mode staying on the imaginary axis in the range of momenta we consider. This mode can be thought of as the prolongation of the diffusion mode into the unbroken phase.

Application of the determinant method.

The equations of motion in the broken phase couple the scalar fluctuations η, σ to the longitudinal vector components a_t, a_x

$$0 = f\eta'' + \left(f' + \frac{2f}{\rho}\right)\eta' + \left(\frac{\phi^2}{f} + \frac{2}{L^2} + \frac{\omega^2}{f} - \frac{k^2}{\rho^2}\right)\eta - \frac{2i\omega\phi}{f}\sigma - \frac{i\omega\psi}{f}a_t - \frac{ik\psi}{r^2}a_x\,, \tag{6.47}$$

$$0 = f\sigma'' + \left(f' + \frac{2f}{\rho}\right)\sigma' + \left(\frac{\phi^2}{f} + \frac{2}{L^2} + \frac{\omega^2}{f} - \frac{k^2}{\rho^2}\right)\sigma + \frac{2\phi\psi}{f}a_t + \frac{2i\omega\phi}{f}\eta\,, \tag{6.48}$$

$$0 = fa_t'' + \frac{2f}{\rho}a_t' - \left(\frac{k^2}{\rho^2} + 2\psi^2\right)a_t - \frac{\omega k}{\rho^2}a_x - 2i\omega\psi\,\eta - 4\psi\phi\,\sigma\,, \tag{6.49}$$

$$0 = fa_x'' + f'a_x' + \left(\frac{\omega^2}{f} - 2\psi^2\right)a_x + \frac{\omega k}{f}a_t + 2ik\psi\,\eta\,. \tag{6.50}$$

This system of four coupled equations is subject to the constraint

$$\frac{\omega}{f}a_t' + \frac{k}{\rho^2}a_x' = 2i\left(\psi'\,\eta - \psi\,\eta'\right)\,, \tag{6.51}$$

where the left hand side known from the unbroken phase is amended by the condensate terms on the right. Note that the real part σ of the scalar fluctuation is not involved in the constraint.

The constraint can be interpreted as the Ward identity of current conservation in the presence of the condensate. We expand the gauge fields near the boundary and note that $a_0' = \langle n\rangle/\rho^2$ and $a_x' = -\langle j_x\rangle/\rho^2$, where j_x is the x-component of the current. Expanding also the r.h.s. and comparing the leading orders in ρ we find

$$\partial_\mu\langle j^\mu\rangle = 2\langle O_i\rangle\eta_0^i\,, \tag{6.52}$$

where η_0^i is the source for the insertion of the imaginary part of the operator O_i, i.e. the Goldstone field in the dual field theory. This equation is to be understood as the local Ward identity encoding current conservation in the presence of the condensate $\langle O_i\rangle$. It

follows for example that the two point function of the divergence of the current with the operator $O_i^{(\eta)}$ is zero only up to a contact term $\left\langle \partial_\mu j^\mu(x) O_i^{(\eta)}(y) \right\rangle = \langle O_i \rangle \, \delta(x-y)$.

The gauge field component a_y being transverse to the momentum decouples from the above system and assumes the form

$$0 \;=\; f\, a_y{}'' + f' a_y{}' + \left(\frac{\omega^2}{f} - \frac{k^2}{\rho^2} - 2\psi^2 \right) a_y \,. \tag{6.53}$$

Since we do not expect any hydrodynamic modes in the transverse vector channel we will not study this equation further.

Applying the indicial procedure to the system (6.47) to find the exponents for the singular and the coefficients for the regular parts of the fields, we obtain the following behavior at the horizon

$$\eta \;=\; (\rho-1)^\zeta \left(\eta^{(0)} + \eta^{(1)}(\rho-1) + \dots \right) , \tag{6.54}$$

$$\sigma \;=\; (\rho-1)^\zeta \left(\sigma^{(0)} + \sigma^{(1)}(\rho-1) + \dots \right) , \tag{6.55}$$

$$a_t \;=\; (\rho-1)^{\zeta+1} \left(a_t^{(0)} + a_t^{(1)}(\rho-1) + \dots \right) , \tag{6.56}$$

$$a_x \;=\; (\rho-1)^\zeta \left(a_t^{(0)} + a_t^{(1)}(\rho-1) + \dots \right) , \tag{6.57}$$

with the exponent $\zeta = -i\omega/3$ obeying the incoming wave boundary condition.

Due to the constraint we can choose only three of the four parameters at the horizon. Using the constraint and without loss of generality we can eliminate the time component a_t^0 and parametrize the solutions by $(\eta^{(0)}, \sigma^{(0)}, a_x^{(0)})$. We choose three linearly independent combinations I, II, III. A fourth solution can be found from the gauge transformations

$$\eta^{IV} = i\lambda\psi \,, \quad \sigma^{IV} = 0 \,, \quad a_t^{IV} = \lambda\omega \,, \quad a_x^{IV} = -\lambda k \,, \tag{6.58}$$

with λ being an arbitrary constant with respect to ρ. It is not an algebraic solution to the equations of motion since η has non trivial dependence on the bulk variable ρ. The gauge solution solves the equations (6.47) not exactly but only up to terms proportional to the background equations (6.4).

Our goal is to find the poles in the retarded correlation functions of the four fields appearing in the coupled system of equations of motion (6.47). A convenient way of imposing the appropriate boundary conditions is given by redefining the scalar fields as

$$\tilde\eta(\rho) = \rho\eta(\rho) \quad , \quad \tilde\sigma(\rho) = \rho\sigma(\rho) \,. \tag{6.59}$$

Then the most general solution for each field $\varphi_i \in \{\tilde\eta, \tilde\sigma, a_t, a_x\}$ including gauge degrees of freedom can be written

$$\varphi_i = \alpha_1 \varphi_i{}^I + \alpha_2 \varphi_i{}^{II} + \alpha_3 \varphi_i{}^{III} + \alpha_4 \varphi_i{}^{IV} \,. \tag{6.60}$$

In the theory with the dimension two operator the sources for the various gauge invariant operators are given by $\varphi_i(\Lambda)$. We are interested in the quasinormal modes of the system (6.47) and as we have argued in the previous section these are the special values of the frequency where the determinant spanned by the values $\varphi_i^{I,II,III,IV}$ vanishes. Expanding this determinant we get

$$\begin{aligned} 0 &= \frac{1}{\lambda}\det\begin{pmatrix} {\varphi_\eta}^I & {\varphi_\eta}^{II} & {\varphi_\eta}^{III} & {\varphi_\eta}^{IV} \\ {\varphi_\sigma}^I & {\varphi_\sigma}^{II} & {\varphi_\sigma}^{III} & {\varphi_\sigma}^{IV} \\ \varphi_t^I & \varphi_t^{II} & \varphi_t^{III} & \varphi_t^{IV} \\ \varphi_x^I & \varphi_x^{II} & \varphi_x^{III} & \varphi_x^{IV} \end{pmatrix} = i\varphi_\eta^{IV}\det\begin{pmatrix} {\varphi_\sigma}^I & {\varphi_\sigma}^{II} & {\varphi_\sigma}^{III} \\ \varphi_t^I & \varphi_t^{II} & \varphi_t^{III} \\ \varphi_x^I & \varphi_x^{II} & \varphi_x^{III} \end{pmatrix} \\ &+ \omega\det\begin{pmatrix} {\varphi_\eta}^I & {\varphi_\eta}^{II} & {\varphi_\eta}^{III} \\ {\varphi_\sigma}^I & {\varphi_\sigma}^{II} & {\varphi_\sigma}^{III} \\ \varphi_x^I & \varphi_x^{II} & \varphi_x^{III} \end{pmatrix} + k\det\begin{pmatrix} {\varphi_\eta}^I & {\varphi_\eta}^{II} & {\varphi_\eta}^{III} \\ {\varphi_\sigma}^I & {\varphi_\sigma}^{II} & {\varphi_\sigma}^{III} \\ \varphi_t^I & \varphi_t^{II} & \varphi_t^{III} \end{pmatrix}, \end{aligned} \tag{6.61}$$

which needs to be evaluated at the cutoff $\rho = \Lambda$. The first term in (6.61) vanishes at the cutoff since $\varphi_4^{IV} = \Lambda\psi = 0$ is just the condition that the operator O_2 is not sourced by the background.

We first find three linearly independent numerical solutions and then solve condition (6.61) numerically. Explicit checks confirm that the choice of a solution basis $\varphi^{I,II,III,IV}$ is completely arbitrary and does not change the results. Note also that in our present case all the remaining determinants can not be factorized. But if the momentum is set to zero, the only remaining term is the one with ω and the determinant factorizes into a scalar part and a vector part since the system of equations decouples.

In the theory with the dimension one operator the sources are given by $-\Lambda^2\tilde{\eta}$ and $-\Lambda^2\tilde{\sigma}$ for the scalar fields. Let us call $\varphi_1 = -\rho^2\tilde{\eta}'$ and $\varphi_2 = -\rho^2\tilde{\sigma}'$ in this case. The determinant has therefore the same form and again the first term vanishes due to the absence of sources for O_1 in the background solution. The quasinormal modes can again be found by integrating three arbitrary solutions with infalling boundary conditions from the horizon to the cutoff and finding numerically the zeroes of the determinant (6.61).

Hydrodynamic and Goldstone modes.

Sound mode The scalar modes originally destabilizing the unbroken phase turn into Goldstone modes at T_c instead of becoming tachyonic. Below T_c they evolve into the two second sound modes. Figure 6.4 shows their movement when momentum is changed at different temperatures. Note that we focus on the positive real frequency axis because of the mirror symmetry sketched in figure 6.3. From the dispersion relation at small frequencies and long wavelengths we extract the speed of second sound v_s and the second

sound attenuation Γ_s using the hydrodynamic equation

$$\omega = v_s k - i\Gamma_s k^2 \,. \tag{6.62}$$

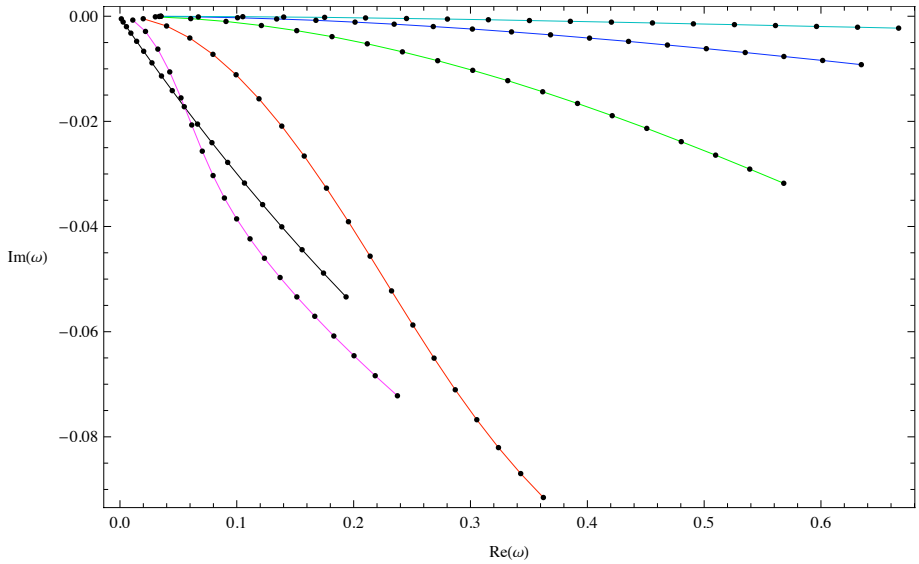

Figure 6.4: *Movement of the positive frequency sound pole away from $\omega = 0$ with increasing spatial momentum. Distinct curves correspond to temperatures below the phase transition $T/T_c =$ 0.999 (black), 0.97 (pink), 0.91 (red), 0.71 (green), 0.52 (blue), 0.26 (light blue). Dots on one curve are separated by $\Delta k = 0.05$. All curves start at $k = 0.05$ and end at $k = 1.00$.*

It turns out that the hydrodynamic regime, i.e. that range of momenta in which the dispersion relation is well approximated by (6.62), is very narrow for temperatures just below the critical one since the speed of sound vanishes at T_c. Fits to the hydrodynamic form at a high temperature $T \approx 0.9999 T_c$ are plotted in figure 6.5 for the O_2-theory, the results for the O_1 theory are qualitatively similar.

The speed of second sound is shown in figure 6.6. We have a good numerical agreement with the thermodynamic value of the second sound velocity given in [75]. This nicely confirms validity of our method. In particular, within our numerical precision we find that the value of the square of the speed of sound tends to $v_s^2 \approx 1/3$ in the O_1 theory and to $v_s^2 \approx 1/2$ in the O_2 theory[3]. However, the numerics becomes rather unstable for low temperatures, especially for the O_1 theory. Near but below the critical temperature we

[3]In [158] it was argued that conformal symmetry implies $v_s^2 = 1/2$ at zero temperature. Due to the divergence in the order parameter for the O_1 theory conformal symmetry could be broken and allow thus for a different value.

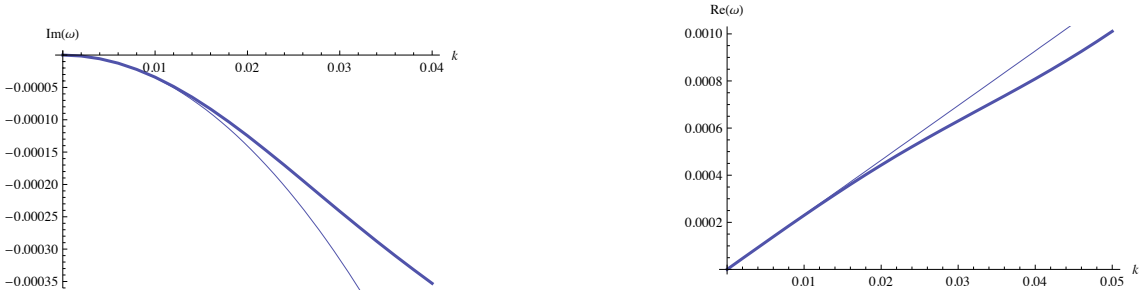

Figure 6.5: *Fits of the real and imaginary part of the hydrodynamic modes in the broken phase to the lowest order approximation $\omega = v_s k - i\Gamma_s k^2$. The left figure shows the real part and the right one the imaginary part. The thick lines are the numerical results and the thin lines are the linear and quadratic fits. The fit is done for a temperature just below the critical one where the range of the approximation is rather small.*

find

$$v_s^2 \approx 1.9\left(1-\frac{T}{T_c}\right) \qquad \mathrm{O}_1-\mathrm{Theory}\,, \tag{6.63}$$

$$v_s^2 \approx 2.8\left(1-\frac{T}{T_c}\right) \qquad \mathrm{O}_2-\mathrm{Theory}\,. \tag{6.64}$$

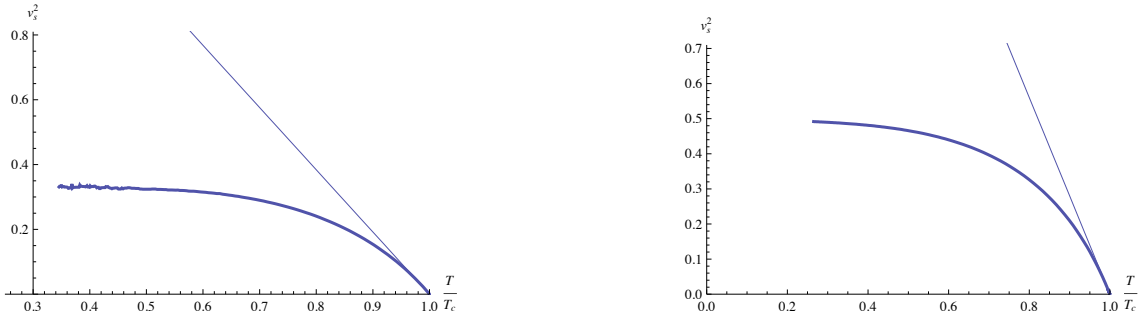

Figure 6.6: *The plots show the squares of the speed of sound as extracted from the location of the lowest quasinormal mode in the broken phase. The left figure is for the O_1 theory and the right one for the O_2 theory. We also indicate the linear behavior close to T_c. As can be seen the numerics for the O_1 theory becomes somewhat unstable for low temperatures.*

Moreover, as a benefit of our effort considering the fluctuations, we are also able to extract non-thermodynamic quantities in this channel. Specifically we examine the attenuation of the second sound mode as shown in figure 6.7. The curve shows how attenuation smoothly asymptotes to zero as the superfluid becomes more and more ideal at low temperatures. This effect is however much stronger in the O_2 theory. Near T_c the attenuation is growing. Within our numerical precision it seems however that the attenuation constant is taking a finite value at the critical temperature. Numerically we

find

$$\Gamma_s = 1.87T_c \quad \text{at} \quad T = 0.9991T_c \quad \mathrm{O}_1 - \text{Theory}\,, \tag{6.65}$$

$$\Gamma_s = 1.48T_c \quad \text{at} \quad T = 0.9998T_c \quad \mathrm{O}_2 - \text{Theory}\,. \tag{6.66}$$

A similar behavior has been observed in [162], where the attenuation of the normal sound mode asymptotes to a finite value near a phase transition.

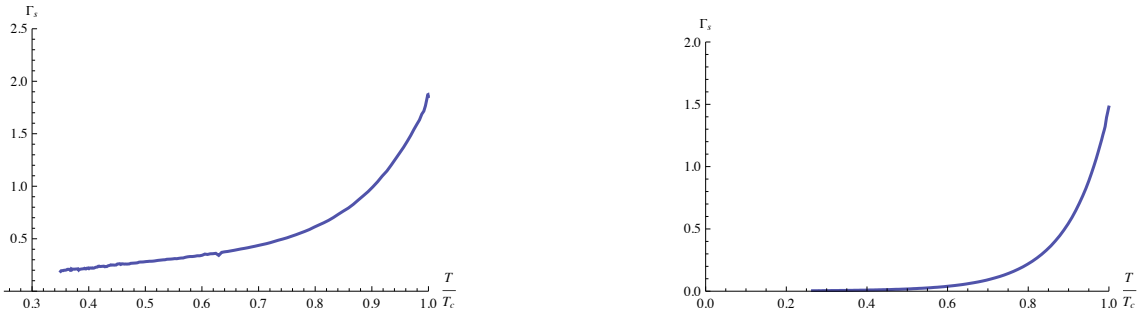

Figure 6.7: *The plots show the attenuation constants of second sound as extracted from the location of the lowest quasinormal mode in the broken phase. The left figure is for the O_1 theory and the right one for the O_2 theory. Again it can be noticed that the O_1 theory is numerically more challenging at low temperatures.*

(Pseudo) diffusion mode The vector diffusion mode from the unbroken phase turns into a (pseudo) diffusion mode below T_c[4]. For not too low temperatures and not too large momenta the dispersion relation for this mode is well approximated by

$$\omega = -iDk^2 - i\gamma(T)\,, \tag{6.67}$$

with a gap $\gamma \in \mathbb{R}$ in imaginary frequency direction. Thus the pole is shifted from its unbroken phase position such that it does not approach zero at vanishing momentum any more, i.e. it is not anymore a hydrodynamic mode.

In figure 6.8 we have plotted the gap γ as a function of the reduced temperature and we can see that it vanishes linearly near T_c.

$$\gamma \approx 15.4T_c\left(1 - \frac{T}{T_c}\right) \quad \mathrm{O}_1 - \text{Theory}\,, \tag{6.68}$$

$$\gamma \approx 8.1T_c\left(1 - \frac{T}{T_c}\right) \quad \mathrm{O}_2 - \text{Theory}\,. \tag{6.69}$$

Figure 6.9 shows the dispersion relation for the diffusion pole at different temperatures. The offset at $k = 0$ is the gap size γ depending linearly on T only near T_c. This implies

[4] An analytical result obtained for second sound in a non-abelian model [159] also shows the appearance of a pseudo diffusion mode with a gap that vanishes as the condensate goes to zero.

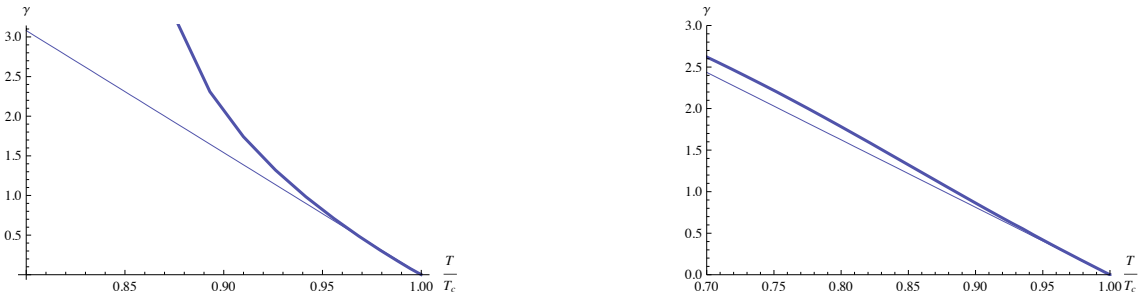

Figure 6.8: *The plots show the gap of the pseudo diffusion mode as a function of reduced temperature. On the left the O_1 theory and on the right the O_2 theory.*

that the relation (6.67) asymptotes to the ordinary diffusion equation near the critical temperature. As expected the highest temperature curve $T = 0.999T_c$ (black) matches the hydrodynamic approximation (thin line) very well at small momenta. That agreement becomes worse around $k \sim 0.25$. Also as the condensate grows below T_c the behavior of this (pseudo) diffusion mode becomes less hydrodynamic.

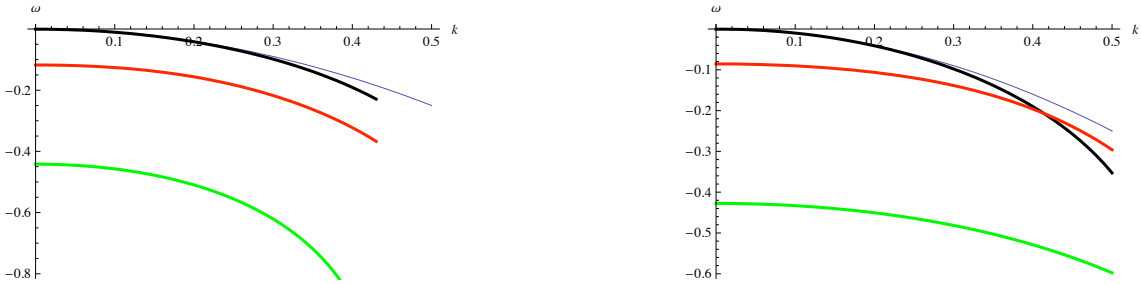

Figure 6.9: *The plots show the dispersion relations for the pseudo diffusion mode at different temperatures and the diffusion dispersion relation with $D = 3/(4\pi T)$ (note that even in the unbroken phase the latter approximates the diffusive quasinormal mode only for small momenta). On the left we have the O_1 theory at temperatures $T = 0.999T_c$ (black), $T = 0.97Tc$ (red) and $T = 0.91T_c$ (green). On the right the same for the O_2 theory at temperatures $T = 0.999T_c$ (black), $T = 0.97T_c$ (red) and $T = 0.87T_c$ (green).*

Higher quasinormal modes

In addition to the hydrodynamic sound modes and the pseudo diffusion mode there are higher quasinormal modes. We have not studied them in detail, however, we have traced the prolongation of the second and third quasinormal modes in the scalar sector from the unbroken phase into the broken phase.

The former scalar modes evolve continuously into higher modes of the coupled system through the phase transition as seen from the two kinked dashed (unbroken phase) and solid (broken phase) lines in figure 6.10. The kink indicates that the poles move con-

tinuously but change direction at the critical temperature. We show only the plot for the theory with the dimension two operator, similar results hold for the O_1 theory. At the critical temperature the locations of the quasinormal frequency calculated with the Frobenius method in the unbroken phase and by the method of finding the zeroes of the determinant spanned by the solutions match with impressively high precision. We might take this as a highly non trivial test of the accuracy of the numerical integration method.

We expect that all quasinormal frequencies are shifted *continuously* in the complex frequency plane across the phase transition. This means that there are no jumps in any of the dispersion relations. There is simply an infinite set of poles corresponding to the degrees of freedom of the system which are continuously shifted when parameters are changed.

Our numerical invesigations also reveal poles developing an increasing real part with decreasing temperature which most likely originate from the longitudinal vector modes in the unbroken phase. Note that we have not shown these modes for simplicity.

The two higher modes shown in figure 6.10 move parallel to the real axis and to each other with decreasing temperature [5]. At low temperatures their real parts are almost the same. This is also true for the longitudinal vectors as far as we can tell within our numerical uncertainties. We suspect that this *alignment of higher poles* has to do with the appearence of the conductivity gap showing up at low temperatures [66].

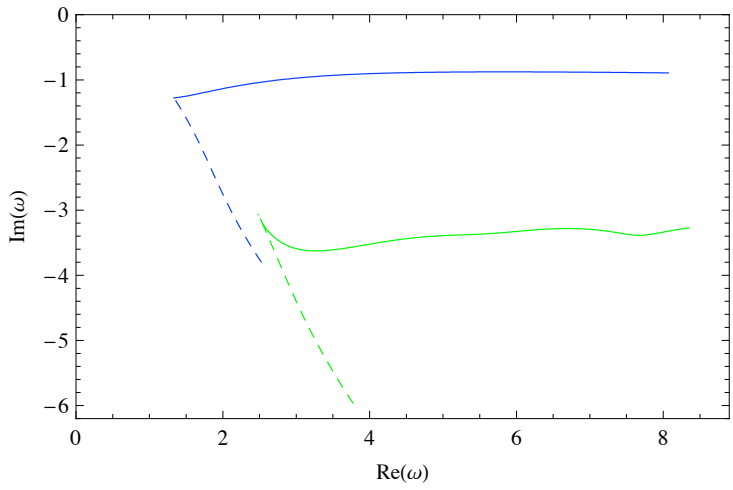

Figure 6.10: *Movement of the higher poles in the complex frequency plane at vanishing momentum $k = 0$. Scalar modes 2 (blue) and 3 (green) in the unbroken phase (dashed) evolve continuously into the higher poles of the broken phase (solid). The right end points are evaluated for $T/T_c = 0.25$.*

[5] Note that this behavior is very different from the behavior usually found in five-dimensional holographic setups when temperature is decreased [139, 140, 163].

6.4 Conclusions

We have studied the hydrodynamics of a holographic model of a superfluid. The model is an Abelian gauge field model with a charged scalar field in a four dimensional AdS black hole background.

As is well known by now the holographic dictionary allows to interpret the quasinormal frequencies as the poles of the retarded Green functions of the dual field theory. By calculating the low lying quasinormal frequencies numerically in the broken and unbroken phases we were able to identify the hydrodynamics. We found that at high temperatures, $T > T_c$ there is only one hydrodynamic mode representing the diffusion of the conserved $U(1)$ charge. As one lowers the temperature reaching the critical temperature T_c two of the quasinormal frequencies of the charged scalar field approach the origin of the complex frequency plane. Precisely at the critical temperature at the onset of the phase transition these modes become massless, giving rise to new hydrodynamic variables. We also have calculated the residue of these modes and found that it stays finite at $T = T_c$ resulting in a divergence of the order parameter susceptibility, as expected.

Below the critical temperature these modes stay massless and show a dispersion relation with a linear real part and a quadratic imaginary one, allowing an interpretation as the modes of second sound in the superfluid. On the other hand the diffusion mode starts to develop a gap and stops to be hydrodynamic. The counting is therefore one hydrodynamic mode at high temperatures, three at the critical temperature and two at low temperatures.

In the low temperature phase we were able to calculate the speed of sound as well as its attenuation constant as a function of temperature. Also the gap in the pseudo diffusion mode has been determined. We have also been able to follow some of the higher quasinormal modes through the phase transition and found that they evolve continuously albeit non-smoothly with temperature in the complex frequency plane, showing a sharp kink at the critical temperature.

On a technical side we have developed a method to determine the quasinormal frequencies and the holographic Green functions for systems of coupled differential equations and without using gauge invariant variables. The quasinormal frequencies correspond simply to the zeroes of the determinant spanned by a maximal set of linearly independent solutions. We have furthermore seen that the poles of the Green functions stemming from bulk gauge fields are gauge invariant as expected.

There are now several interesting questions that should be investigated in the future. The most obvious one is to apply the methods developed here to the model where the backreaction of the matter and gauge field onto the metric are properly taken into account. Due to the presence of the metric fluctuations the hydrodynamics of such a model is

certainly much richer. In addition to the diffusion and second sound modes found here one expects also shear and sound modes stemming from bulk metric fluctuations. The corresponding system of differential equations promises to be rather involved. However there should be no principal obstacle to apply our methods also in these cases.

Another interesting direction of research should be to reinterpret the results obtained here and analogous ones for related models with different scalar mass and living in different dimensions from the point of view of dynamical critical phenomena [164]. We have seen already that the speed of sound scales with exponent one half, whereas the gap in the pseudo diffusion mode scales with exponent one. The situation for the sound attenuation is unfortunately less clear. As far as our numerics indicates the sound attenuation reaches a finite value at $T = T_c$. An extensive study of related models possibly with enhanced numerical efforts might give new insights here.

Of course an effort should also be undertaken to extend the results at hand to models of p-wave superconductors [69]. For infinitesimal condensates and analytic study of the hydrodynamics has already been done in [159]. It might be of interest to supplement these analytical result with a numeric study that allows to go further away from the phase transition point deep into the broken phases. Another very interesting class of holographic p-wave superconductors are the ones realized on $D7$ brane embeddings [70, 72, 151]. Due to the presence of fundamental matter these should be especially interesting to study.

Summary and Outlook

Let us summarize the main results of this work and the some possible future research directions related to them.

We have seen that the quasinormal spectra of black holes, and thus of the poles of corresponding retarded correlators, are related to geometric properties of the black holes, in particular to its causal structure. In the large frequency limit the location of the singularities of thermal correlators can be explained in terms of null geodesics bouncing in the singularities and the boundaries of an eternal AdS black hole. This computation is related to the Schwinger-Keldish formalish up to identification of the fields living in different boundaries with insertion of operators in different pieces of the SK path. An interesting extension of this work is to study whether the geometric analysis of null geodesics can be generalized to other backgrounds like rotating or charged black holes, or to other geometries like asymptotically flat spaces where there is no boundary like in aAdS, so the space does not act like a box. It can also be interesting to study the effects of quantum corrections to the background, what implies to go beyond the large N limit or equivalently to introduce higher curvature corrections.

We have seen that the response to small external perturbations is completely determined by the poles of the retarded propagators and their associated residues and used it to study the linear response of the plasma phase of the strongly coupled $\mathcal{N} = 4$ SYM theory. This allows us to explore the validity of the hydrodynamic regime, based on integrating out all the modes but the hydrodynamic ones, in two different ways: defining a hydrodynamic time and legth scales that measure from when on the contribution of the hydrodynamic modes becomes dominant and by analyzing in which range of wavelengths and frequencies the hydrodynamic modes alone give a reliable description of the system. The very short hydrodynamic times obtained indicate that the perturbed plasma thermalises extremely fast, a result that can be used as an indication of fast thermalization at RHIC. The breakdown of the hydrodynamic approximation is somehow built into the theory: when decreasing the wavelength, more and more quasinomal modes have to be taken into account to describe the system. The weight of collective excitations in the plasma depends crucially on the value of the residues. For the shear and R-charge diffusion modes, it shows an oscillatory decaying behavior, signaling their decoupling at small momentum. It would be interesting to examine if that behavior is universal of hydrodynamic diffusion modes. *A priori* there is an indication that something drastic happens at short wavelength coming from the observation that causality is preserved but at the same

time first order hydrodynamic (that is acausal) is reproduced at long wavelengths. At RHIC there are processes taking place that cannot be described within the linear response theory. Therefore it would be of high interest to go beyond this approximation in order to have a more meaningful definition of the hydrodynamic scale that might be relevant for RHIC experiments in which the scale of thermalization is crucial. All the discussion only contains adjoint matter. To really have a predictive model relevant for real world experiments it would be nice to repeat the analysis including fundamental matter, achieved by the addition of new sets of branes in the string background.

Finally, we have studied the hydrodynamic behavior of the holographic superfluid given by an abelian gauge model with a massive scalar field in a fixed AdS black hole background. The lowest quasinormal mode of the charged scalar field becomes tachyonic at a certain value of the temperature. This instability indicates that the scalar field condenses and the system undergoes a second order phase transition. At the phase transition this scalar mode is massless and its susceptibility diverges, so it can be identified with the Goldstone boson appearing at the SSB. Below the critical temperature this mode is identified with the second sound. Using holography, we have been able to compute reactive transport coefficients as the speed of second sound, computed directly from thermodynamic considerations in other works, and also non-thermodynamic quantities like absorptive transport coefficients, as is the case of attenuation of the second sound or the diffusion constant. As a side result, we have developed a method to compute the physical quasinormal modes of coupled systems in terms of the non-gauge invariant variables. In this analysis the backreaction due to the presence of the scalar and gauge fields has been neglected. An obvious extension is to consider the backreacted model in which metric fluctuations are allowed and the dynamics of the system is richer. In that model even for a neutral scalar field there exist a phase transition at a finite temperature due to the instability of the background. For small charge of the scalar two competing mechanisms responsible of the condensation are present, the coupling to the gauge field and the instability of the metric. It will be interesting to find which mode is the order parameter of the phase transition for each case and what happens in the broken phase in the second case. It is also interesting the study of the interplay between normal and second sound. The complete investigation of the backreacted case hopefully will shed some light on the origin of the conductivity gap in these models. Another natural extension of this model is to consider high curvature corrections to examine whether or not the phase transition takes place and how the phase diagram is modified. Another extension of interest would be the explicit breaking of conformal invariance introducing for instance a mass deformation and study how the transition is affected.

Appendix

A.1 Computing quasinormal modes and residues

Let us explain how to compute quasinormal modes and their residues numerically in a holographic setup. Concretely, we present the cases of fluctuations of the metric and of a vector field in a Schwarzschild-AdS background given by the metric (2.14) up to dimensional reduction on the 5-sphere. This corresponds to find the quasinormal spectrum of energy-momentum and R-charge excitations, respectively, in the dual gauge theory. In the following we will use the coordinate $u = r_{\rm H}^2/r^2$ such that the horizon sits at $u = 1$ and the boundary at $u = 0$.

Energy-momentum tensor.

The equations of motion for the diffeomorphism-invariant quantities defined in (5.18) are

$$Z_1'' + \frac{(\mathfrak{w}^2 - q^2 f(u))f(u) - u\mathfrak{w}^2 f'(u)}{uf(u)(\mathfrak{q}^2 f(u) - \mathfrak{w}^2)} Z_1' + \frac{\mathfrak{w}^2 - \mathfrak{q}^2 f(u)}{uf(u)^2} Z_1 = 0 \ , \tag{A.70a}$$

$$Z_2'' - \frac{3\mathfrak{w}^2(1+u^2) + \mathfrak{q}^2(2u^2 - 3u^4 - 3)}{uf(u)(3\mathfrak{w}^2 + \mathfrak{q}^2(u^2-3)} Z_2' + \\ + \frac{3\mathfrak{w}^4 + \mathfrak{q}^4(3 - 4u^2 + u^4) + \mathfrak{q}^2(4u^5 - 4u^3 + 4\mathfrak{w}^2u^2 - 6\mathfrak{w}^2)}{uf(u)^2(3\mathfrak{w}^2 + \mathfrak{q}^2(u^2-3))} Z_2 = 0 \ , \tag{A.70b}$$

$$Z_3'' + \frac{1+u^2}{uf(u)} Z_3' + \frac{\mathfrak{w} - \mathfrak{q}^2 f(u)}{uf(u)^2} Z_3 = 0 \ . \tag{A.70c}$$

Both the boundary and the horizon are regular singular points. At the horizon ($u = 1$), there are two possible local solutions

$$Z_{(a)} \simeq (1-u)^{-i\mathfrak{w}/2}\, \varphi^{\rm in}_{(a)} + (1-u)^{i\mathfrak{w}/2}\, \varphi^{\rm out}_{(a)} \ , \quad a = 1, 2, 3. \tag{A.71}$$

As explained in section 3.1, in order to compute the retarded Green function, we must pick infalling boundary conditions $\varphi^{\rm out}_{(a)} \equiv 0$. According to the holographic prescription the retarded Green function is proportional to the ratio of the connection coefficients, (3.19), that relate the local solution at the horizon with ingoing boundary conditions to the non-normalizable ($\mathcal{A}_a$) and normalizable ($\mathcal{B}_a$) solutions at the boundary ($u = 0$)

$$Z^{\rm in}_{(a)} = \mathcal{A}_{(a)}\varphi^1_{(a)} + \mathcal{B}_{(a)}u^2\varphi^2_{(a)} \ . \tag{A.72}$$

The Green functions in the different channels are determined by three scalar functions $G_{(a)}$ given by

$$G_{(a)} = -\pi^2 N^2 T^4 \frac{\mathcal{B}_{(a)}}{\mathcal{A}_{(a)}} \,. \tag{A.73}$$

The quasinormal modes are normalizable solutions where $\mathcal{A}_{(a)} = 0$. The ratio $\mathcal{B}_{(a)}/\mathcal{A}_{(a)}$ follows from demanding that the solution is smooth at a matching point in the interior of the interval $(0, 1)$

$$\frac{\mathcal{B}_{(a)}}{\mathcal{A}_{(a)}} = \frac{Z^{\rm in}_{(a)}(Z^1_{(a)})' - (Z^{\rm in}_{(a)})' Z^1_{(a)}}{Z^2_{(a)}(Z^{\rm in}_{(a)})' - (Z^2_{(a)})' Z^{\rm in}_{(a)}} \,. \tag{A.74}$$

We have computed the Frobenius series up to order 50. Matching the series expansions, we see that the ratio (A.74) remains constant for a fair interval in the radial coordinate. We have chosen $x = 0.53$ to evaluate the ratio.

The residue R_n for the quasinormal mode $\mathfrak{w}_n$ can be computed as

$$R_n = \left[\frac{\partial}{\partial \mathfrak{w}} \left(\frac{\mathcal{A}_a}{\mathcal{B}_a} \right) \Big|_{\mathfrak{w}=\mathfrak{w}_n} \right]^{-1} \,. \tag{A.75}$$

Global current.

The equations of motion for the gauge invariant combinations (section 5.3) of the plane-wave vector field perturbations are

$$E_T'' + \frac{f'(u)}{f(u)} E_T' + \frac{\mathfrak{w}^2 - f(u)\mathfrak{q}^2}{(uf(u)^2} E_T = 0 \,, \tag{A.76a}$$

$$E_L'' + \frac{\mathfrak{w}^2 f'(u)}{f(u)(\mathfrak{w}^2 - f(u)\mathfrak{q}^2)} E_L' + \frac{\mathfrak{w}^2 - f(u)\mathfrak{q}^2}{uf(u)^2} E_L = 0 \,. \tag{A.76b}$$

Defining $(\alpha) := (T, L)$ as the two gauge-invariant components components, we can follow the same procedure as with the energy-momentum tensor components. The infalling solution can be expanded at the boundary in the non-normalizable and normalizable modes

$$E^{\rm in}_{(\alpha)}(u) = \mathcal{A}_{(\alpha)} E^1_{(\alpha)}(u) + \mathcal{B}_{(\alpha)} E^2_{(\alpha)}(u) \,, \tag{A.77}$$

where $E^2_{(\alpha)}(u) \sim u$. The retarded Green function is determined by the longitudinal and transverse polarization

$$\Pi^{(\alpha)} = -\frac{N^2 T^2}{8} \frac{\mathcal{B}_{(\alpha)}}{\mathcal{A}_{(\alpha)}} \,, \tag{A.78}$$

which are proportional to the ratio between the connection coefficients

$$\frac{\mathcal{B}_{(\alpha)}}{\mathcal{A}_{(\alpha)}} = \frac{E^{\rm in}_{(\alpha)}(E^1_{(\alpha)})' - (E^{\rm in}_{(\alpha)})' E^1_{(\alpha)}}{E^2_{(\alpha)}(E^{\rm in}_{(\alpha)})' - (E^2_{(\alpha)})' E^{\rm in}_{(\alpha)}} \,. \tag{A.79}$$

We have computed the Frobenius series up to order 50. Matching the series expansions, we see that the ratio (A.79) remains constant for a fair interval in the radial coordinate. We have chosen $x = 0.53$ to evaluate the ratio and have checked that the spectral function agrees with previous numerical (for non-zero momentum) and exact (for zero momentum) results [139, 165, 166]. The quasinormal modes correspond to the frequencies where there is a pole $\mathcal{A} = 0$. We can apply equation (A.75) to compute the residues.

A.2 Zeros of hydrodynamic residues

We have seen that the residues of the diffusion and the shear mode have an oscillatory behavior with the momentum. We now show how to find the location of the zeros of the residues. We will use that the equations of motion for the for the vector field and vector component of the metric are Heun equations (c.f. [102, 137])[6]

$$y''(x) + \left(\frac{\gamma}{x} + \frac{\delta}{x-1} + \frac{\epsilon}{x-2}\right) y'(x) + \frac{\alpha\beta x - Q}{x(x-1)(x-2)}\, y(x) = 0 \ . \tag{A.80}$$

In the case of the vector field, we define $V_0(z) = A_0'(z)$, $V_L(z) = A_L'(z)$. In the $x = 1 - z^2$ coordinate, the Heun equations are found using the new variables

$$\begin{aligned} V_0(x) &= x^{-i\mathfrak{w}/2}(x-1)^{1/2}(x-2)^{-\mathfrak{w}/2} y(x) \ , \\ V_L(x) &= x^{-1-i\mathfrak{w}/2}(x-1)^{1/2}(x-2)^{-1-\mathfrak{w}/2} y(x) \ . \end{aligned} \tag{A.81}$$

In both cases we find the same parameters for the Heun equation

$$\begin{aligned} \alpha &= -\frac{\mathfrak{w}}{2}(1+i) \ , \quad \beta = 2 - \left(\frac{\mathfrak{w}}{2}(1+i)\right) \ , \quad Q = \mathfrak{q}^2 - (1+3i)\frac{\mathfrak{w}}{2} - (2-i)\frac{\mathfrak{w}^2}{2} \ , \\ \gamma &= 1 - i\mathfrak{w} \ , \quad \delta = 1 \ , \quad \epsilon = 1 - \mathfrak{w} \ . \end{aligned} \tag{A.82}$$

For the shear component we use the gauge-invariant variable ψ_V proposed in [167]. The Heun equation is found for the new variable

$$\psi_V(x) = x^{-i\mathfrak{w}/2}(x-1)^{3/4}(x-2)^{-\mathfrak{w}/2} y(x) \ , \tag{A.83}$$

with parameters

$$\begin{aligned} \alpha\beta &= \frac{\mathfrak{w}}{2}(1+i)\left(\frac{\mathfrak{w}}{2}(1+i) - 3\right) \ , \quad Q = \mathfrak{q}^2 - (1+5i)\frac{\mathfrak{w}}{2} - (2-i)\frac{\mathfrak{w}^2}{2} \ , \\ \gamma &= 1 - i\,\mathfrak{w} \ , \quad \delta = 2 \ , \quad \epsilon = 1 - \mathfrak{w} \ . \end{aligned} \tag{A.84}$$

[6] There is a factor of two difference with the conventions used here for the frequency and the momentum.

The coefficients of the Frobenius series at $x = 0$ should satisfy the recursion relation

$$2(n+2)(n+1+\gamma)a_{n+2} + A_n(\mathfrak{w},\mathfrak{q})\, a_{n+1} + B_n(\mathfrak{w},\mathfrak{q})\, a_n = 0 \ , \quad n \geq 0 \ , \tag{A.85}$$

where

$$A_n(\mathfrak{w},\mathfrak{q}) = -((n+1)(2\delta+\epsilon+3(n+\gamma))+Q) \ , \tag{A.86}$$

$$B_n(\mathfrak{w},\mathfrak{q}) = (n+\alpha)(n+\beta) \ , \tag{A.87}$$

and $2\gamma a_1 - Q a_0 = 0$. This recursion relation has in general a unique solution. However, when the continued fraction

$$r_n = \frac{a_{n+1}}{a_n} = -\frac{B_n(\omega,q)}{A_n(\omega,q)+r_{n+1}} \tag{A.88}$$

converges, Pincherle's theorem states that an extra solution to the three term recursion relation (A.85) exists [91, 94, 168]. This is equivalent to finding a solution that is analytic both at the boundary and at the horizon. Notice that at the horizon ($x = 0$), the critical exponents are 0 and $1-\gamma = i\mathfrak{w}$, so the analytic solution usually corresponds to the first solution, that is the one associated to infalling boundary conditions. However, when $\mathfrak{w} = -ik$, with $k = 1, 2, \ldots$, the analytic solution will be in general the outgoing solution, since it corresponds to the largest integer critical exponent, while the infalling solution will have a logarithmic contribution. This is reflected in the recursion relations, since the coefficient of the a_{n+2} term vanishes when $n+2 = k$, implying that the series start at x^k. The reason for this is that the first k recursion relations form a closed subsystem of linear equations for k unknowns. Then, the general solution to the Heun equation will be of the form

$$y(x) = \alpha_1 x^k \sum_{n=0}^{\infty} a_n x^n + \alpha_2 \left(\sum_{n=0}^{\infty} b_n x^n + c(\mathfrak{q}) \log(x) x^k \sum_{n=0}^{\infty} a_n x^n \right) \ . \tag{A.89}$$

In principle, there could be special values of the momentum where the coefficient of the logarithm vanishes $c(\mathfrak{q}) = 0$ and the two solutions at the horizon are analytic. This actually happens when the rank of the subsystem of the first k recursion relations is zero. In that case, we can find trivially two solutions satisfying the recursion relations without having to check the convergence of (A.88).

The diffusion and shear modes are located at negative imaginary values of the frequency, larger as the momentum is increased. This implies that for some large enough value of the momentum, the frequency will have the special value $\mathfrak{w} = -ik$. However, the mode has to be analytic at the boundary and the horizon, so the value of the momentum when the special value is reached must be determined by the condition $c(\mathfrak{q}) = 0$. When we compare the analytic result with the numerical computation, we find that this is indeed the case, the first points are $(i\mathfrak{w}, \mathfrak{q}^2) = (1, 1/2)$, $(2, \sqrt{3}-1)$, $(3, \sqrt{6}-3/2)$ for the diffusion

mode and $(i\mathfrak{w}, \mathfrak{q}^2) = (1, \sqrt{6})$, $(2, 3.2266)$, $(3, 3.91764)$ for the shear mode. On the other hand, at the special point the analytic solution that is found as the limit of the hydro mode $\mathfrak{w} \to -ik$ is a linear combination of the normalizable and non-normalizable modes. This implies that the pole disappears from the retarded Green function or in other words, that the residue is zero.

A.3 Front velocity

Wave propagation in dispersive media has been studied long ago in the classic work of Brillouin and Sommerfeld [169–171]. It has been pointed out there that the group velocity $v_g = \mathrm{d}\omega/\mathrm{d}q$ is not a reliable indicator if one wants to study the question of how fast can a signal be transmitted through the dispersive medium. In fact it is the so called front velocity which limits the speed of propagation of a signal through the medium. The front velocity is defined as the velocity with which the onset of a signal travels. In dispersive media this is not yet sufficient to guarantee that the signal travels with this speed and therefore one also has to define a signal velocity, which is the speed with which practically usable signals travel. This signal velocity is always smaller than the front velocity. For matters of principle, i.e. answering the question if causality is preserved it is therefore the front velocity that is important. We will briefly review here the reasoning leading to the definition of the front velocity. We want to study how fast a perturbation can travel through the medium, for this purpose we will switch on a periodic signal with frequency ν at time $t = 0$. We model this by a source of the form $\Theta(t)\mathrm{e}^{-i\nu t}\delta(x)$.[7] To compute the response of the system we expand the retarded Green function in its poles in the complexified momentum plane (for simplicity we will also restrict our considerations to effectively $1 + 1$ dimensions)

$$\langle \Phi(x,t) \rangle = -\int \frac{\mathrm{d}\omega}{2\pi} \frac{\mathrm{d}q}{2\pi} \sum_n \frac{R_n(\omega, q)}{q - q_n} \frac{i}{\omega - \nu + i\epsilon} \mathrm{e}^{-i\omega t + iqx} \ . \tag{A.90}$$

The poles in the momentum k have real and imaginary parts $q_n(\omega) = q_n^R(\omega) + iq_n^I(\omega)$ and from [102, 137] we know that they have to lie symmetrically in the first and third quadrants. We consider therefore only the region with $x > 0$ since the response in $x < 0$ is just the mirror image. Assuming $x > 0$ we have

$$\langle \Phi(x,t) \rangle = -\int \frac{\mathrm{d}\omega}{2\pi} \sum_n R_n(\omega, q_n) \frac{i}{\omega - \nu + i\epsilon} \mathrm{e}^{-i\omega t + iq_n^R x} \mathrm{e}^{-q_n^I x} \ . \tag{A.91}$$

To pick up a non vanishing signal we have to close the contour of integration now in the lower half plane. This demands however that $\lim_{\omega\to\infty}(t - x\frac{q_n^R(\omega)}{\omega}) \geq 0$ showing that we

[7] For simplicity we chose to localize the source in space, it is not important for the general argument.

can pick up the first front of the signal only at space time points where $x/t \leq v_{\mathrm{F}}$, where we have defined the front velocity [8]

$$v_{\mathrm{F}} := \lim_{\omega\to\infty} \frac{\omega}{q^R} \ . \tag{A.92}$$

It follows that causality is preserved if the front velocity is smaller that the speed of light $v_{\mathrm{F}} \leq c$. Results for the complex momentum modes for the shear channel and the diffusion channel in [102, 137] and for the sound channel in figure 5.7, show that the imaginary parts go to zero if we extrapolate to the large frequency limit, i.e. $\omega \to \infty$, while the real part approaches from below the dispersion relation $\omega = q$. Moreover, the evolution of the hydrodynamic modes in this limit is the same as the evolution of the higher modes, finding numerically that $\lim_{\omega\to\infty} \frac{\omega}{q} = 1$. This provides a numerical proof that the strongly coupled $\mathcal{N}=4$ plasma behaves causally even when we take into account the hydrodynamic modes.

[8] Since this implies a linear relation between ω and q for large frequencies and (real) wave numbers it is usually written as $v_{\mathrm{F}} = \lim_{q\to\infty} \frac{\omega}{q}$. It also follows that the diffusion equation violates causality since from the dispersion relation we find $\omega = 2Dq^2$ and therefore $\omega/q = 2Dq$ with no finite limit for the front velocity.

Part III

Secciones en castellano

Introducción

Esta tesis doctoral versa sobre la aplicación de la correspondencia AdS/CFT a la dinámica de teorías *gauge* en acoplo fuerte, prestando una atención especial al comportamiento hidrodinámico de las mismas. En particular estamos interesados en el estudio de la respuesta del plasma de *quarks* y *gluones* fuertemente acoplado frente a perturbaciones pequeñas empleando técnicas holográficas así como en examinar la validez de la aproximación hidrodinámica en dicho sistema. También estamos interesados en el estudio del régimen hidrodinámico de superconductores de alta temperatura en el marco de la dualidad gauge/gravedad.

La corespondencia AdS/CFT establece una equivalencia entre teorías cuánticas de campos y teorías de cuerdas en espacios curvos con la peculiaridad de ser una dualidad de acoplo fuerte/débil. Cuando la constante de acoplo gauge es grande, la teoría de campos se encuentra en un régimen no perturbativo, mientras que la teoría de cuerdas puede aproximarse por su límite clásico a bajas energías, supergravedad. La correspondencia nos proporciona una herramienta teórica con la que describir la dinámica de teorías gauge en interacción fuerte. Particularmente interesante es el caso del plasma de quarks y gluones fuertemente acoplado (sQGP) descubierto en el *Relativistic Heavy Ion Collider* (RHIC). El sQGP se comporta prácticamente como un fluido perfecto y puede ser descrito en términos hidrodinámicos en el límite de bajas energías. El acelerador RHIC crea un medio de materia muy densa y caliente, constituida de quarks y gluones, mediante colisiones de núcleos pesados. La 'bola de fuego' creada termaliza rápidamente, se expande y se enfría volviendo al estado de gas de hadrones, pero mientras tanto, cuando es un plasma de quarks y gluones, reproduce las condiciones del plasma primordial existente durante los primeros microsegundos posteriores al Big Bang. Al final de la era de Gran Unificación (10^{-36} segundos) el universo estaba hecho de una 'sopa' de partículas que se expandía y enfriaba. Aproximadamente 10^{-11} segundos tras la explosión, la fuerza electrodébil se desacopló de la fuerza nuclear fuerte y las interacciones entre partículas fueron lo bastante energéticas como para permitir la formación de partículas pesadas como los bosones Z y W. El Universo Primitivo estaba entonces ocupado por el plasma de quarks y gluones, aún en expansión y enfriamiento, hasta que éste alcanzó una temperature de unos 200 MeV, que son unos 2×10^{12}K, cuando la transición de fase *confinamiento/deconfinamiento* tuvo lugar. El QGP hadronizó formando protones y neutrones una decena de microsegundos después del Big Bang. Transcurridos unos minutos, la temperatura fue lo bastante baja como para permitir la formación de enlaces entre nucleones y los primeros núcleos ligeros

aparecieron. El estado del Universo Primitivo justo antes de la transición de fase entre quarks y hadrones se reproduce aproximadamente en RHIC y pronto lo será también en el experimento ALICE en el LHC. Estos experimentos proporcionan información de gran valor sobre la fase de deconfinamiento de QCD y sobre la física del plasma primordial. Obtener un entendimiento teórico de éstos es una tarea complicada e interesante además de un reto, y parece que la correspondencia puede ser de gran ayuda en esta empresa.

Recientemente, la correspondencia AdS/CFT se ha revelado como una herramienta muy útil también en el marco de la física de la materia condensada, dado que ésta nos proporciona un gran número de sistemas fuertemente correlacionados que no pueden ser tratados empleando los paradigmas convencionales, como es el caso de los sistemas críticos cuánticos. Existen muchos materiales fuertemente acoplados que pueden ser manipulados y estudiados en laboratorios, dificilmente tratables desde el punto de vista de materia condensada y para los que parece posible que la dualidad gauge/gravedad pueda ser de ayuda para llegar a comprender mejor su comportamiento. Es de esperar que los superfluidos y los superconductores de alta temperatura pertenezcan a esta familia de sistemas de materia condensada a los que pueden ser aplicadas técnicas holográficas. Por otro lado, este gran número de sistemas de materia condensada nos proporciona una gran variedad de Lagrangianos efectivos, de modo que empleando técnicas experimentales podría ser posible 'crear' un material cuyo dual holográfico sea conocido, dando lugar a un AdS/CFT experimental que podría permitir un mayor entendimiento de la gravedad cuántica a través de la física atómica, invirtiendo la dirección habitual del uso de la correspondencia. Por tanto, la correspondencia AdS/CM aparece como un tema de estudio muy rico e interesante. En esta tesis nos limitaremos a emplear la correspondencia para modelizar sistemas simples de materia condensada y ver que información podemos obtener de ella.

La tesis está organizada en dos partes. La primera parte está dedicada a presentar los ingredientes y herramientas básicos que serán empleados más adelante, es decir, los sistemas fuertemente acoplados a los que pretendemos aplicar la correspondencia así como las técnicas hológraficas que emplearemos para ello:

Capítulo 1: Presentamos las características principales de los sistemas en acoplo fuerte, centrándonos en la fase de sQGP de QCD, exponiendo algunos de los resultados más relevantes de RHIC que apuntan a que el plasma formado se encuentra fuertemente acoplado, y en el fenómeno de 'criticalidad cuántica' especialmente en el caso de superconductores de alta temperatura y superfluidos. También presentamos algunos conceptos básicos relativos a la teoría de respuesta lineal y a la hidrodinámica, que son las principales herramientas para el estudio de perturbaciones en estos sistemas.

Capítulo 2: Este capítulo está dedicado a explicar los conceptos básicos de la correspondencia AdS/CFT, evitando en la medida de lo posible entrar en detalles que no serán útiles a continuación. Nos centramos en aquellos aspectos de la correspondencia y sus extensiones más relevantes para sus aplicaciones a los sistemas antes mencionados: cómo añadir temepratura y cómo añadir potenciales químicos a la teoría gauge.

Capítulo 3: El poder de la dualidad gauge/gravedad radica en su capacidad para realizar cálculos en tiempo real. En este capítulo presentamos la que será la herramienta de cálculo principal en el resto de la tesis: una prescripción para calcular holográficamente correladores a temperatura finita. También se presentan algunos resultados de la correspondencia relativos a las singularidades de los propagadores y al espectro de modos cuasinormales de agujeros negros, así como las restricciones que la estabilidad impone en su localización.

En la segunda parte de esta tesis, presentamos varias aplicaciones de la correspondencia para el estudio de la física de sistemas con interacción fuerte:

Capítulo 4: Se examina una propiedad muy interesante de la dualidad relacionada con el espectro de modos cuasinormales de un agujero negro: en el límite de largas frecuencias, la localización de los polos de propagadores retardados puede ser explicada en términos de rayos nulos 'rebotando' en una geometría de agujero negro, de modo que el espectro de modos cuasinormales está relacionado con la estructura causal del agujero negro. Esta relación es consistente con la prescripción dada en el capítulo anterior para el cálculo de correladores.

Capítulo 5: La física de procesos cerca del equilibrio en la teoría gauge esta codificada en funciones de correlación de operadores a dos puntos en tiempo real y está completamente determinada por las singularidades de éstos, que en el caso holográfico son simplemente polos. Calculamos el espectro de modos cuasinormales y los correspondientes residuos de distintos tipos de perturbaciones para medir la contribución de cada uno de los modos colectivos que se propagan en un plasma de gluones. Presentamos los resultados para los modos hidrodinámicos y estudiamos el régimen de validez de una descripción hidrodinámica basada sólo en estos modos. También somos capaces de definir un límite inferior para el tiempo de termalización del plasma.

Capítulo 6: Se estudia el modelo holográfico de superfluido más simple: la ruptura espontánea de una simetría global mediante la formación de un condensado de Bose es

realizada holográficamente a través de un campo escalar cargado condensando en un espacio asintóticamente AdS con un agujero negro cargado. A bajas temperaturas el escalar adquiere un valor esperado y el sistema entra en la fase superfluida. Encontramos el bosón de Goldstone esperado en la ruptura de una simetría $U(1)$ y lo seguimos en la fase superfluida. Por debajo de la temperatura crítica se propaga como el sonido: el llamado segundo sonido de la componente superfluida.

La primera parte de este trabajo es básicamente un compendio de múltiples artículos y estudios sobre los temas correspondientes. El trabajo original aquí presentado corresponde a la segunda parte de esta tesis doctoral y está basado en nuestras publicaciones [1–4].

Conclusiones

Hemos visto que el espectro de modos cuasinormales de un agujero negro, y por lo tanto los polos del correspondiente correlador retardado, está relacionado con las propiedades geométricas del agujero negro, en particular con su estructura causal. En el límite de frecuencias largas la localización de las singularidades de correladores a temperatura finita pueden ser explicados en términos de geodésicas nulas rebotando en las singularidades y en las fronteras de un agujero negro eterno en AdS. Este cálculo está relacionado con el formalismo de Schwinger-Keldish bajo la identificación de los campos viviendo en diferentes fronteras con la inserción de operadores en diferentes segmentos del contorno de SK. Una extensión interesante de este trabajo es estudiar si el análisis geómetrico basado en geodésicas nulas puede ser generalizado a otro tipo de geometrías como la dada por un agujero negro en rotación o cargado, o incluso para espacios asintóticamente planos en los que no hay una frontera como en aAdS, de modo que el espacio no actua como una caja. También podría ser interesante estudiar el efecto de correcciones cuánticas, que implica introducir correcciones al límite de N grande o equivalentemente a la curvatura.

Hemos visto que la respuesta frente a perturbaciones pequeñas está completamente determinada por los polos de los propagadores retardados y por sus correspondientes residuos y lo hemos usado para estudiar la respuesta lineal de la fase de plasma de $\mathcal{N} = 4$ SYM en acoplo fuerte. Esto nos permite explorar la validez de la aproximación hidrodinámica, basada en *integrar out* todos los modos salvo los modos hidrodinámicos, de dos formas distintas: definiendo escalas hidrodinámicas de tiempo y distancia que miden a partir de que momento la contribución de los modos hidrodinámicos pasa a ser dominante y analizando en que rango de longitudes de onda y frecuencias los modos hidrodinámicos proporcionan una descripción fiable del sistema. Los tiempos hidrodinámicos obtenidos indican que el plasma perturbado termaliza extremadamente rápido, resultado que puede considerarse como un indicativo de rápida termalización también en RHIC. El fin de la validez de la aproximación hidrodinámica forma parte de la propia teoría: a menor longitud de onda de la perturbación, más y más modos cuasinormales tienen que ser considerados para describir el sistema. El peso de las excitaciones colectivas en el plasma depende de modo crucial del valor de los residuos. Para los modos de cizalladura y de difusión de carga, el residuo muestra un decaimiento oscilatorio, señalando que se desacoplan para momento pequeño. Sería interesante estudiar si este comportamiento es universal de los modos hidrodinámicos que describen difusión. A priori hay una indicación de que algo drástico ocurre a longitudes de onda cortas que viene de la observación de que se preserva causalidad mientras

al mismo tiempo al ir a longitudes de onda largas se reproduce hidrodinámica a primer orden, que es acausal. En RHIC tienen lugar procesos que no pueden ser descritos dentro de la teoría de respuesta lineal. Por lo tanto, sería de gran interés ir más allá de esta aproximación para poder tener una definición de la escala hidrodinámica más significativa que pudiese ser relevante para los experimentos en RHIC, para los que fijar la escala de termalización resulta crucial. Toda la discusión sólo contiene materia en la representación adjunta. Para poder realmente tener un modelo predictivo relevante para experimentos del mundo real, estaría muy bien repetir el análisis incluyendo materia en la fundamental, lo cual desde la teoría de cuerdas se consigue introduciendo nuevos sets de branas.

Finalmente, hemos estudiado el comportamiento hidrodinámico de un superfluido holográfico dado por un modelo gauge abeliano con un campo escalar masivo cargado en un espacio AdS con un agujero negro. El modo cuasinormal más bajo del campo escalar cargado se convierte en taquiónico a un cierto valor de la temperatura. Esta inestabilidad indica que el campo escalar condensa y el sistema sufre una transición de fase de segundo orden. En la transición de fase este modo escalar no tiene masa y su suceptibilidad es divergente, de modo que puede identificarse con el bosón de Goldstone que aparece en la ruptura espontánea de simetría. Por debajo de la temperatura crítica este modo puede identificarse con el segundo sonido. Empleando holografía hemos sido capaces de calcular coeficientes de transporte como la velocidad de propagación del segundo sonido, calculado directamente a partir de consideraciones termodinámicas en otros trabajos, pero también cantidades no termodinámicas como coeficientes de transporte 'absortivos', como la atenuación del segundo sonido o la constante de difusión. Como resultado complementario hemos desarrollado un método para calcular los modos cuasinormales físicos de un sistema acoplado en términos de las variables no invariantes gauge. En el análisis la *backreaction* debida a la presencia de los campos gauge y escalar ha sido despreciada. Una extensión obvia es considerar el modelo en el que su efecto es tenido en cuenta y en el cual las fluctuaciones de la métrica sí estan permitidas dando lugar a una dinámica mucho más rica. En este modelo la transición de fase a temperatura finita puede ocurrir incluso para un escalar neutro debido a la inestabilidad de la propia geometría. Cuando la carga del escalar es pequeña dos mecanismos responsables de la condensación compiten, el acoplo al campo gauge y la inestabilidad de la métrica. Sería interesante encontrar cuál es el parámetro de orden de la transición de fase para cada caso y qué es lo que ocurre en la fase superconductora en el segundo caso. También resultaría interesante estudiar la relación entre el sonido normal y el segundo sonido en dicha fase. El estudio completo del caso con *backreaction* podría arrojar luz sobre el origen del gap en la conductividad en estos modelos. Otra extensión natural de este modelo es considerar correcciones a la curvatura para examinar cuándo o cuándo no tiene lugar la transición de fase y cómo se ve afectado el diagrama de fases. Otra extensión interesante sería romper explicitamente la invariancia conforme y estudiar cómo afecta a la transición.

Agradecimientos

En cuanto a Física se refiere, a quién podría estar agradecida sino a Karl? Gracias a él esta tesis ha sido posible y aunque puede que no todo lo que a ambos nos gustaría, me atrevo a decir que finalmente algo de física sí que he aprendido en estos años! Karl, ha sido un gran placer trabajar contigo y espero poder repetir.

Por supuesto también estoy agradecida a la gente con la que he colaborado a lo largo de todo este tiempo. Especialmente a mi 'hermano mayor', Sergio, de quien también he aprendido mucho y con quien he pasado tan buenos ratos (se te echa de menos en el despacho!) y a Choyos, que tan bien me acogió en la soleada Swansea.

A nivel más personal, gracias a los que me han hecho más llevadera la a veces estresante vida en la Universidad, a todos los que han sido compañeros de despacho pero sobretodo a vosotros con los que he compartido las 'estupendas' comidas de la UAM durante los últimos 4 años (que se dice pronto), cafes, meriendas, las cervezas en la terracita, conciertos, salidas nocturnas, viajes por el mundo... Creo que entre todos hemos conseguido mantener la cordura! Espero que seais conscientes del aprecio que os tengo, chicos, un placer haber contado con vuestra compañia en este viaje, o en un tramo del mismo (por los que ya se han ido de aquí...).

Por último, aunque en realidad sean los primeros, a mis padres, a mi familia, que aunque creo que nunca les ha quedado muy claro de qué va ésto, han sido un apoyo incondicional y no podría estar más orgullosa de ellos. Muchas gracias de corazón.

Bibliography

[1] Irene Amado and Carlos Hoyos-Badajoz. *AdS black holes as reflecting cavities*. *JHEP*, **09**:118, 2008. arXiv:0807.2337 [hep-th].

[2] Irene Amado, Carlos Hoyos-Badajoz, Karl Landsteiner, and Sergio Montero. *Residues of Correlators in the Strongly Coupled N=4 Plasma*. *Phys. Rev.*, **D77**:065004, 2008. arXiv:0710.4458 [hep-th].

[3] Irene Amado, Carlos Hoyos-Badajoz, Karl Landsteiner, and Sergio Montero. *Hydrodynamics and beyond in the strongly coupled N=4 plasma*. *JHEP*, **07**:133, 2008. arXiv:0805.2570 [hep-th].

[4] Irene Amado, Matthias Kaminski, and Karl Landsteiner. *Hydrodynamics of Holographic Superconductors*. *JHEP*, **05**:021, 2009. arXiv:0903.2209 [hep-th].

[5] L. H. Ryder. *Quantum Field Theory*. Cambridge, UK: Univ. Pr. 2nd edition (1996) 507 p.

[6] Sidney R. Coleman and David J. Gross. *Price of asymptotic freedom*. *Phys. Rev. Lett.*, **31**:851–854, 1973.

[7] D. J. Gross and Frank Wilczek. *Ultraviolet Behavior of Non-Abelian Gauge Theories*. *Phys. Rev. Lett.*, **30**:1343–1346, 1973.

[8] H. David Politzer. *Reliable Perturbative Results For Strong Interactions?* *Phys. Rev. Lett.*, **30**:1346–1349, 1973.

[9] R. Hagedorn. *Statistical thermodynamics of strong interactions at high-energies*. *Nuovo Cim. Suppl.*, **3**:147–186, 1965.

[10] Edward V. Shuryak. *Quark-Gluon Plasma and Hadronic Production of Leptons, Photons and Psions*. *Phys. Lett.*, **B78**:150, 1978.

[11] O. K. Kalashnikov and V. V. Klimov. *Phase Transition in Quark-Gluon Plasma*. *Phys. Lett.*, **B88**:328, 1979.

[12] Joseph I. Kapusta. *Quantum Chromodynamics at High Temperature*. *Nucl. Phys.*, **B148**:461–498, 1979.

[13] Frithjof Karsch. *Lattice QCD at high temperature and density*. *Lect. Notes Phys.*, **583**:209–249, 2002. hep-lat/0106019.

[14] Y. Aoki, G. Endrodi, Z. Fodor, S. D. Katz, and K. K. Szabo. *The order of the quantum chromodynamics transition predicted by the standard model of particle physics*. *Nature*, **443**:675–678, 2006. hep-lat/0611014.

[15] Y. Aoki, Z. Fodor, S. D. Katz, and K. K. Szabo. *The QCD transition temperature: Results with physical masses in the continuum limit*. *Phys. Lett.*, **B643**:46–54, 2006. hep-lat/0609068.

[16] Christian Schmidt. *Lattice QCD at finite density*. *PoS*, **LAT2006**:021, 2006.

[17] J. D. Bjorken. *Highly Relativistic Nucleus-Nucleus Collisions: The Central Rapidity Region*. *Phys. Rev.*, **D27**:140–151, 1983.

[18] Obtained at `http://www.bnl.gov/rhic/physics.asp`.

[19] Derek Teaney. *Effect of shear viscosity on spectra, elliptic flow, and Hanbury Brown-Twiss radii*. *Phys. Rev.*, **C68**:034913, 2003. `nucl-th/0301099`.

[20] P. Huovinen, P. F. Kolb, Ulrich W. Heinz, P. V. Ruuskanen, and S. A. Voloshin. *Radial and elliptic flow at RHIC: further predictions*. *Phys. Lett.*, **B503**:58–64, 2001.

[21] Hans-Joachim Drescher, Adrian Dumitru, Clement Gombeaud, and Jean-Yves Ollitrault. *The centrality dependence of elliptic flow, the hydrodynamic limit, and the viscosity of hot QCD*. *Phys. Rev.*, **C76**:024905, 2007.

[22] L. P. Csernai, J. I. Kapusta, and L. D. McLerran. *Properties of the quantum fluid at RHIC*. *J. Phys.*, **G32**:S115–S121, 2006.

[23] Matthew Luzum and Paul Romatschke. *Conformal Relativistic Viscous Hydrodynamics: Applications to RHIC results at sqrt(s_NN) = 200 GeV*. *Phys. Rev.*, **C78**:034915, 2008.

[24] S. Sachdev. *Quantum Phase Transitions*. Cambridge, UK: Univ. Pr. (1999) 368 p.

[25] Sidney R. Coleman. *There are no Goldstone bosons in two-dimensions*. *Commun. Math. Phys.*, **31**:259–264, 1973.

[26] N. D. Mermin and H. Wagner. *Absence of ferromagnetism or antiferromagnetism in one-dimensional or two-dimensional isotropic Heisenberg models*. *Phys. Rev. Lett.*, **17**:1133–1136, 1966.

[27] P. C. Hohenberg. sl Existence of Long-Range Order in One and Two Dimensions. *Phys. Rev.*, **158**:383–386, 1967.

[28] Subir Sachdev. *Quantum magnetism and criticality*. *Nature Physics*, **4**:173, 2008. `arXiv:0711.3015 [cond-mat.str-el]`.

[29] Matthew P. A. Fisher, Peter B. Weichman, G. Grinstein, and Daniel S. Fisher. *Boson localization and the superfluid-insulator transition*. *Phys. Rev.*, **B40**:546–570, 1989.

[30] Kedar Damle and Subir Sachdev. *Non-zero temperature transport near quantum critical points*. *Phys. Rev.*, **B56**:8714, 1997. `cond-mat/9705206`.

[31] M. J. Bhaseen, A. G. Green, and S. L. Sondhi. *Magnetothermoelectric Response at a Superfluid–Mott Insulator Transition*. *Phys. Rev. Lett.*, **98**:166801, 2007. `cond-mat/0610687`.

[32] R. D. Parks. *Superconductivity*. Marcel Dekker Inc. (1969).

[33] Joseph Polchinski. *Effective field theory and the Fermi surface*. 1992. `hep-th/9210046`.

[34] E. W. Carlson, V. J. Emery, S. A. Kivelson, and D. Orgad. *Concepts in High Temperature Superconductivity*. 2002. `cond-mat/0206217`.

[35] D. M. Broun. *What lies beneath the dome?* *Nature Physics*, **4**:170, 2008.

[36] Subir Sachdev. *Where is the quantum critical point in the cuprate superconductors ?* 2009.

[37] L. D. Landau and E. M. Lifshitz. *Fluid Mechanics*. Pergamon Press. (1987).

[38] A. Atland and B. Simons. *Condensed matter field theory*. Cambridge, UK: Univ. Pr. (2006).

[39] D. T. Son. *Hydrodynamics of relativisic systems with broken continuous symmetries*. *Int. J. Mod. Phys.*, **A16S1C**:1284–1286, 2001. `hep-th/0011246`.

[40] Gerard 't Hooft. *Dimensional reduction in quantum gravity*. 1993. `gr-qc/9310026`.

[41] Leonard Susskind. *The World as a hologram*. *J. Math. Phys.*, **36**:6377–6396, 1995. hep-th/9409089.

[42] Jacob D. Bekenstein. *Entropy bounds and black hole remnants*. *Phys. Rev.*, **D49**:1912–1921, 1994. gr-qc/9307035.

[43] Juan Martin Maldacena. *The large N limit of superconformal field theories and supergravity*. *Adv. Theor. Math. Phys.*, **2**:231–252, 1998. hep-th/9711200.

[44] Gerard 't Hooft. *A Planar Diagram Theory For Strong Interactions*. *Nucl. Phys.*, **B72**:461, 1974.

[45] S. S. Gubser, Igor R. Klebanov, and Alexander M. Polyakov. *Gauge theory correlators from non-critical string theory*. *Phys. Lett.*, **B428**:105–114, 1998. hep-th/9802109.

[46] Edward Witten. *Anti-de Sitter space and holography*. *Adv. Theor. Math. Phys.*, **2**:253–291, 1998. hep-th/9802150.

[47] Ofer Aharony, Steven S. Gubser, Juan Martin Maldacena, Hirosi Ooguri, and Yaron Oz. *Large N field theories, string theory and gravity*. *Phys. Rept.*, **323**:183–386, 2000. hep-th/9905111.

[48] Eric D'Hoker and Daniel Z. Freedman. *Supersymmetric gauge theories and the AdS/CFT correspondence*. 2002. hep-th/0201253.

[49] Sean A. Hartnoll. *Lectures on holographic methods for condensed matter physics*. *Class. Quant. Grav.*, **26**:224002, 2009.

[50] Christopher P. Herzog. *Lectures on Holographic Superfluidity and Superconductivity*. *J. Phys.*, **A42**:343001, 2009. arXiv:0904.1975 [hep-th].

[51] Alexander M. Polyakov. *String theory and quark confinement*. *Nucl. Phys. Proc. Suppl.*, **68**:1–8, 1998. hep-th/9711002.

[52] Alexander M. Polyakov. *The wall of the cave*. *Int. J. Mod. Phys.*, **A14**:645–658, 1999. hep-th/9809057.

[53] Joseph Polchinski. *Dirichlet-Branes and Ramond-Ramond Charges*. *Phys. Rev. Lett.*, **75**:4724–4727, 1995. hep-th/9510017.

[54] Edward Witten. *String theory dynamics in various dimensions*. *Nucl. Phys.*, **B443**:85–126, 1995. hep-th/9503124.

[55] Edward Witten. *Bound states of strings and p-branes*. *Nucl. Phys.*, **B460**:335–350, 1996. hep-th/9510135.

[56] J. A. Minahan and K. Zarembo. *The Bethe-ansatz for N = 4 super Yang-Mills*. *JHEP*, **03**:013, 2003. hep-th/0212208.

[57] Niklas Beisert, Rafael Hernandez, and Esperanza Lopez. *A crossing-symmetric phase for AdS(5) x S**5 strings*. *JHEP*, **11**:070, 2006. hep-th/0609044.

[58] Niklas Beisert, Burkhard Eden, and Matthias Staudacher. *Transcendentality and crossing*. *J. Stat. Mech.*, **0701**:P021, 2007. hep-th/0610251.

[59] Leonard Susskind and Edward Witten. *The holographic bound in anti-de Sitter space*. 1998. hep-th/9805114.

[60] G. W. Gibbons and S. W. Hawking. *Cosmological event horizons, thermodynamics, and particle creation*. *Phys. Rev.*, **D15**:2738–2751, 1977.

[61] S. S. Gubser, Igor R. Klebanov, and A. W. Peet. *Entropy and Temperature of Black 3-Branes*. *Phys. Rev.*, **D54**:3915–3919, 1996. `hep-th/9602135`.

[62] Igor R. Klebanov and A. A. Tseytlin. *Entropy of Near-Extremal Black p-branes*. *Nucl. Phys.*, **B475**:164–178, 1996. `hep-th/9604089`.

[63] Edward Witten. *Anti-de Sitter space, thermal phase transition, and confinement in gauge theories*. *Adv. Theor. Math. Phys.*, **2**:505–532, 1998. `hep-th/9803131`.

[64] S. W. Hawking and Don N. Page. *Thermodynamics of Black Holes in anti-De Sitter Space*. *Commun. Math. Phys.*, **87**:577, 1983.

[65] Steven S. Gubser. *Breaking an Abelian gauge symmetry near a black hole horizon*. *Phys. Rev.*, **D78**:065034, 2008. `arXiv:0801.2977 [hep-th]`.

[66] Sean A. Hartnoll, Christopher P. Herzog, and Gary T. Horowitz. *Building a Holographic Superconductor*. *Phys. Rev. Lett.*, **101**:031601, 2008. `arXiv:0803.3295 [hep-th]`.

[67] Sean A. Hartnoll, Christopher P. Herzog, and Gary T. Horowitz. *Holographic Superconductors*. *JHEP*, **12**:015, 2008. `arXiv:0810.1563 [hep-th]`.

[68] Steven S. Gubser. *Colorful horizons with charge in anti-de Sitter space*. *Phys. Rev. Lett.*, **101**:191601, 2008. `arXiv:0803.3483 [hep-th]`.

[69] Steven S. Gubser and Silviu S. Pufu. *The gravity dual of a p-wave superconductor*. *JHEP*, **11**:033, 2008. `arXiv:0805.2960 [hep-th]`.

[70] Martin Ammon, Johanna Erdmenger, Matthias Kaminski, and Patrick Kerner. *Superconductivity from gauge/gravity duality with flavor*. *Phys. Lett.*, **B680**:516–520, 2009. `arXiv:0810.2316 [hep-th]`.

[71] Christopher P. Herzog. *An Analytic Holographic Superconductor*. 2010. `arXiv:1003.3278 [hep-th]`.

[72] Martin Ammon, Johanna Erdmenger, Matthias Kaminski, and Patrick Kerner. *Flavor Superconductivity from Gauge/Gravity Duality*. *JHEP*, **10**:067, 2009. `arXiv:0903.1864 [hep-th]`.

[73] Frederik Denef and Sean A. Hartnoll. *Landscape of superconducting membranes*. *Phys. Rev.*, **D79**:126008, 2009. `arXiv:0901.1160 [hep-th]`.

[74] Steven S. Gubser, Christopher P. Herzog, Silviu S. Pufu, and Tiberiu Tesileanu. *Superconductors from Superstrings*. *Phys. Rev. Lett.*, **103**:141601, 2009.

[75] C. P. Herzog, P. K. Kovtun, and D. T. Son. *Holographic model of superfluidity*. *Phys. Rev.*, **D79**:066002, 2009. `arXiv:0809.4870 [hep-th]`.

[76] Massimo Bianchi, Daniel Z. Freedman, and Kostas Skenderis. *Holographic Renormalization*. *Nucl. Phys.*, **B631**:159–194, 2002. `hep-th/0112119`.

[77] Dam T. Son and Andrei O. Starinets. *Minkowski-space correlators in AdS/CFT correspondence: Recipe and applications*. *JHEP*, **09**:042, 2002. `hep-th/0205051`.

[78] C. P. Herzog and D. T. Son. *Schwinger-Keldysh propagators from AdS/CFT correspondence*. *JHEP*, **03**:046, 2003. `hep-th/0212072`.

[79] Kostas Skenderis and Balt C. van Rees. *Real-time gauge/gravity duality*. *Phys. Rev. Lett.*, **101**:081601, 2008. arXiv:0805.0150 [hep-th].

[80] Juan Martin Maldacena. *Eternal black holes in Anti-de-Sitter*. *JHEP*, **04**:021, 2003. hep-th/0106112.

[81] Vijay Balasubramanian, Per Kraus, Albion E. Lawrence, and Sandip P. Trivedi. *Holographic probes of anti-de Sitter space-times*. *Phys. Rev.*, **D59**:104021, 1999. hep-th/9808017.

[82] Gary T. Horowitz and Donald Marolf. *A new approach to string cosmology*. *JHEP*, **07**:014, 1998. hep-th/9805207.

[83] Bruno G Carneiro da Cunha. *Inflation and holography in string theory*. *Phys. Rev.*, **D65**:026001, 2002. hep-th/0105219.

[84] W. Israel. *Thermo field dynamics of black holes*. *Phys. Lett.*, **A57**:107–110, 1976.

[85] Michel Le Bellac. *Thermal Field Theory*. Cambridge, UK: Univ. Pr. (2000) 270 p.

[86] W. G. Unruh. *Notes on black hole evaporation*. *Phys. Rev.*, **D14**:870, 1976.

[87] Kostas D. Kokkotas and Bernd G. Schmidt. *Quasi-normal modes of stars and black holes*. *Living Rev. Rel.*, **2**:2, 1999. gr-qc/9909058.

[88] Hans-Peter Nollert. *Topical Review: Quasinormal modes: the characteristic 'sound' of black holes and neutron stars*. *Class. Quant. Grav.*, **16**:R159–R216, 1999.

[89] Gary T. Horowitz and Veronika E. Hubeny. *Quasinormal modes of AdS black holes and the approach to thermal equilibrium*. *Phys. Rev.*, **D62**:024027, 2000. hep-th/9909056.

[90] Vitor Cardoso and Jose P. S. Lemos. *Quasi-normal modes of Schwarzschild anti-de Sitter black holes: Electromagnetic and gravitational perturbations*. *Phys. Rev.*, **D64**:084017, 2001. gr-qc/0105103.

[91] Danny Birmingham, Ivo Sachs, and Sergey N. Solodukhin. *Conformal field theory interpretation of black hole quasi-normal modes*. *Phys. Rev. Lett.*, **88**:151301, 2002. hep-th/0112055.

[92] Giuseppe Policastro, Dam T. Son, and Andrei O. Starinets. *From AdS/CFT correspondence to hydrodynamics*. *JHEP*, **09**:043, 2002. hep-th/0205052.

[93] Giuseppe Policastro, Dam T. Son, and Andrei O. Starinets. *From AdS/CFT correspondence to hydrodynamics. II: Sound waves*. *JHEP*, **12**:054, 2002. hep-th/0210220.

[94] Andrei O. Starinets. *Quasinormal modes of near extremal black branes*. *Phys. Rev.*, **D66**:124013, 2002. hep-th/0207133.

[95] Alvaro Nunez and Andrei O. Starinets. *AdS/CFT correspondence, quasinormal modes, and thermal correlators in $N = 4$ SYM*. *Phys. Rev.*, **D67**:124013, 2003. hep-th/0302026.

[96] Vitor Cardoso, Roman Konoplya, and Jose P. S. Lemos. *Quasinormal frequencies of Schwarzschild black holes in anti-de Sitter spacetimes: A complete study on the asymptotic behavior*. *Phys. Rev.*, **D68**:044024, 2003. gr-qc/0305037.

[97] Jose Natario and Ricardo Schiappa. *On the classification of asymptotic quasinormal frequencies for d-dimensional black holes and quantum gravity*. *Adv. Theor. Math. Phys.*, **8**:1001–1131, 2004. hep-th/0411267.

[98] Pavel K. Kovtun and Andrei O. Starinets. *Quasinormal modes and holography*. *Phys. Rev.*, **D72**:086009, 2005. hep-th/0506184.

[99] Suphot Musiri, Scott Ness, and George Siopsis. *Perturbative calculation of quasi-normal modes of AdS Schwarzschild black holes*. *Phys. Rev.*, **D73**:064001, 2006. hep-th/0511113.

[100] Joshua J. Friess, Steven S. Gubser, Georgios Michalogiorgakis, and Silviu S. Pufu. *Expanding plasmas and quasinormal modes of anti-de Sitter black holes*. *JHEP*, **04**:080, 2007. hep-th/0611005.

[101] Emanuele Berti, Vitor Cardoso, and Andrei O. Starinets. *Quasinormal modes of black holes and black branes*. *Class. Quant. Grav.*, **26**:163001, 2009. arXiv:0905.2975 [hep-th].

[102] Irene Amado, Carlos Hoyos-Badajoz, Karl Landsteiner, and Sergio Montero. *Absorption Lengths in the Holographic Plasma*. *JHEP*, **09**:057, 2007. arXiv:0706.2750 [hep-th].

[103] N. Andersson and K. E. Thylwe. *Complex angular momentum approach to black hole scattering*. *Class. Quant. Grav.*, **11**:2991–3001, 1994.

[104] Vijay Balasubramanian and Simon F. Ross. *Holographic particle detection*. *Phys. Rev.*, **D61**:044007, 2000.

[105] Jorma Louko, Donald Marolf, and Simon F. Ross. *On geodesic propagators and black hole holography*. *Phys. Rev.*, **D62**:044041, 2000.

[106] Per Kraus, Hirosi Ooguri, and Stephen Shenker. *Inside the horizon with AdS/CFT*. *Phys. Rev.*, **D67**:124022, 2003.

[107] Lukasz Fidkowski, Veronika Hubeny, Matthew Kleban, and Stephen Shenker. *The black hole singularity in AdS/CFT*. *JHEP*, **02**:014, 2004.

[108] Guido Festuccia and Hong Liu. *Excursions beyond the horizon: Black hole singularities in Yang-Mills theories. I*. *JHEP*, **04**:044, 2006.

[109] Veronika E Hubeny, Hong Liu, and Mukund Rangamani. *Bulk-cone singularities & signatures of horizon formation in AdS/CFT*. *JHEP*, **01**:009, 2007.

[110] Notes by M. Blau, *"Plane waves and Penrose limits"*,. Available at http://www.unine.ch/phys/string/Lecturenotes.html.

[111] Timothy J. Hollowood and Graham M. Shore. *The Causal Structure of QED in Curved Spacetime: Analyticity and the Refractive Index*. *JHEP*, **12**:091, 2008.

[112] Vitor Cardoso, Jose Natario, and Ricardo Schiappa. *Asymptotic quasinormal frequencies for black holes in non- asymptotically flat spacetimes*. *J. Math. Phys.*, **45**:4698–4713, 2004. hep-th/0403132.

[113] Vijay Balasubramanian, Klaus Larjo, and Joan Simon. *Much ado about nothing*. *Class. Quant. Grav.*, **22**:4149–4170, 2005.

[114] Daniel N. Kabat and Gilad Lifschytz. *Gauge theory origins of supergravity causal structure*. *JHEP*, **05**:005, 1999.

[115] Gary T. Horowitz and N. Itzhaki. *Black holes, shock waves, and causality in the AdS/CFT correspondence*. *JHEP*, **02**:010, 1999.

[116] M. Porrati and R. Rabadan. *Boundary rigidity and holography*. *JHEP*, **01**:034, 2004.

[117] Sean A. Hartnoll and S. Prem Kumar. *AdS black holes and thermal Yang-Mills correlators*. *JHEP*, **12**:036, 2005. hep-th/0508092.

[118] Pavel Kovtun and Laurence G. Yaffe. *Hydrodynamic fluctuations, long-time tails, and supersymmetry. Phys. Rev.*, **D68**:025007, 2003.

[119] G. Policastro, D. T. Son, and A. O. Starinets. *The shear viscosity of strongly coupled N = 4 supersymmetric Yang-Mills plasma. Phys. Rev. Lett.*, **87**:081601, 2001. `hep-th/0104066`.

[120] P. Kovtun, D. T. Son, and A. O. Starinets. *Viscosity in strongly interacting quantum field theories from black hole physics. Phys. Rev. Lett.*, **94**:111601, 2005. `hep-th/0405231`.

[121] Mauro Brigante, Hong Liu, Robert C. Myers, Stephen Shenker, and Sho Yaida. *Viscosity Bound Violation in Higher Derivative Gravity. Phys. Rev.*, **D77**:126006, 2008. `arXiv:0712.0805 [hep-th]`.

[122] Mauro Brigante, Hong Liu, Robert C. Myers, Stephen Shenker, and Sho Yaida. *The Viscosity Bound and Causality Violation. Phys. Rev. Lett.*, **100**:191601, 2008. `arXiv:0802.3318 [hep-th]`.

[123] Yevgeny Kats and Pavel Petrov. *Effect of curvature squared corrections in AdS on the viscosity of the dual gauge theory. JHEP*, **01**:044, 2009. `arXiv:0712.0743 [hep-th]`.

[124] Alex Buchel, Robert C. Myers, and Aninda Sinha. *Beyond eta/s = 1/4pi. JHEP*, **03**:084, 2009. `arXiv:0812.2521 [hep-th]`.

[125] Berndt Muller and James L. Nagle. *Results from the Relativistic Heavy Ion Collider. Ann. Rev. Nucl. Part. Sci.*, **56**:93–135, 2006. `nucl-th/0602029`.

[126] W. Israel. *Nonstationary irreversible thermodynamics: A Causal relativistic theory. Ann. Phys.*, **100**:310–331, 1976.

[127] I. Müller. *Zum Paradoxon der Wärmeleitungstheorie. Zeitschrift für Physik A Hadrons and Nuclei*, **198**:329, 1967.

[128] Stewart J.M. *On Transient Relativistic Thermodynamics and Kinetic Theory. Proc. Roy. Soc.*, **357**:59, 1977.

[129] W. Israel and J. M. Stewart. *Transient relativistic thermodynamics and kinetic theory. Ann. Phys.*, **118**:341–372, 1979.

[130] Michal P. Heller and Romuald A. Janik. *Viscous hydrodynamics relaxation time from AdS/CFT. Phys. Rev.*, **D76**:025027, 2007. `hep-th/0703243`.

[131] Rudolf Baier, Paul Romatschke, Dam Thanh Son, Andrei O. Starinets, and Mikhail A. Stephanov. *Relativistic viscous hydrodynamics, conformal invariance, and holography. JHEP*, **04**:100, 2008. `arXiv:0712.2451 [hep-th]`.

[132] Sayantani Bhattacharyya, Veronika E Hubeny, Shiraz Minwalla, and Mukund Rangamani. *Nonlinear Fluid Dynamics from Gravity. JHEP*, **02**:045, 2008. `arXiv:0712.2456 [hep-th]`.

[133] Makoto Natsuume and Takashi Okamura. *Causal hydrodynamics of gauge theory plasmas from AdS/CFT duality. Phys. Rev.*, **D77**:066014, 2008. `arXiv:0712.2916 [hep-th]`.

[134] Ulrike Kraemmer and Anton Rebhan. *Advances in perturbative thermal field theory. Rept. Prog. Phys.*, **67**:351, 2004. `hep-ph/0310337`.

[135] Jean-Paul Blaizot and Edmond Iancu. *The quark-gluon plasma: Collective dynamics and hard thermal loops. Phys. Rept.*, **359**:355–528, 2002. `hep-ph/0101103`.

[136] R. A. Konoplya. *On quasinormal modes of small Schwarzschild-anti-de-Sitter black hole. Phys. Rev.*, **D66**:044009, 2002. `hep-th/0205142`.

[137] Carlos Hoyos-Badajoz, Karl Landsteiner, and Sergio Montero. *Holographic Meson Melting*. *JHEP*, **04**:031, 2007. hep-th/0612169.

[138] Carlos Hoyos-Badajoz, Karl Landsteiner, and Sergio Montero. *Quasinormal modes and meson decay rates*. *Fortsch. Phys.*, **55**:760–764, 2007.

[139] Robert C. Myers, Andrei O. Starinets, and Rowan M. Thomson. *Holographic spectral functions and diffusion constants for fundamental matter*. *JHEP*, **11**:091, 2007. arXiv:0706.0162 [hep-th].

[140] Angel Paredes, Kasper Peeters, and Marija Zamaklar. *Mesons versus quasi-normal modes: undercooling and overheating*. *JHEP*, **05**:027, 2008. arXiv:0803.0759 [hep-th].

[141] Edward V. Shuryak and Ismail Zahed. *Rethinking the properties of the quark gluon plasma at T approx. T(c)*. *Phys. Rev.*, **C70**:021901, 2004. hep-ph/0307267.

[142] Gerald E. Brown, Chang-Hwan Lee, Mannque Rho, and Edward Shuryak. *The anti-q q bound states and instanton molecules at t >= T(C)*. *Nucl. Phys.*, **A740**:171–194, 2004. hep-ph/0312175.

[143] Edward V. Shuryak and Ismail Zahed. *Towards a theory of binary bound states in the quark gluon plasma*. *Phys. Rev.*, **D70**:054507, 2004. hep-ph/0403127.

[144] Robert C. Myers and Aninda Sinha. *The fast life of holographic mesons*. *JHEP*, **06**:052, 2008. arXiv:0804.2168 [hep-th].

[145] Tameem Albash and Clifford V. Johnson. *A Holographic Superconductor in an External Magnetic Field*. *JHEP*, **09**:121, 2008. arXiv:0804.3466 [hep-th].

[146] Eiji Nakano and Wen-Yu Wen. *Critical magnetic field in a holographic superconductor*. *Phys. Rev.*, **D78**:046004, 2008. arXiv:0804.3180 [hep-th].

[147] Wen-Yu Wen. *Inhomogeneous magnetic field in AdS/CFT superconductor*. 2008. arXiv:0805.1550 [hep-th].

[148] Matthew M. Roberts and Sean A. Hartnoll. *Pseudogap and time reversal breaking in a holographic superconductor*. *JHEP*, **08**:035, 2008. arXiv:0805.3898 [hep-th].

[149] Kengo Maeda and Takashi Okamura. *Characteristic length of an AdS/CFT superconductor*. *Phys. Rev.*, **D78**:106006, 2008. arXiv:0809.3079 [hep-th].

[150] Pallab Basu, Anindya Mukherjee, and Hsien-Hang Shieh. *Supercurrent: Vector Hair for an AdS Black Hole*. *Phys. Rev.*, **D79**:045010, 2009. arXiv:0809.4494 [hep-th].

[151] Pallab Basu, Jianyang He, Anindya Mukherjee, and Hsien-Hang Shieh. *Superconductivity from D3/D7: Holographic Pion Superfluid*. *JHEP*, **11**:070, 2009. arXiv:0810.3970 [hep-th].

[152] Gary T. Horowitz and Matthew M. Roberts. *Holographic Superconductors with Various Condensates*. *Phys. Rev.*, **D78**:126008, 2008. arXiv:0810.1077 [hep-th].

[153] Steven S. Gubser and Abhinav Nellore. *Low-temperature behavior of the Abelian Higgs model in anti-de Sitter space*. *JHEP*, **04**:008, 2009. arXiv:0810.4554 [hep-th].

[154] Andy O'Bannon. *Toward a Holographic Model of Superconducting Fermions*. *JHEP*, **01**:074, 2009. arXiv:0811.0198 [hep-th].

[155] Anton Rebhan, Andreas Schmitt, and Stefan A. Stricker. *Meson supercurrents and the Meissner effect in the Sakai- Sugimoto model*. *JHEP*, **05**:084, 2009. arXiv:0811.3533 [hep-th].

[156] Nick Evans and Ed Threlfall. *Chemical Potential in the Gravity Dual of a 2+1 Dimensional System*. *Phys. Rev.*, **D79**:066008, 2009. arXiv:0812.3273 [hep-th].

[157] George Koutsoumbas, Eleftherios Papantonopoulos, and George Siopsis. *Exact Gravity Dual of a Gapless Superconductor*. *JHEP*, **07**:026, 2009. arXiv:0902.0733 [hep-th].

[158] Amos Yarom. *Fourth sound of holographic superfluids*. *JHEP*, **07**:070, 2009. arXiv:0903.1353 [hep-th].

[159] Christopher P. Herzog and Silviu S. Pufu. *The Second Sound of SU(2)*. *JHEP*, **04**:126, 2009. arXiv:0902.0409 [hep-th].

[160] P. M. Chaikin and T. C. Lubensky. *Principles of Condensed Matter Physics*. Cambridge University Press (2000).

[161] Alex S. Miranda, Jaqueline Morgan, and Vilson T. Zanchin. *Quasinormal modes of plane-symmetric black holes according to the AdS/CFT correspondence*. *JHEP*, **11**:030, 2008. arXiv:0809.0297 [hep-th].

[162] Alex Buchel and Chris Pagnutti. *Bulk viscosity of N=2* plasma*. *Nucl. Phys.*, **B816**:62–72, 2009. arXiv:0812.3623 [hep-th].

[163] Johanna Erdmenger, Matthias Kaminski, and Felix Rust. *Holographic vector mesons from spectral functions at finite baryon or isospin density*. *Phys. Rev.*, **D77**:046005, 2008. arXiv:0710.0334 [hep-th].

[164] P.C. Hohenberg and B. I. Halperin. *Theory of dynamic critical phenomena*. *Rev. Mod. Phys.*, **49**:435, 1977.

[165] Derek Teaney. *Finite temperature spectral densities of momentum and R-charge correlators in $N = 4$ Yang Mills theory*. *Phys. Rev.*, **D74**:045025, 2006. hep-ph/0602044.

[166] Pavel Kovtun and Andrei Starinets. *Thermal spectral functions of strongly coupled $N = 4$ supersymmetric Yang-Mills theory*. *Phys. Rev. Lett.*, **96**:131601, 2006. hep-th/0602059.

[167] Hideo Kodama and Akihiro Ishibashi. *A master equation for gravitational perturbations of maximally symmetric black holes in higher dimensions*. *Prog. Theor. Phys.*, **110**:701–722, 2003. hep-th/0305147.

[168] E. W. Leaver. *An Analytic representation for the quasi normal modes of Kerr black holes*. *Proc. Roy. Soc. Lond.*, **A402**:285–298, 1985.

[169] A. Sommerfeld. *Ein Einwand gegen die Relativtheorie der Elektrodynamik und seine Beseitigung*. *Physikalische Zeitschrift*, **8**:841, 1907.

[170] L. Brillouin. *Über die Fortpflanzung des Lichts in dispergierenden Medien*. *Annalen Phys.*, **10**:203, 1914.

[171] L. Brillouin. *Wave Propagation and Group Velocity*. Academic Press (1960).